TECTONIC FEATURES AND STRUCTURAL EVOLUTION OF THE YALVAÇ - YARIKKAYA NEOGENE BASIN

Fuzuli YAĞMURLU*

ABSTRACT— Yalvaç-Yarıkkaya Neogene basin, which has a triangular shape, with its margins bordered largely by normal faults, is located in the central pan of a regional-scale structure, the so-called Isparta flexure. Ordovician mete-sedimentiles comprising the Sultan Mountains, and Triassic-Cretaceous aged carbonate rocks border the basin in the east and north, respectively. The Anamas Mountains, bordering the basin in the south, comprise largely a carbonate rock sequence of Triassic to Cretaceous, whose thickness reaches 5000 m. An ophiolilic complex, described as the "inner Tauride ophiolitic complex nappe" by the former investigators, and whose emplacement in the region has been ascribed to Upper Lutetian, forms the boundary of the basin in south and west. The Neogene sequence, reaching a total thickness of 800 m. in the region, dominantly comprise alluvial fan, fluvial and lacustrine sediments. Alluvial and lacustrine sediments exhibit intervened stratigraphic relations laterally at the margins of the basin. Neogene sediments, which are distributed extensively in the region, have been deposited under the control of growthfaults. These faults, bordering the basin, have a general trend in the N, NE and NW directions, and exhibit parallel en echelon structural features. Structural elements in the study area and in near vicinity have developed under the influence of compressional and tensional tectonic regimes, that prevailed in different epochs. In Langian, due to the compressional tectonic regime that progressed in the N-S direction, many intersecting shear-faults developed in the NE and NW direction, which shaped the Isparta flexure, in addition to many folded and thrusled structures. In the period following the Langian compressional regime, Yalvaç Neogene basin opened by the transformation of previously formed strike-faults into normal-faults, due to tensional tectonics.

FACIES AND DEPOSITIONAL ENVIRONMENTS OF THE MIOCENE SEDIMENTARY SEQUENCE IN NORTH OF TORBALI, IZMIR

Ugur İNCİ**

ABSTRACT— A Late Miocene sedimentary sequence, over 900 m., crops out in the north-northeast trending graben type depression developed at the western margin (north of Torbalı) of the Bozdağ high. This sequence is represented with the several complete and incomplete sedimentary cycles which are mainly composed of, in ascending order, conglomerate, sandstone and algal limestone segments. According to the lithofacies analyses, the clastic rocks of this normal fault-boundered depression deposited in the alluvial fan and plain environmental conditions by rapid deposition of the sedimentary load of the gravel-sand dominated hyperconcentrated flood flows originated from the Nif Dağı and Bozdağ high. In consequence of these floods, the small, variable boundered, occasionally wavered and fringing with swamps, ephemeral freshwater lake environments formed characterizing with algal limestones.

Mineral Res. Expl. Bull., 112, 1 - 16, 1991

POSSIBLE PAN-AFRICAN METAVOLCANICS IN THE ÖDEMİŞ, SUBMASSIF OF THE MENDERES MASSIF, WESTERN TURKEY

Osman CANDAN* and Nejat KUN*

ABSTRACT. - Menderes massif located in the Western Anatolia, in Turkey, is made up of the old crystalline rocks. The last main metamorphism of this massif has been completed during Upper Paleocene - Lower Eocene. The general sequence of the study area which is situated in the Ödemiş submassif of the Menderes massif consists of, in ascending order, basal gneiss complex, blue augen gneiss, leptite (metavolcanic), schist and marble. This metamorphic sequence was cut by the post-metamorphic acidic and basic plutons and covered by the young volcanics. Leptites occuring between gneiss and schist units are the metamorphic equivalents of the dacitic and rhyolitic volcanics. These island arc volcanics have a calc-alkaline kindred. According to the age, geological position and chemical characteristics, these metavolcanics of the Ödemiş submassif may be correlated with the island arc volcanic bell widely exposed in the NE Africa and Arabian Peninsula, in relation to the late phases of the Pan-African orogenesis.

INTRODUCTION

Menderes massif consists of the old crystalline rocks which are exposed widely in Western Anatolia, in Turkey. The previous studies began with Phillippson (1911) and continued later by various investigators until today. The presence of some different rock types from the others such as gneiss, schist and phyllite in the Menderes massif was first noted by Schuiling (1962). It was determined by Kun (1983) that these rocks exposed in the Çine submassif of the Menderes massif were clearly originated from the old volcanic rocks and they were called as leptite by the same auther based on the similar chemical properties, with those of in Sweden.

In recent years, the relation between the volcanics of the Pan-African orogenesis exposed in NE Africa and Arabian Peninsula and the metavolcanics which show widespread distribution in the Menderes massif has been the subject of investigation by many investigators. In this paper, an attempt is made to solve the problem of the origin and geotectonic position of the leptites in the Ödemiş submassif of the Menderes massif in Turkey.

LITHOSTRATIGRAPHY

The study area is located in the Ödemiş submassif of the Menderes massif, in Western Anatolia in Turkey (Fig. 1 A-B). The generalized columnar section of this area can be given as follows: The lowest level of the rock succession consist of a basal gneiss complex made up of migmatite, augen, granitic and banded gneisses (Fig. 2). In these rocks which contain almandine-rich garnet, the feldspar porphyroblasts amount up to 7-8 cm in length. Through the microscobic studies, the general mineral assamblage of the gneisses which show widely cataclastic texture, was found as "Quartz-plagioclasc (oligoclase)-K. feldspar (orthoclase and microcline)-biotite-muscovite-garnet-tourmaline-zircon and apatite".

The blue augen gneisses which have been firstly pbserved in the Menderes massif, are found near the contacts of the leptites and basal gneisses as interlayers and lenses in both unit with different lengths. This kind of gneisses typified by the very large blue-violet K-feldspar porphyroblasts, show great similarity to the basal gneiss complex occuring at the bottom of the sequence in terms of mineralogical composition. But, by contrast with basal gneisses, sillimanite is accompanied to garnet in these rocks. The bluc-augen gneisses containing abundant relicts of leptite are appearently related to the volcanic origin.

The leptite which lies conformably on the gneisses, vary in thickness from 20-25 m to several kilometers. Some key minerals, such as sillimanite and kyanite, are found in these metavolcanics. The leptites are overlain by the schists with an

* Dokuz Eylül Üniversitesi, Jeoloji Mühendisliği Bölümü, İzmir-Turkey.

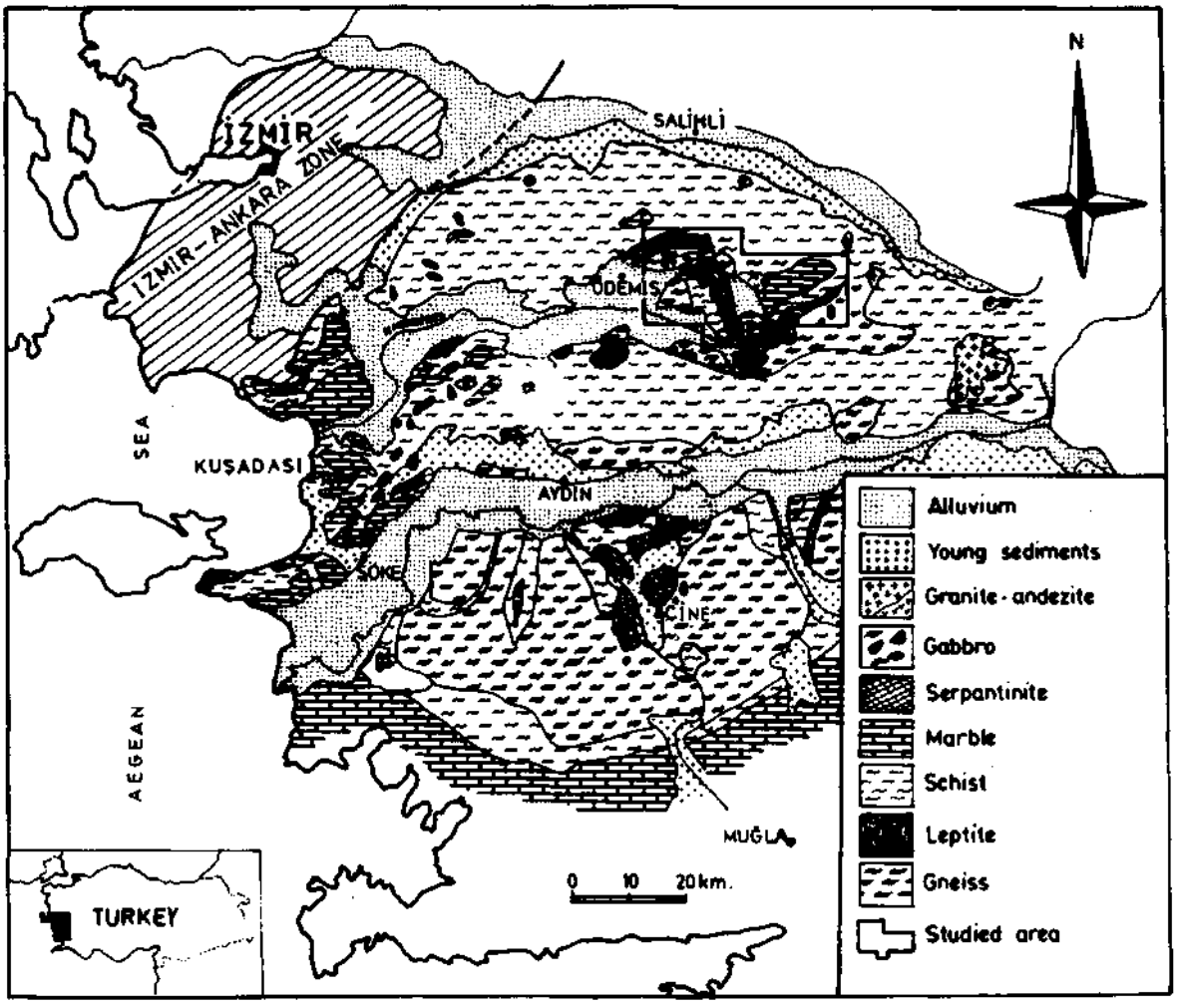

Fig. 1 A - Location map of the study area.

appearently conformable contact. The schist series starts with the kyanite-staurolite-gamet schist at the base and passes to the garnet-mica schists towards the upper level.

Phyllite, marble and muscovite-quartz schists occure as interlayers and lenses in this schist sequence with highly variable thicknesses. Coarse-grained kyanite-staurolite-gamet schists contain widely distributed kyanite-pegmatoid lenses which are parallel to the schistosity. This schist unit consist of Quartz-plagioclasc-kyanite-staurolite-garnet-biotite-muscovite-chlorite-rutil-apatite and zircon". Also, garnet-mica schists are mainly composed of "Quartz-plagioclase-biotite-muscovite-chlorite-gamet-apatite-tourmaline and zircon". The phyllites which are observed as interlayers and lenses show a number of different mineral paragenesis as follows:

Quartz-muscovite-garnet-chloritoid;

Quartz-muscovite-garnet-chloritoid-slaurolite;

Quartz-muscovite-gamet-staurolite;

Quartz-muscovite-garnet-staurolite-kyanite.

Fig. 1 B - Geological map of the study area.

The marble interlayers become dominant at the upper level of the metamorphic sequence and these rocks form thick calcerous series at the NE part of the study area.

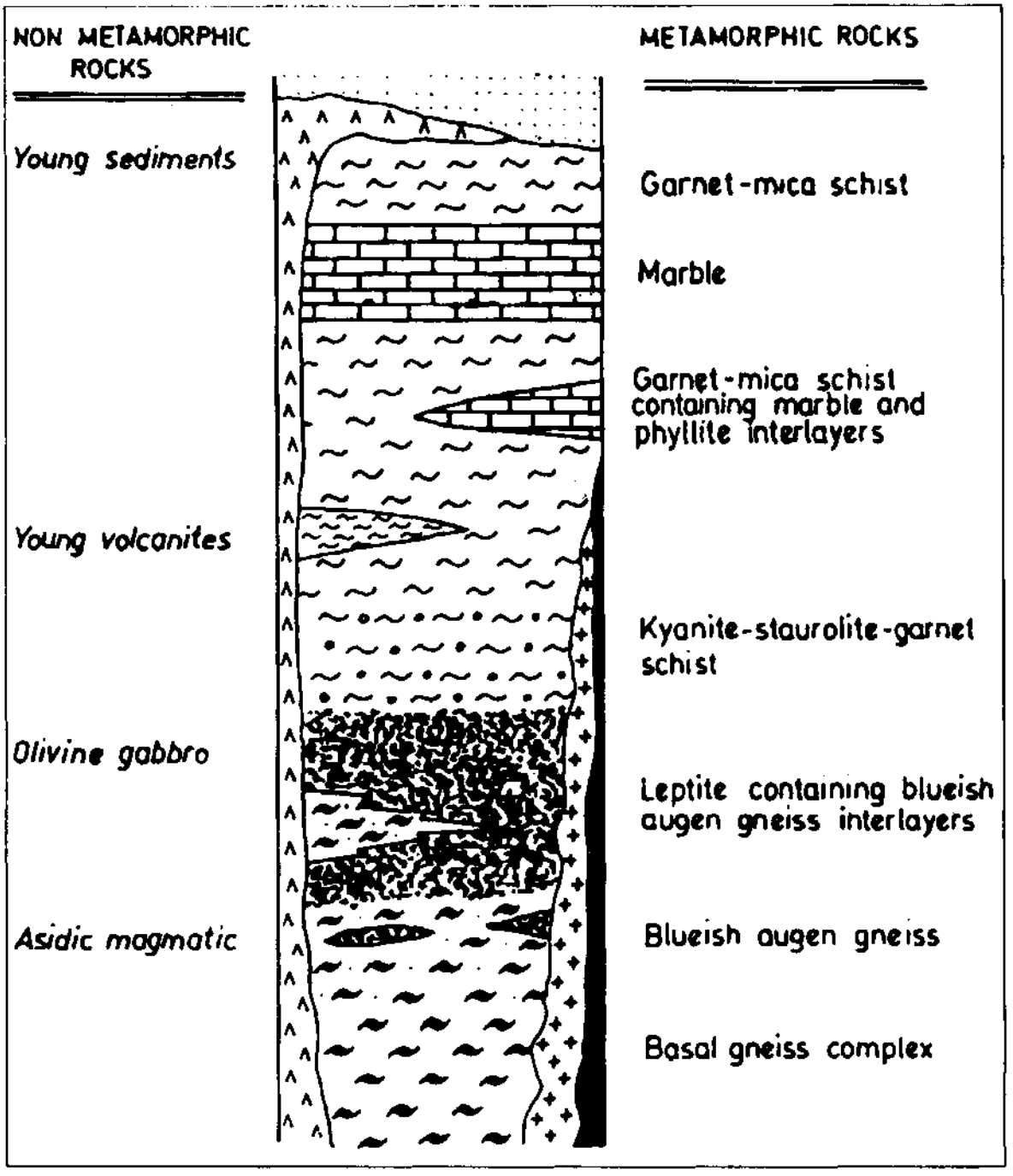

Fig. 2 - Generalized columnar section of the Ödemiş submassif.

All these metamorphic units were cut by the unmetamorphosed acidic and basic plutons and covered by the Neogene aged volcanic rocks. The acidic magmatitcs which arc of granitic and granodioritic composition, are exposed in gneisses and leplitcs as slocks with different sizes. The general mineral composition of these rocks were determined as

"Quartz+plagioclase+orthoclase+biotite+muscovite+apatite+zircon±sillimanite and ±gamet". The basic plutons, olivine gabbros, were observed as stocks with different sizes in the blue-augen gneisses, at the vicinity of Birgi town. The mineral composition of these unmetamorphosed basic plutons consists of "Plagioclase + orthopyroxene + clinopyroxene +olivine + biotite+apatite + zoisite + zircon and +garnet". The extrusive rocks which are the volcanic equivalents of these basic and acidic plutons are observed at two different parts of the area. According to their mineralogical and chemical composition, these volcanic rocks arc of andesite and basalt in composition. All the rock units exposed at the investigated area are unconformably covered by the Neogene aged unmetamorphosed sedimentary rocks.

PETROGRAPHY OF THE LEPTITES

Leptites show a widespread distribution in the Ödemiş submassif, the middle part of the Menderes massif. These rocks which occur between the basal gneiss and schist vary in thickness from 20-25 m to several kilometers. Purple, grayish and gray coloured leptites are hard, massive and generally badly schistozed rocks. These metavolcanites are often cut by the pegmatitic veins, ranging from mm to m in thickness. These pegmatitic veins arc composed of feldspar, quartz, muscovite and tourmaline. In the field, one of the characteristic features of the leptites is the presence of the old sills and dykes which exhibit hornfelsic texture and rich-in pyroxene and anorlhite (Kun and Candan, 1987). These gabbroic vein rocks were simullanously metamorphosed with the leptites.

The locally preserved old porphyritic texture can be observed in the leptilcs. This evidence clearly suggests that the origin of these rocks called as leptites in this paper, is volcanic. In these porphyric rocks which show a foliated andesitic appcarence, the old phenocrystals were oriented by the metamorphism (Fig. 3). These phcnocrystal relicts were filled by some light coloured minerals such as quartz, muscovite, feldspar, sillimanite, and gamet.

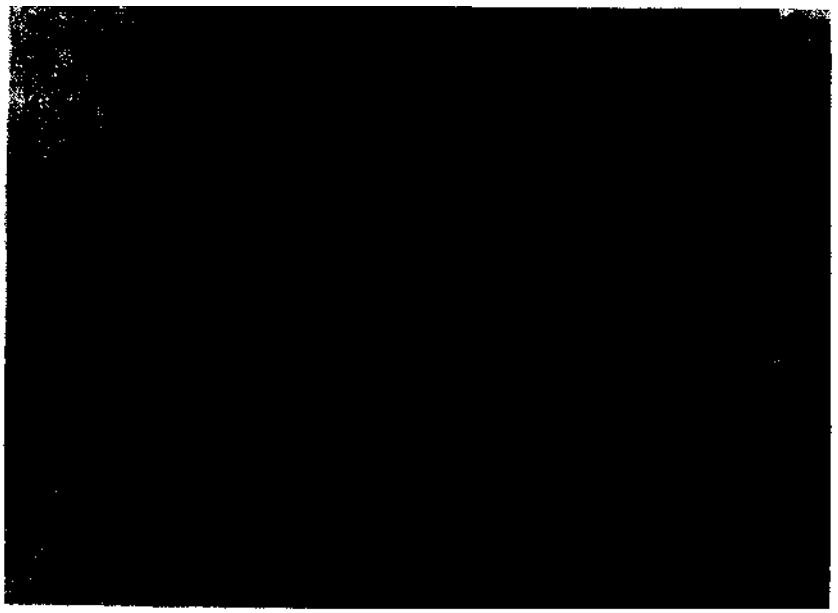

Fig. 3 - Photograph of the relict porphyritic texture of the primary volcanics observed in leptites.

The field observations show that leptiles occur as a gide horizon between the basal gneiss complex which were derived from graywackeys, and schists in the Menderes massifs But, because of the presence of the blue-augen gneisses most probably of volcanic origin like leptites the contact mapped between the basal gneiss complex and leptite, docs not correspond to the primary graywackey/volcanic rock boundary (Fig. 4).

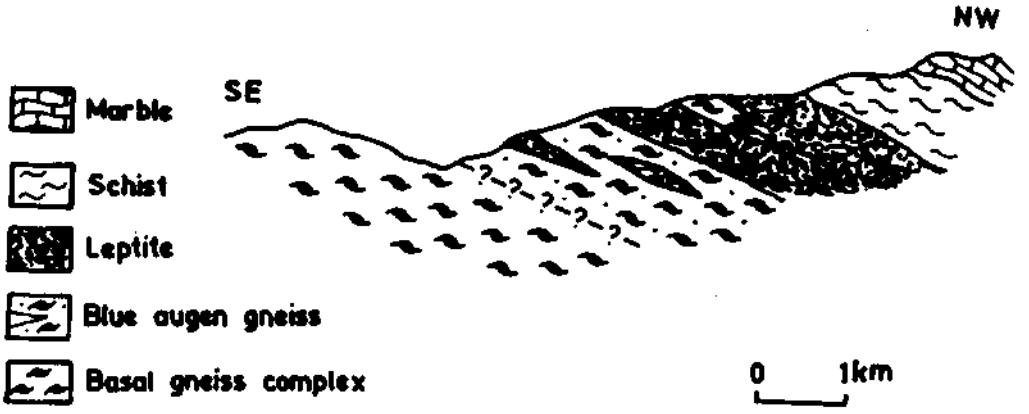

Fig. 4 - Cross-section showing the contact relation between blue augen gneiss and leptite.

From the petrographic studies, it has been observed that the leptites exhibit a typical fine-grained, nondirectional granoblastic and hornfelsic texture (Fig. 5). But some samples, especially those which are rich-in biotite, may show a poorly developed schistosity. The general mineral compositions of the leptites consist of "Quartz-plagioclase-orthoclase-garnet-biotite-muscovite-epidote-sillimanite-kyanite-tourmaline-zircon and apatite". The leptites can be divided into three major groups according to their macro and micro features: 1 - Garnet-biotite leptites; 2 - Sillimanite-kyanite leptites; 3 - Spotted-. leptites.

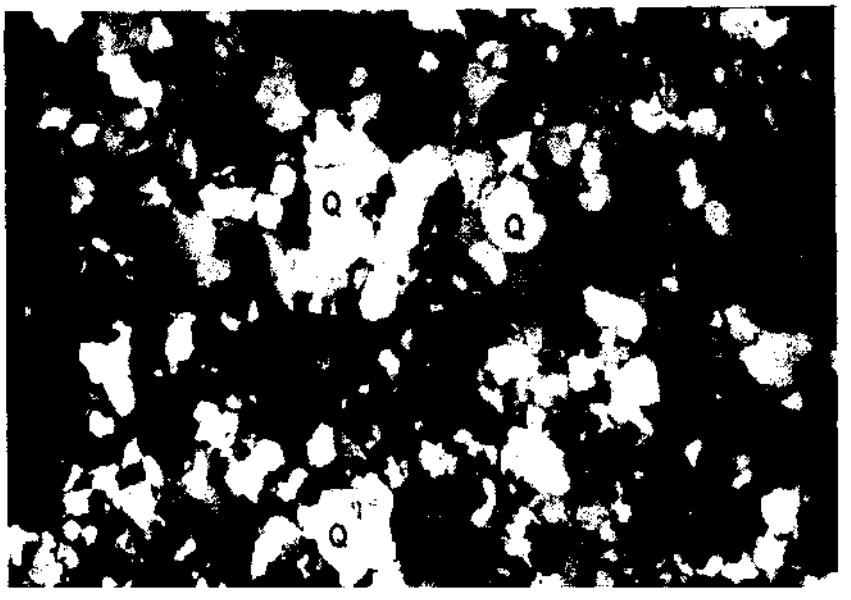

Fig. 5 - Photomicrograph showing the typical fine-grained, nondirectional hornfelstic texture in leptites. 2.5 X, crossed nicols. Q: Quartz, Plj: Plagioclase.

1 - Garnet-biotite leptites

The great majority of the leptites exposed in the study area belongs to this group. While the percentage of garnet reaches up to 35 % and biotite up to 40 %, muscovite is always present in the amounts of less than 5 % in these rocks. Garnet-biotite leptites which exhibit a poorly developed schistosity consist mainly of quartz, orthoclase, plagioclase, biotite, muscovite, garnet, epidote, zoisite, apatite, tourmaline and zircon.

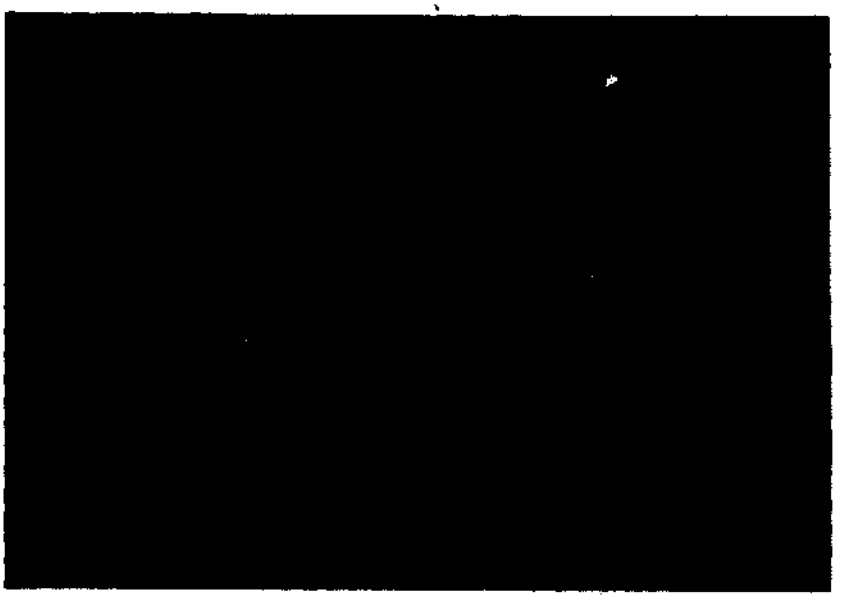

Fig. 6 - Sillimanite fibrolites occuring at the contacts of the feldspars. Sil: Sillimanite, 10 X, plane light.

2 - Sillimanite-kyanite leptites

This type of leptites closely resemble the garnet-biotite leptites. The distribution of the sillimanite-kyanite leptites in the investigated area may be only identified by the microscopic studies. With the increasing percentage of the sillimanite content, these rocks exhibit a harder and rougher appearence. The percentage of the, sillimanite ranges from 1 % to 15 % (Fig. 6). But, the kyanite content of these leptites does not exceed 3 %. The formation of the sillimanites can be divided into two groups by their textural evidences. 1) Sillimanites, which occur as fibrolites at the contacts of the feldspars, and 2) Sillimanilcs, which replace the garnet and biotite crystals (Fig. 7).

Fig. 7 - Sillimanite crystalls occuring by the replacement of the biotites. Sil: Sillimanite; Bio: Biotite; 10 X, plane light.

3 - Spotted leptites

These leptites, which were rarely observed can be easily recognized in the field by their white spots. These appearance are caused by the preserved relict porphiritic textures of the primary volcanic rocks, and are of great importance to clarify the parent rocks of the leptites. These spots were generally filled by the light coloured minerals such as quartz, feldspar and muscovite. In general, an euhedral garnet crystal is situated at the center of these voids and this core is rimmed by the sillimanite and biotite zones (Fig. 8). The general mineral compositions of the spotted leptites show a great similarity to the sillimanite-kyanite leptites and consist of "Quartz-orthoclase-plagioclase-muscovite-biotite-sillimanite-kyanite-gamet-zircon and apatite".

Fig. 8 - Photomicrograph of the white-spots in the leptites. An euhedral garnet crystall is situated at the center of these voids. Sil: Sillimanite; Gr: Garnet; 10 X, plane light.

CHEMISTRY OF THE LEPTITES

In general, the leptites exhibit more or less a homogeneous mineral composition. But, of course, the amount of garnet, biotite and sillimanite in the rocks affect the chemical composition of the leptites. The average contents of SiO2, Al2O3, FeO, CaO, MgO, Na2 and K_2O in the leptites can be given as 61-74 %, 11-18 %, 4-6 %, 0.7-2.6 %, 1-3 %, 1.64.3 % and 2-4.5 % respectively. TiO2 is always present in amounts of less than 1 % (Table 1). A comparision of the Sweden (Löfgren, 1979) leptites with those of the study area in terms of SiO2 contents is given in Table 2. The leptites from Sweden are divided into 6 different groups. But, the leptites in Ödemiş submassif of the Menderes massif show only 3 groups and don't contain the extreme acidic and basic groups.

The chemical analysis were plotted on several diagrams to find out the properties of the original volcanics of the leptites. In order to eliminate the influences of possible element migrations during the high grade metamorphism, in addition to the major oxides, the diagrams based on the trace elements were also used.

In the Na2O+K2O/SiO2 diagram proposed by Zanettin-(1984), the leptites are concentrated in rhyolite, dacite and andesite areas (Fig. 9). In Kistler and Evernden (1971), Winchester and Floyd (1977) diagrams based on the Rb vs Sr and SiO_2 % versus Zr/TiO2 respectively, all the examined metavolcanics plot in the fields of andesite, rhyodacite and rhyolite (Fig. 10 and11).

Table 1 - Comparation of the Sweden and Ödemiş submassif leptites in terms of SiO_2 contents

	Group 1 *% SiO_2* *50-55*	*Group 2* *% SiO_2* *55-60*	*Group 3* *% SiO_2* *60-65*	*Group 4* *% SiO_2* *65-70*	*Group 5* *% SiO_2* *70-75*	*Group 6* *% SiO_2* *75-80*
Leptites of Sweden						
SiO_2	53.66	57.45	62.82	67.20	72.64	77.28
Al_2O_3	18.74	16.49	15.92	14.67	13.06	12.00
TiO_2	.93	1.06	.59	.52	.26	16
Fe_{tot}	8.89	8.33	5.08	4.34	2.60	1.35
MgO	4.18	3.54	2.58	1.81	1.14	80
CaO	5.70	5.06	3.27	2.10	1.36	70
Na_2O	2.86	2.58	2.58	2.46	2.42	3.93
K_2O	3.36	2.93	3.96	4.94	4.90	2.97
Leptites of the Ödemiş submassif						
SiO_2			63.38	65.70	71.68	
Al_2O_3			15.27	15.01	13.09	
TiO_2			.88	.80	.73	
Fe_{tot}			5.40	4.77	3.92	
MgO			2.58	1.98	1.67	
CaO			1.55	1.54	1.33	
Na_2O			3.19	3.02	3.24	
K_2O			3.34	3.11	2.62	

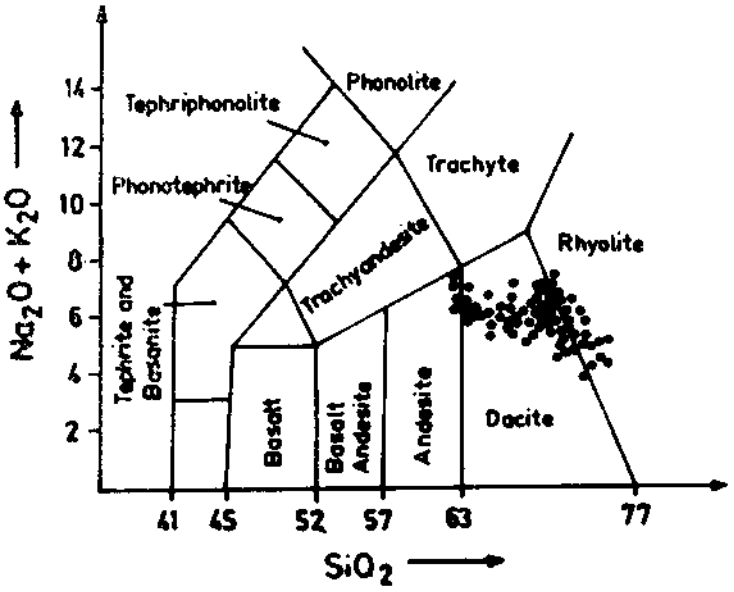

Fig. 9- $Na_2O + K_2O$ versus SiO_2 diagram after Zanettin (1984).

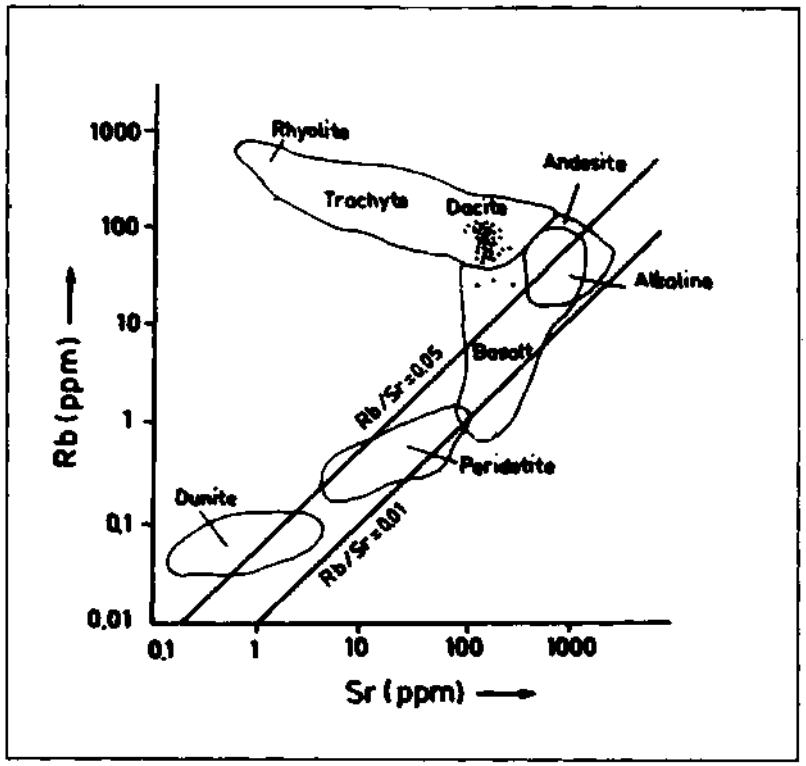

Fig. 10 - Rb (ppm) - Sr (ppm) variation diagram after Kistler and Evernden (1971).

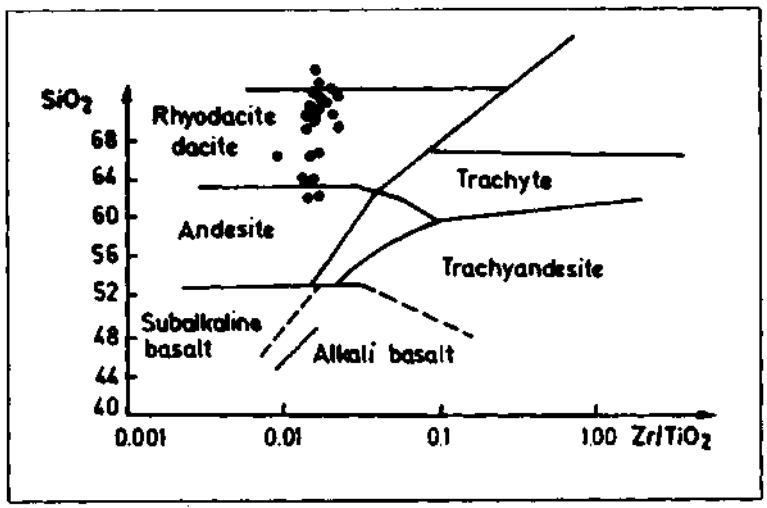

Fig. 11 - SiO_2 (Wt %) vs Zr (ppm) / TiO_2 (Wt %) diagram after Winchester and Floyd (1977).

In order to determine the kindred of the primary volcanics, several diagrams based on major oxides are used. In the Rittmann (1962) diagram, all the leptites are accumulated in the field of calc-alkaline series (Fig. 12). In another diagram using the same oxides, the great majority of the rocks are concentrated in the calc-alkalinc series but only a few samples extended into the tholeiitic area (Fig. 13). In the Miyashiro (1975) diagram, where FeO*/MgO versus SiO_2 is plotted the samples fall again in the calc-alkaline field (Fig. 14).

Table 2- Chemical analyses of the metavolcanics (leptites) in Ödemiş submassif of the Menderes Masif

	O-305	Ş-206/A	Ş-51	Ş-178	O-202/A	O-11B	O-226	O-316/A	O-292	O-303/C
SiO_2	69.85	71.28	69.24	65.69	70.10	64.01	72.08	71.69	71.57	68.60
Al_2O_3	14.23	13.36	14.60	16.26	13.74	16.88	13.16	13.96	14.14	15.00
TiO_2	.69	.65	.65	.76	.81	.78	.63	.60	.54	.68
Fe_2O_3	1.59	2.02	1.87	4.52	2.25	3.37	.99	3.90	1.54	2.79
FeO	2.78	1.96	2.54	1.52	2.17	2.54	2.70	.00	1.90	1.96
MnO	05	.06	.07	.07	.05	.08	.06	.04	.06	.05
MgO	1.86	1.43	1.78	2.61	1.58	2.54	1.46	1.36	1.35	1.91
CaO	1.09	1.44	1.57	.70	.95	.97	1.16	.76	.98	.83
Na_2O	2.32	2.79	3.63	1.69	2.74	2.33	3.35	2.40	4.07	3.02
K_2O	3.18	3.36	3.08	4.07	3.08	3.84	2.31	2.60	2.20	3.11
P_2O_5	14	18	18	.16	.17	.20	.12	.12	.18	.17
H_2O	1.36	1.36	93	.95	1.37	1.92	.85	2.02	.84	1.53
Total	**99.14**	**99.89**	**100.14**	**99.00**	**99.01**	**99.46**	**98.96**	**99.45**	**99.37**	**99.65**
Zn	73	50	0	128	60	125	51	52	48	70
Ni	61	54	56	40	47	66	45	57	43	49
Cu	3	3	5	24	7	13	6	12	15	14
Cr	120	124	114	133	152	144	125	120	104	125
V	93	86	89	106	100	115	89	82	67	90
Zr	193	238	183	186	337	171	224	206	183	205
Y	23	22	23	24	25	27	21	23	19	21
Sr	192	196	222	131	209	155	258	208	231	201
Rb	118	88	97	133	111	124	78	89	107	102
Hf	8	8	6	8	9	6	10	6	7	8

	A-39	A-18/A	Ş-209/B	G-22	O-203/A	O-26B	G-40	480/B
SiO_2	70.37	71.58	69.12	66.90	70.40	69.25	64.82	67.73
Al_2O_3	15.06	13.65	14.64	16.01	13.83	14.14	16.63	14.40
TiO_2	.67	.78	1.01	.72	.84	.70	.84	.70
Fe_2O_3	3.64	5.03	5.16	6.37	4.78	5.30	6.75	5.18
MgO	.96	1.43	1.50	1.76	1.43	1.54	1.91	2.75
CaO	1.87	1.72	2.23	1.04	2.61	2.26	.89	1.64
Na_2O	3.30	3.75	3.53	2.12	4.00	3.59	2.21	4.36
K_2O	4.33	2.33	2.51	3.76	2.17	2.82	4.16	2.33
K.K.	.24	.37	.28	1.19	.22	.38	1.90	.72
Total	**100.44**	**100.64**	**99.98**	**99.87**	**100.28**	**99.98**	**100.11**	**99.96**
Ba	653.3	305.0	921.9	637.0	468.8	510.4	694.9	281.5
Nb	8.9	10.5	15.5	19.2	14.9	11.6	13.6	13.6
Zr	128.0	191.6	122.6	154.9	139.1	125.6	130.4	156.9
Y	19.7	13.7	27.7	14.0	2.5	E	27.2	11.8
Sr	115.5	226.2	480.0	145.7	305.6	260.2	164.3	38.0
Rb	128.8	79.5	64.0	124.3	68.1	96.5	126.2	65.1

	448	431	486	465/A	Ş-24	Ş-22/D	463/A	Ş-101	Ş-44	Ş-65	A-27
SiO_2	71.66	74.23	71.94	70.99	65.87	71.06	63.30	71.33	72.67	69.02	62.96
Al_2O_3	12.24	11.71	12.91	13.18	16.76	13.93	16.94	14.12	13.28	14.50	16.76
TiO_2	66	.73	.75	.76	.88	.70	.86	.64	.71	.85	.88
Fe_2O_3	4.21	4.36	4.39	4.56	5.08	4.21	5.97	4.03	3.77	4.21	6.50
MgO	2.28	1.65	1.72	1.64	1.86	1.43	2.08	1.43	1.34	1.47	3.03
CaO	.99	.82	1.96	1.21	.70	.84	2.66	1.16	.97	2.27	2.36
Na_2O	3.47	2.76	3.34	2.90	2.54	2.91	4.22	3.57	3.17	4.17	3.20
K_2O	3.19	2.27	2.24	2.60	3.85	2.99	2.43	2.58	2.74	2.27	2.66
K.K.	85	1.22	.54	1.27	1.94	1.64	1.50	1.02	1.12	1.02	1.43
Total	**99.55**	**99.75**	**99.79**	**99.11**	**99.48**	**99.71**	**99.96**	**99.88**	**99.77**	**99.78**	**99.78**
Ba	563.9	423.2	451.6	598.3	618.3	707.6	468.2	594.2	609.6	485.6	1038.2
Nb	10.8	13.6	15.2	5.3	18.9	—	12.9	13.4	11.7	8.8	13.1
Zr	111.8	148.4	141.7	126.5	151.5	—	137.4	149.4	180.8	266.9	181.3
Y	14.1	20.7	6.6	19.4	27.7	—	13.9	21.4	17.1	14.0	12.5
Sr	179.0	191.9	182.0	180.2	181.3	—	279.2	247.7	246.5	34.9	272.6
Rb	81.6	77.4	73.0	79.7	104.1	—	94.5	80.7	81.2	77.2	55.9

	465/C	467	449	432/A	463/D	426	437/B	380	469	363	466/C
SiO_2	73.16	64.82	72.03	71.51	71.50	69.65	63.04	71.29	72.76	66.56	62.11
Al_2O_3	10.68	15.15	12.99	12.96	12.69	12.99	16.19	12.19	11.97	14.27	18.26
TiO_2	.98	.81	.59	.70	.72	.90	1.09	.84	.79	1.15	.85
Fe_2O_3	5.25	5.37	3.94	3.95	4.54	4.47	6.04	4.57	4.94	6.02	6.34
MgO	2.29	3.07	2.11	2.14	2.35	2.32	3.17	2.40	1.41	2.17	2.29
CaO	1.68	2.01	1.71	1.28	1.00	3.16	2.81	1.54	1.34	2.35	.95
Na_2O	2.99	4.31	3.52	4.22	3.11	3.55	3.99	3.50	2.94	3.08	1.66
K_2O	2.18	2.43	2.35	2.16	2.58	2.31	2.46	2.35	2.33	2.77	4.72
K.K.	.59	1.53	.85	.76	1.27	.85	.80	1.05	1.32	1.22	1.79
Total	**99.80**	**99.50**	**100.09**	**99.68**	**99.79**	**100.20**	**99.59**	**99.73**	**99.80**	**99.59**	**98.98**
Ba	655.6	363.6	426.3	413.3	820.0	442.3	639.4	530.7	528.2	604.0	704.1
Nb	12.3	13.6	12.9	14.9	11.6	13.6	—	10.1	12.8	5.8	13.0
Zr	282.1	116.3	117.1	104.9	131.3	161.5	—	190.6	214.1	188.0	120.1
Y	17.0	16.7	12.1	14.8	10.0	21.0	—	114.4	17.9	14.4	27.3
Sr	172.1	143.0	182.3	203.2	183.3	405.7	—	35.1	37.9	257.4	111.6
Rb	57.3	109.1	79.1	78.5	76.5	52.9	—	76.4	75.2	94.9	131.8

	482/B	391	Ş-59	432/B	447	O-316	463/B	Ş-102	Ş-167	467	476
SiO_2	66.61	71.79	67.27	69.50	68.06	65.40	61.62	62.96	66.94	64.15	66.55
Al_2O_3	15.74	12.14	16.05	13.82	14.00	17.04	18.26	16.94	15.12	17.58	15.65
TiO_2	.82	.86	.82	.81	.77	.77	.95	.91	.85	.80	.75
Fe_2O_3	6.26	5.32	5.18	4.75	5.53	5.53	5.97	6.41	5.09	6.65	6.15
MgO	2.16	1.65	1.74	1.76	1.86	1.79	2.30	2.47	1.54	2.95	3.28
CaO	1.21	1.18	.80	2.58	1.75	.80	1.88	.65	2.13	.29	.14
Na_2O	2.94	2.39	2.60	3.14	3.44	2.48	4.48	2.62	3.11	2.85	2.11
K_2O	3.30	2.71	3.86	2.86	2.75	3.42	3.07	4.50	3.24	3.16	3.59
MnO	.06	.07	04	.05	.05	.05	—	—	.07	.04	.03
K.K	1.13	1.26	1.49	.80	1.23	2.69	.83	.39	1.29	1.25	1.68
Total	**100.23**	**99.37**	**99.85**	**100.07**	**99.44**	**99.97**	**99.36**	**99.85**	**99.38**	**99.72**	**99.93**
Ba	952.8	583.4	624.9	715.9	536.0	599.0	857.2	710.6	539.09	—	699.6
Nb	11.8	13.7	12.0	—	10.7	14.1	14.3	15.6	11.6	—	8.3
Zr	76.6	240.0	133.0	—	103.2	122.7	123.9	125.1	172.0	—	72.5
Y	10.6	17.0	22.6	—	12.0	13.8	33.5	40.3	25.3	—	11.4
Sr	157.7	172.5	169.9	—	266.7	189.2	275.4	182.3	134.2	—	121.1
Rb	109.9	85.1	118.0	—	128.3	114.5	101.9	142.7	102.7	—	115.2

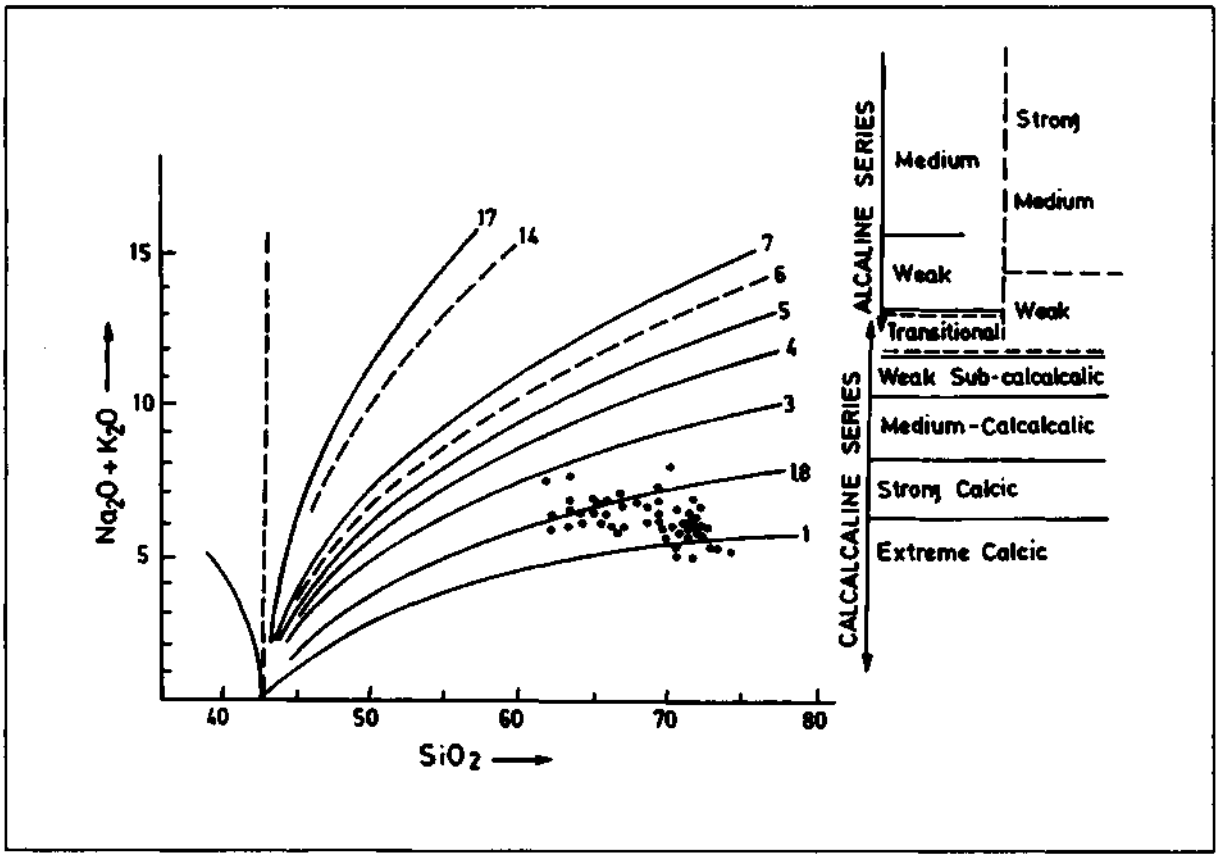

Fig. 12 - Place of the Ödemiş leptites on Rittmann (1962) diagram.

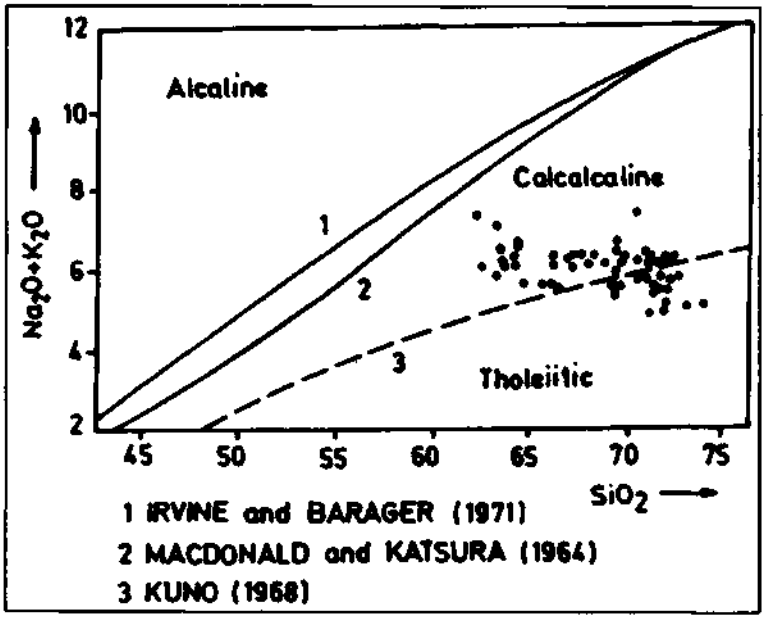

Fig. 13 - Place of the Ödemiş submassif leptites on alkali-silica diagram.

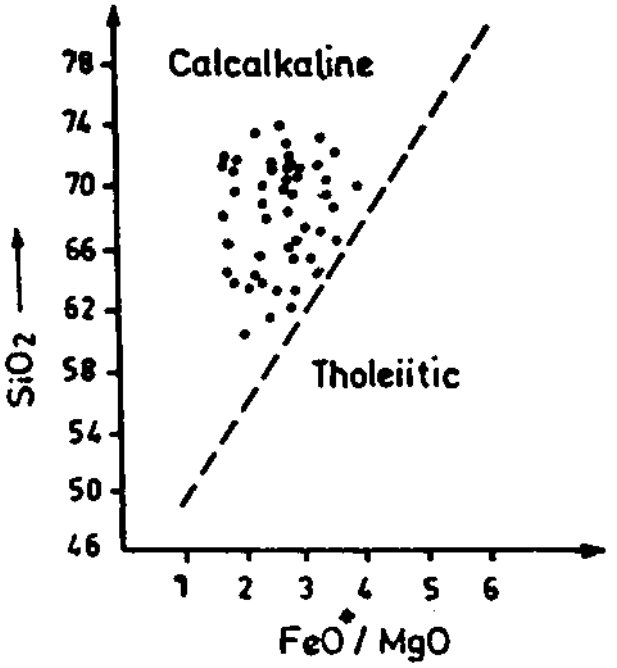

Fig. 14 - FeO* / MgO versus SiO_2 diagram after Miyashiro (1975).

In the log t versus log d diagram suggested by Gottini (1968), all the samples fall in the sialic origin (Fig. 15). There are several diagrams to explain the tectonic environment of the volcanics on the light of the plate tectonic theory. In the Morrison (1980) diagram, where K_2O are plotted against SiO_2 , all the samples lie within the calc-alkaline island arc fields (Fig. 16). In the TiO_2 versus FeO/MgO diagram advanced by Glassley (1974), the leptites of Ödemiş submassif are concentrated in the island arc field too (Fig. 17).

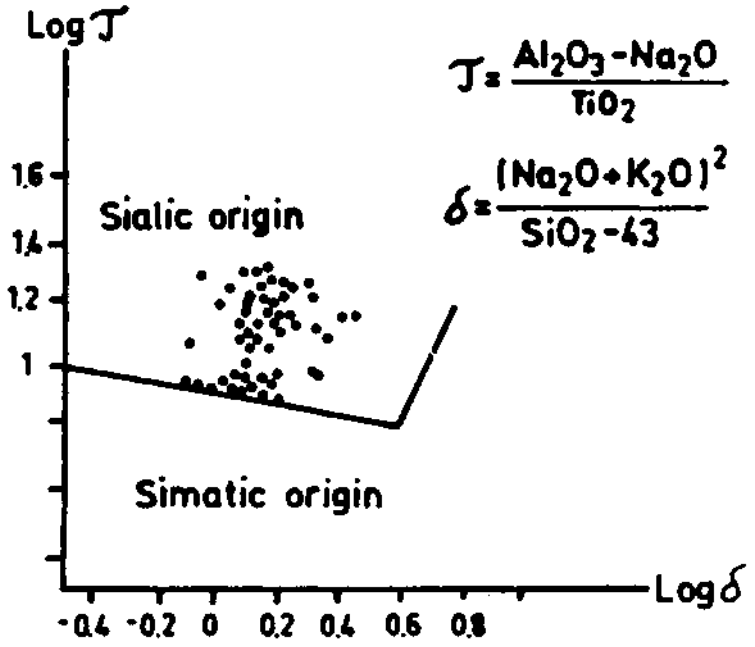

Fig. 15 - Log τ vs log δ diagram after Gottini (1969).

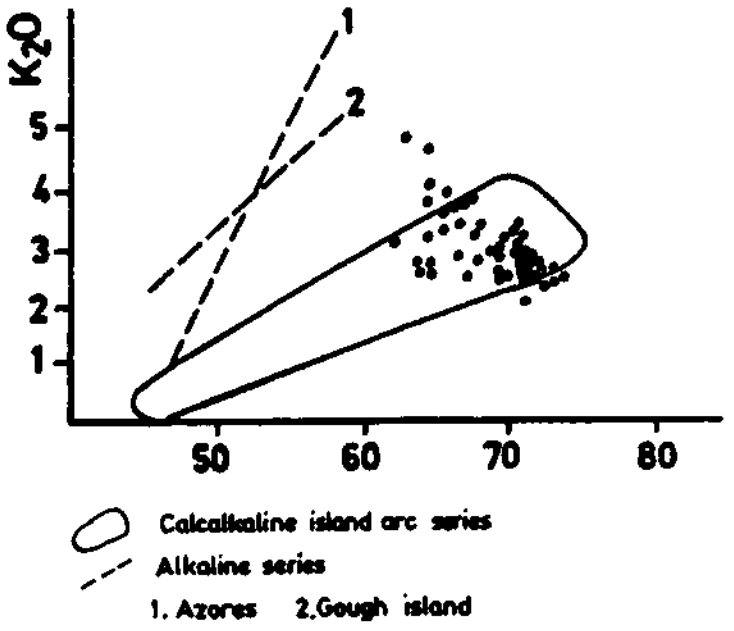

Fig. 16 - Variation diagram of K_2O contents with SiO_2 after Morrison (1980).

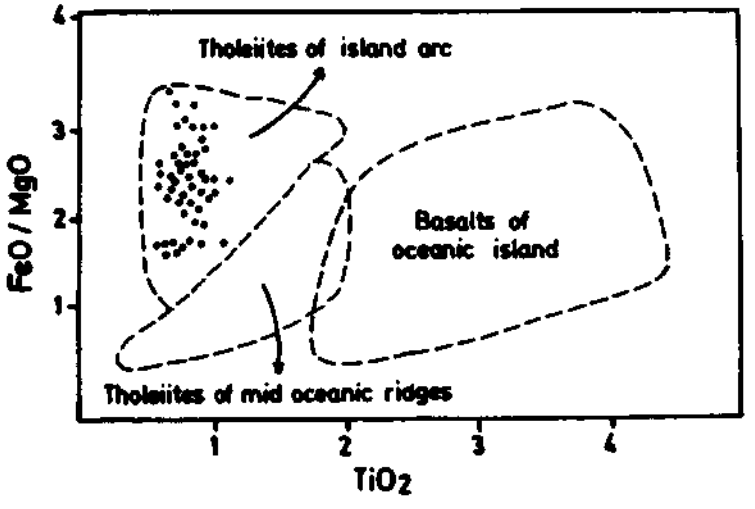

Fig. 17 - TiO_2 versus FeO* / MgO diagram after glassley (1974).

The Tixl0-^{2}/Zr/Yx3, Tixl0-^{2}/Zr/Sr:2 and Ti/Zr diagrams proposed by Pearce and Cann (1973) were applied to the leptites and it has been seen that the original rocks of the leptites were the calc-alkaline island are volcanics(Fig. 18). The analysis of the leptites were plotted on the TiO2 (%) versus Zr (ppm) diagram which was used by Gass (1982) to find out the tectonic environment of the metavolcanics belonging to the Upper Pan-African orogenesis (Fig. 19). It may be concluded from this diagram that the Menderes massif leptites show great similarity with the metavolcanics exposed at the NE Africa and SW Arabian Peninsula.

Finally, it can be suggested that the parent rocks of the leptites in the Ödemiş submassif of the Menderes massif are dacitic and rhyolitic volcanics. These island arc volcanics have sialic origin and dominant calc-alkaline kindred.

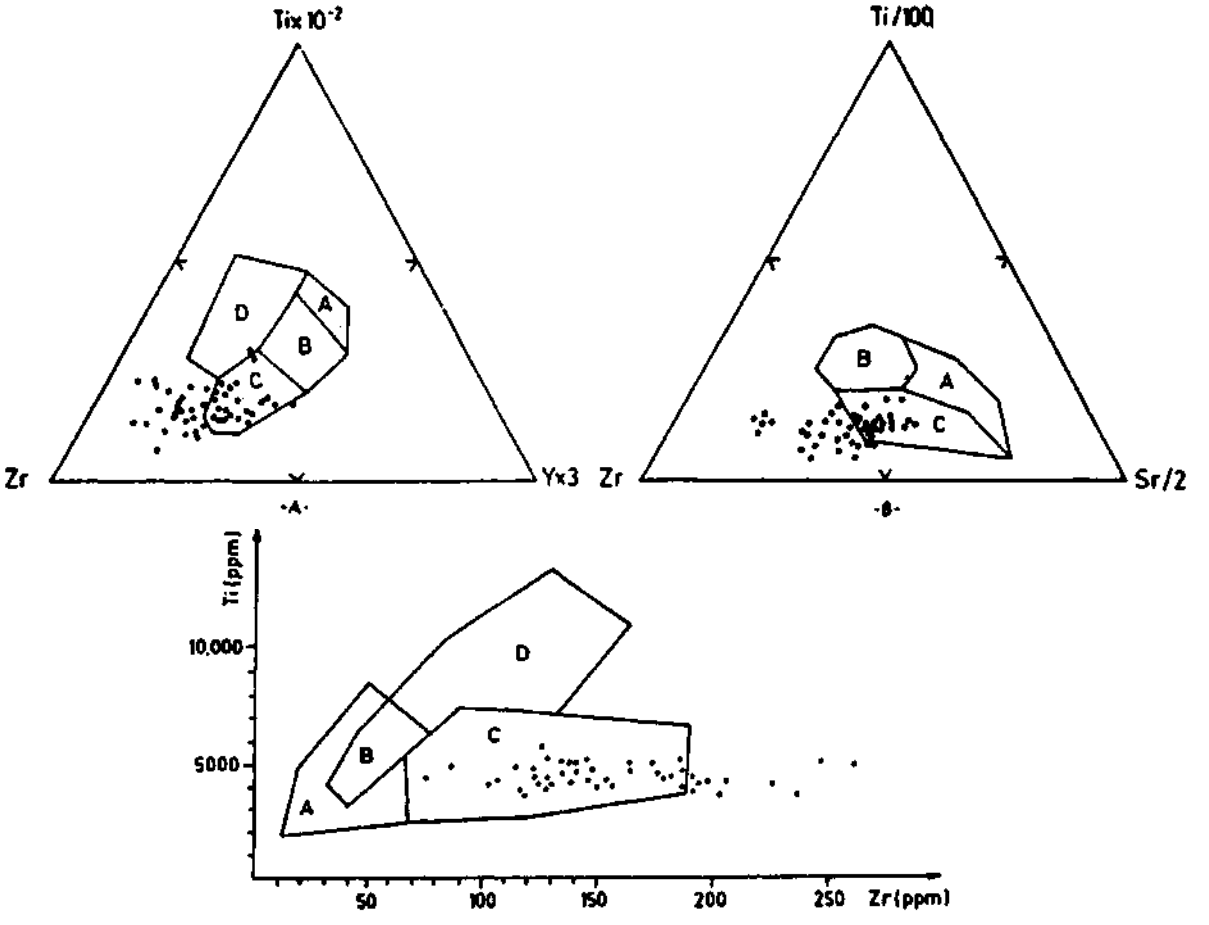

Fig. 18 - Ti x 10^{-2}/Zr/Y x 3, Ti: 100/Zr/Sr: 2 and Ti/Zr diagrams after Pearce and Cann (1973). A = A and B: Low K-Tholeiites, C and B: Calc-alkaline basalts, B: Ocean floor basalts, D: Within plate basalts. B = A: K-Poor tholeiites, B: Ocean floor basalts, C: Calc-alkaline basalts, C = D and B: Ocean floor basalts, A and B: Low K-Tholeiites, C and B: Calc-alkaline basalts.

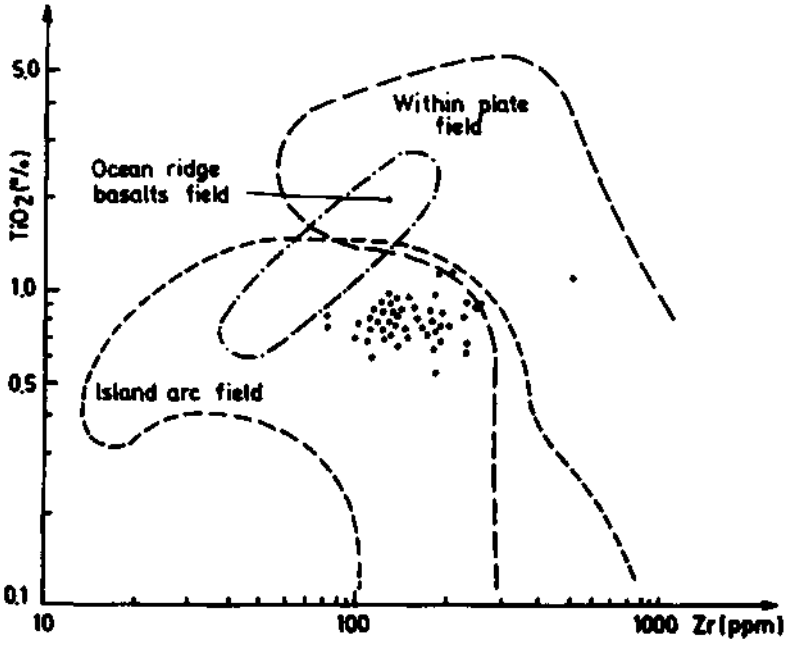

Fig. 19 - Place of the leptites of Ödemiş submassif on the TiO_2(%) / Zr (ppm) diagram.

DISCUSSION AND CONCLUSIONS

The general evolution of the Menderes massif and the position of the leptites (metavolcanics) which are situated at the Ödemiş submassif can be briefly summerized as fallows:

According to the recent studies in the Menderes massif, the initial sedimentation age of the gneisses occuring at the lower level of the metamorphic sequence is about 545-670 Ma old (Satır ve Friedrichsen, 1986). These sediments which were widely composed of graywackeys were subjected to a high grade metamorphism about 500 Ma ago and were cut by the tonalitic-granitic intrusions about 470 Ma ago (Satir and Friedrichsen, 1986). In most places, these gneissic basement was covered by the primary volcanic rocks of the leptits which were the surface equivalents of these post-metamorphic acidic plutons (Kun and Candan, 1987; Dora et al., 1988). These volcanics, rhyolite and dacite in-composition, are the initial rocks of the leptites. In Ordovician, the sedimentation was started in the region and until the Paleocene, sedimentary series which was composed of the flysh type sediments and platform type limestones were deposited on these volcanics (Dürr 1975; Çağlayan et al., 1980; Konak et al., 1987; Dora et al., 1989). The last main metamorphism which was affected the Menderes massif has occured in Upper Paleocene-Lower Eocene time (Dürr, 1975; Dürr et al., 1978; Şengör et al., 1984; Kun and Candan, 1987; Andreissen et al., 1979). The leptites in Ödemiş submassif which are of acidic in-composition were formed by this high grade metamorphism (Kun and Candan, 1987).

In recent years, it has been claimed that the Menderes massif is part of the Pan-African continental crust exposed in NE Africa and Arabian Peninsula (Şengör et al., 1984; Dora et al., 1988). According to Gass (1982), the Upper Pan-African orogenesis in these regions is especially characterized by the silicarich magmatic activity and acidic volcanics which vary in composition from andesite to rhyolite. These island arc type volcanic rocks have a calc-alkaline kindred.

It follows that the leptites (metavolcanics) exposed in the Ödemiş submassif of the Menderes massif shows a great similarity with the Upper Pan-African volcanics in NE Africa in terms of chemical composition and geotectonic position. It may be suggested by these chemical and geological evidences that the leptites of the Ödemiş submassif represent the North-western extension of the island are volcanic belt widely occurring in NE Africa and Arabian Peninsula, in relation to the late phases of the Pan-African orogenesis.

ACKNOWLEDGEMENTS

This work was supported by TÜBİTAK (TBAG-688). We also thank Mualla Gürle for considerable drafting assistance.

Manuscript received February 26,1990

REFERENCES

Andriessen, P.A.; Boerlrijk, N.A.I.M.; Hebeda, E.H.; Priem, H.N.A.; Verdunman, E.A. Th. and Verschure, R.H., 1979, Dating the events of metamorphism and granitic magmatism in the Alpine Orogen of Naxos (Cyclades, Greece): Contrub. Mineral. Petrol., 69, 215-225.

Çağlayan, M.A.; Öztürk, E.M.; Öztürk, Z.; Sav, H. and Akat, U., 1980, Menderes Masifi güney kanadına ait bulgular ve yapısal yorum: Jeo. Müh. Der., 9-17.

Dora, O. Ö.; Kun, N. and Candan, O., 1988, Metavolcanics (leptite) in the Menderes Massif: A possible paleoarc volcanism: ODTÜ Melih Tokay Sempozyumu Bull., (in print).

——— ;———and———, 1989, Menderes Masifi'nin metamorfik tarihçesi ve jeotektonik konumu: Ç.Ü. Ahmet Acar Jeoloji Sempozyumu, Bildiri Özetleri Kitapçığı, p. 5.

Dürr S., 1975, Über alter und geotektonisch stellung des Menderes Kristallins/SW - Anatolien und seine sequivalente in dermittleren Aegaeis: Marburg/Lahn, 107 p.

Dürr, S.; Alther, R.; Keller, J.; Okrusch, M. and Seidel, E., 1978, Alps, Apennines, Hellenides: Inter-Union Commission on Geodyrmnics Scientific Report No: 38, p. 454-477.

Gass, G., 1982, Upper Proterozoic (Pan African) calc-alkaline magmatism in north-eastern African and Arabia: In andesite, cd. Thorpe, R.S., John Willay and Sons.

Glassley, W., 1974, Geochemistry and tectonics of the Crescent volcanic rocks, Olympic peninsula: Geol. Soc. Amer. Bull., 85, 785-794, Washington.

Goltini, V., 1968, The TiO2 frequency in volcanic rocks: Geol. Rdsch., 168 pp.

Kistler, R.W. and Evemden, J.F., 1971, Sierra Nevada Plutonics cycle: Part I., origin of composite granitic batholits: Geol. Soc. Amer. Bull., 82, 853-868.

Konak, N.; Akdeniz, N. and Öztürk, E.M., 1987, Geology of the south of Menderes Massif: IGCP Project No. 5, 42-53, Turkey.

Kun, N., 1983, Cine dolayının petrografisi ve Menderes Masifinin güney kesimine ait petrolojik bulgular: Doktora tezi, DEÜ, İzmir.

———and Candan, O., 1987, Ödemiş Asmasifindeki leptitlerin dağılımı, konumları ve oluşum koşulları: TBAG-688 number of project, 133 P.

———and———, 1988, Menderes Masifindeki Erken Paleozoik yaşlı bazik damar kayaları: Hacettepe Üniversitesi Yerbilimleri Derg. (in print).

Löfgren, C., 1979, Do leptites represent Precambrian island arc rocks: Lithos, 12, 159-165.

Miyashiro, A., 1975, Volcanic rock series and tectonic setting: In annual rewiev of earth and planetary Science, 3, 51-269.

Morrison, G. W., 1980, Characteristics and tectonic setting of the shoshonite rocks association: Lithos, 13, 97-108.

Pearce, J.A. and Cann, J.R., 1973, Tectonic setting of basic volcanic rocks determined using trace clement analysis: Earth planet, Sci. Lett 19, 290-300.

Phillippson, A., 1911, Reisen und forschungen im Westlichen Kleinasien: Petermanns Mitt Erganzonpsheft, 172, Gotha.

Rittmann, A., 1962, Volcanoues and their activity: John Wiley and Sons, Newyork, London, 305 pp.

Satır, M. and Friedrichsen, H., 1986, The origin and evolution of the Menderes Massif, W-Turkey: A rubidium/strontium and oxygen isotope study, Geol. Rundschaus 75/3, 703-714.

Schuiling, R.D., 1962, Türkiye'nin güneybatısındaki Menderes migmatit kompleksinin petrolojisi, yaşı ve yapısı hakkında: MTA Bull. 58, 71-84, Ankara.

Şengör, M.C.; Saur, M. and Akkök, R., 1984, Timing of tectonic events in the Menderes Massif, Western Turkey: Implication for tectonic evolution and evidence for Pan-African basement in Turkey: Tectonics, Vol. 3, no. 7, 693-707.

Winchester, J.A. and Floyd, P.A., 1977, Geochemical discrimination products using immobile elements: Chem. Geol. 20, 325-343.

Zanettin, B., 1984, Proposed new chemical classification of volcanic rocks: Episodes, 714, 19-20.

Mineral Res. Expl. Bull., 112, 17 - 38. 1991

KİSECİK (HATAY) HYDROTHERMAL GOLD VEINS

Ahmet ÇAĞATAY *; İ.Sönmez SAYILI **; Yavuz ULUTÜRK * and M.Ziya ATEŞ *

ABSTRACT .- Solutions, forming Kisecik gold veins, were derived by amphibole bearing quartz-diorite which intruded into the metadiabascs. The solutions, placed along the various fractures with different strikes and dips developed in metadiabase due to intrusion of quartz-diorite brought about the formation of vein type mineralization. Besides the vein type of mineralization, contact metamorphism and hydrothermal alteration decreasing downward in intensity developed along the contact of metadiabase with amphibole bearing quartz-diorite. Veins forming Kisecik gold deposits are seperated into two different groups; as "Kızıltepe and similar veins" and "Deliklikaya Tepe and similar veins". The former is rich in gold content with greater variety of ore minerals. The main ore minerals of this vein are arsenopyrite, pyritc, chalcopyrite, sphalerite, marcasite, loellingite, pyrotite, valleriite, cubanite, native gold, tcllurobismuthite, tellurobismuthite + hessite solid solution mineral, galenite, cinnabar, neodigenite, hematite, magnetite, rutile, anatase, sphene, chromite, ilmenite, tenorite, chalcocite, covellite, limonite, malachite, azurite, siderite, ankerite, scorodite and copper vitriol. Gangue minerals are quartz, chlorite, calcite, dolomite, clay minerals, muscovite and sericite. The ore minerals of Deliklikaya Tepe and similar veins are arsenopyrite, pyrite, sphalerite, marcasite, valleriite, pyrotite, galenite, hematite, rutile, anatase, chromite, sphene, tenorite, chalcocite, covellite, malachite, azurite, limonite, scorodite and copper vitriol. Gangue minerals of these veins are similar to those of Kızıltepe and similar veins, only with higher amount. Chalcopyrite of Kisecik mineralization bear exsolution starlets of sphalerite and show oleander leaf like twinnings. Such kind of structures indicate relatively high temperature of ore formations. The presence of cubanile and valleriite as geologic thermometers among the ore minerals points out that mineralization occurred at temperatures between 250° and 350° C. Moreover, occurrence of mushketovite in the mineralizations also indicate part of mineralization is a contact type. According to the field observations and laboratory investigations, Kızıltepe and similar veins of Kisecik gold deposits can be considered as an occurence or a small deposit from the point of reserves and grades. On the other hand, Deliklikaya Tepe and similar veins contain poor gold mineralizations with non-economic amounts.

INTRODUCTION

Kisecik hydrolhermal gold veins are located at approximately 3 km. northwest of the districts of Kızıltepe and Deliklikaya Tepe near Kisecik village of Hatay (Fig. 1).

Detailed geological studies were implemented on Kızıldağ massif, which includes hydrothermal gold veins, by Blumcnthal (1938), Dubertret (1953), Dean and Krummenacher (1961), Atan (1969), Aslaner (1973), Çoğulu (1973, 1974), Delaloyc et al. (1979, 1980a, 1980b), Selçuk (1981) and Tekeli and Erendil (1986). However, only a few geologist have been interested in the known and probable ore deposits of the Kızıldağ massif. Erickson (1940) investigated the possible petroleum deposits of the area between Hatay and İskenderun. Wijkerslooth (1942) dealt primarily with chromite and gold mineralizations and other mineral resources of the massif. Molly (1955) and Alpan (1985) searched for the possible placer gold accumulations of the above mentioned area. Additionally, Alpan pointed out that the source of placer gold could be the Kisecik gold veins. Finally, Aydal (1989) carried out some studies on the Kisecik gold occurences.

The ancient adits, called "Roman Adits", were discovered during the studies of production adits derived in Kisecik gold veins. Whether these adits were driven during Roman Period, is not clear. Moreover, which of gold and copper was produced from the ore extracted from these adits is not entirely enlightened. According to Alpan (1985), the known oldest gold production from the area dates back to 1910. Later, during the invasion of the area by french army, gold was exploited from the Kisecik gold veins and from the placer gold accumulation of Miocene basal conglomerates of Akıllıçay district.

This paper presents the field observations of the authors on the Kisecik gold mineralizations and contains the mineralogical studies and analytical result of the samples, which were collected in the mineralized area during investigations.

The studies have been realized with the invitation of concessioner of the area, Rasim Yurttaş and the approval of the General Directorate of Mineral Research and Exploration (MTA). The field studies were conducted by Ahmet Çağatay, İ.Sönmez Sayılı, Yavuz Ulutürk and M.Ziya Ateş.

The main objective of the field studies was to collect enough representative samples for mineralogical and petro graphical investigations and to carry out chemical analyses on the Kisecik gold veins and their host rocks. Thus, detailed

* Maden Tetkik ve Arama Genel Müdürlüğü, Maden Etüt ve Arama Dairesi, Ankara-Turkey.
** Ankara Üniversitesi Fen Fakültesi, Jeoloji Mühendisliği Bölümü, Ankara-Turkey.

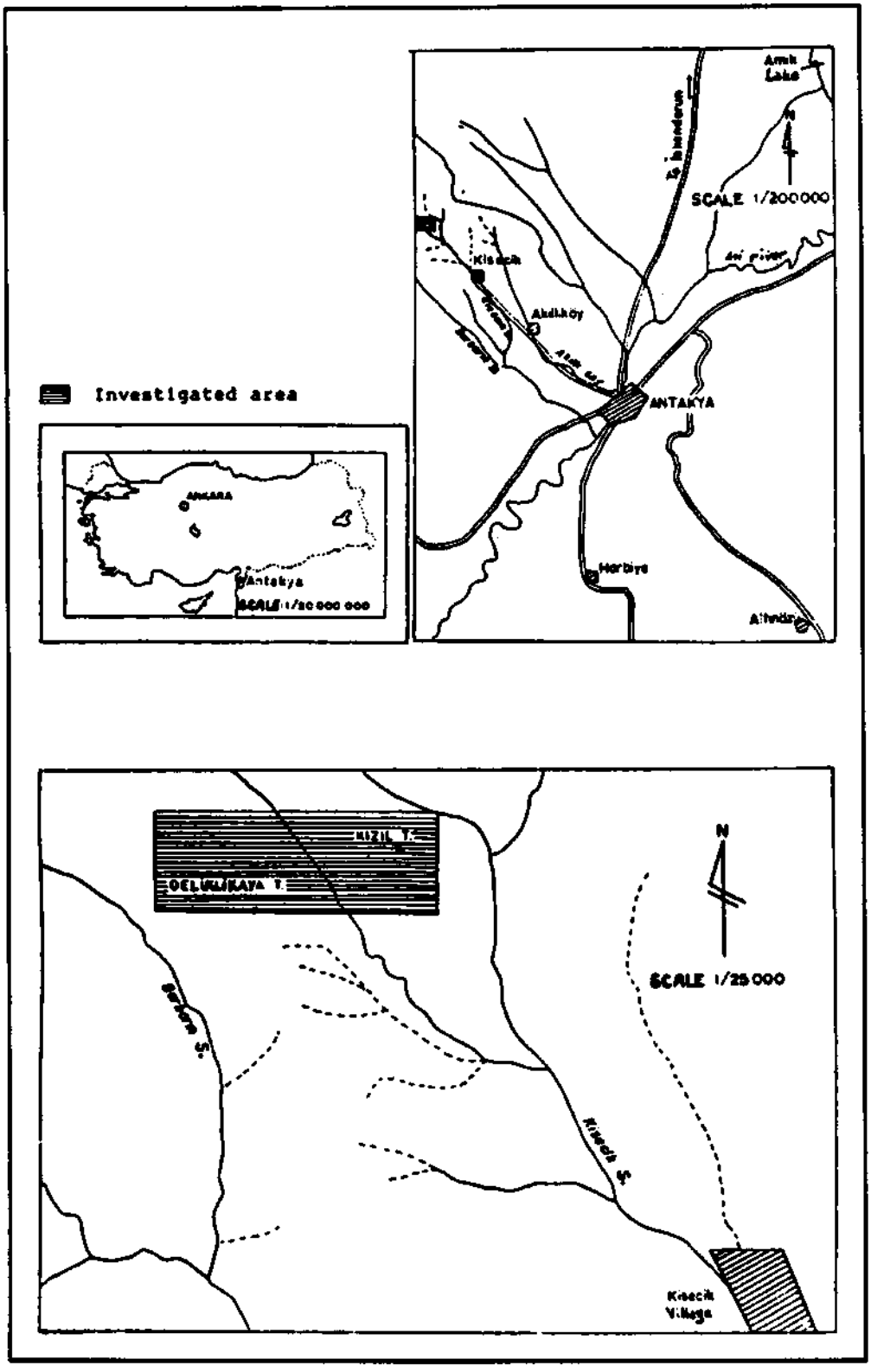

Fig. 1 - Location map of Kisecik (Hatay) hydrothermal gold veins.

mineralogical and petrographical investigations. X-ray diffraction studies and chemical analyses were done on these samples. A genetic model for the formation of Kisecik gold mineralizations was consequently tried to develop using the chemical data together with field observations.

GEOLOGY

Three different magmatic and several sedimentery rocks crop out mainly in the vicinity of the Kisecik gold occurrences (Fig. 2). Among the magmatic rocks, amphibole bearing quartz-diorite is the ore transporter or the mobilizer. Metadiabases host the ore veins. The third magmatic rock, comprised by generally rounded metagabbro, is observed in the amphibolc bearing quartz-dioritc and its contacts with metadiabases. Sedimentery rocks of Miocefie and Quaternary age occur around Kisecik village.

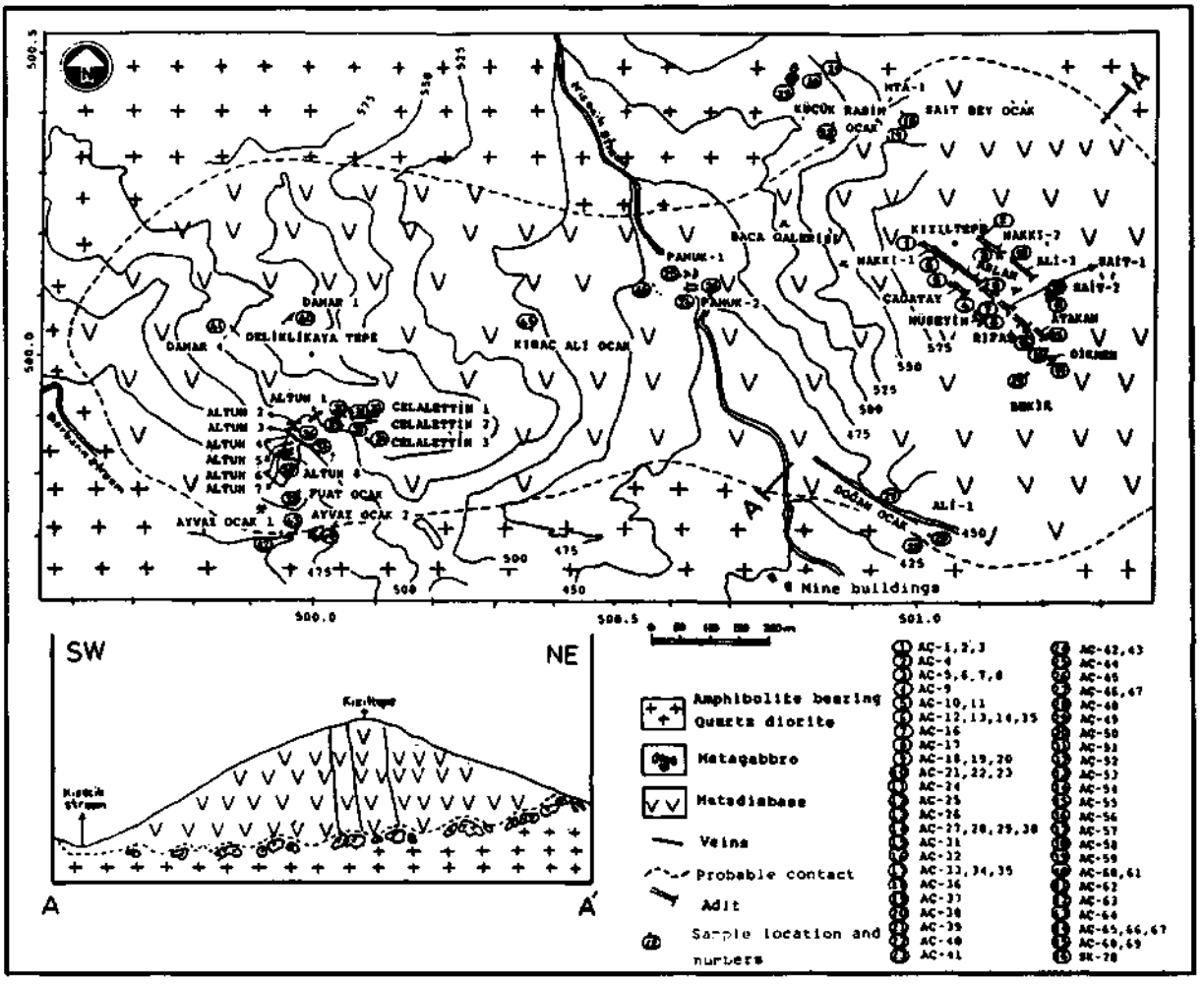

Fig. 2 - Simplified geologic and sample location map of Kisecik gold veins and their surroundings.

Amphibole bearing quartz-diorite

Amphibole bearing quartz-diorite, described as ore transporter or mobilizer rock for Kisecik gold occurrences, is exposed around the mineralizations and intrudes into metadiabases. This rock is intensively altered at the contact with metadiabases. Clinopyroxcnes of this rock are replaced by brownish hornblende and both mineral are later partly altered to actino-

lite-tremolite, biotite and chlorite (Plate I, fig. 1). The plagioclases of amphibole bearing quartz-diorite is saussuritized and partly occur as pseudomorphs after scapolite and sericite. The rock is cut across by mm-thick scapolite veinlets especially close to the contacts with metadiabases. The XRD analyses of the scapolite minerals showed that they are represented by dipyrc type. The hydrothermal effect decreases from the metadiabase contacts downward.

As a result of weathering, the plagioclases of amphibole-bearing quartz-diorite are highly argillized. The types of alteration minerals are defined as montmorillonite and clinozoisite by XRD. As a result of weathering, amphibole bearing quartz-diorite gained a loose structure and, hence, was casily\eroded. Preparation of thin sections and therefore, determination of plagioclase types was not possible due to pervasive argillization of these minerals in amphibole bearing quartz-diorite. Quartz crystals arc observed between altered plagioclases and amphibole minerals of the rock (Plate I, fig. 1). In addition, muscovite was rarely found in amphibole bearing quartz-diorite.

The rock, described as amphibole bearing quartz-diorite in this study, is considered within the "isotrop gabbro" unit by Tekeli and Erendil (1986). The authors point out that isotrop gabbro crops out in a large area and shows various mineral compositions, grain sizes and structures and textures. It is probably that the part of Kisecik gold veins in isotrop gabbro is suggested as a type of plagiogranite by Tekeli and Erendil (1986) representing the final differentiation solutions. Amphibole bearing quartz-diorite is an important rock unit since it forms a hot contact with older metadiabase by intruding in it and acts as an ore mobilizer. As a result of amphibole bearing quartz-diorite emplacement, this rock together with a more acidic rock and ore bearing quartz veins cut the metadiabases along its fractures.

Metadiabase

Gold bearing quartz and ore veins of Kisecik occur in metadiabases. Metadiabase forms two caplike hills with each approximately 600 meters in diameter over the amphibole bearing quartz-diorite in the districts of Kızıltepe and Deliklikaya Tepe of Kisecik gold veins. These metadiabase hills join with each other at Kisecik stream with a narrow ribbon of metadiabasc and, therefore occurs as double humps (Fig. 2). Northwest-southeast trending metadiabase ranges 1.8 to 2 km. in length along its long axis. The rest of the metadiabase, which crop out in a very small area, have already been eroded away.

Around the Kisecik gold veins, metadiabase occurs as a dyke complex composed of several parallel dykes. The dykes trending generally cast-west cut each other in a complex manner. The contact between metadiabase and amphibole bearing quartz-diorite is irregular. Metadiabase is found as enclaves in amphibole bearing quartz-diorite which replaces it.

As a result of amphibole bearing quartz-diorite intrusion into metadiabase, fractures locally parallel to each other but generally different in strikes and dips are formed in metadiabases. These fractures arc filled by quartz and ore minerals which arc transported by amphibole bearing quartz-diorites. Because it serves as host rock for ore veins, metadiabase required detailed investigations. For this reason, some samples collected from meladiabase enclaves, at various distances to the contact between amphibole bearing quartz-diorites and metadiabases and along the contact between ore veins and metadiabases are investigated.

Metadiabase dykes arc generally fine to medium grained and show intersertal textures. The texture is difficult to identifywhere locally obliterated by hydrothermal altcralions. Metadiabase is generally subjected to pervasive chloritization, silicification, carbonization and sericitization. Main constituents of metadiabase are plagioclases (labrador), clinopyroxenes (augite), magnetite and ilmeno-magnetite. Amphibolized clinopyroxenes are replaced by abundant chlorite and plagioclases by sericite, calcite and quartz Clinopyroxenes, amphiboles and plagioclases are observed as relicts in alteration minerals. Magnetite and ilmeno-magnetite are replaced by hematite in their different sections. Metadiabases also contain trace amount of ilmenite, rutile, anatase, sphene and chromite.

The invesligations carried oul on the samples taken from the contacts of amphibole bearing quartz-diorite and ore veins with metadiabases show that these samples do not comprise magnetite, ilmeno-magnetite and ilmenite. The lattice of rutile and rutile and anatas grains are locally replaced by sphene along their borders. The iron content of magnetite, ilmeno-magnetiteand ilmenite is leached from the environment (the rock) as a result of hydrothermal alteration and migrations at these specific pans of mcladiabascs. The remainder in the metadiabases are the titan bearing minerals. This iron is used mainly in the sulphide minerals of ore veins and in other iron bearing rock forming minerals.

Metadiabases are subjected to various kinds of hydrothermal alteration at its enclaves in amphibole bearing quartz-dioritcs and at the contact with the same rock, where intense epidotization, actinolitization-tremolitization and scarce prehnitizalion occur. Additionally, amphiboles are replaced by phlogopites (Plate I, fig.2) and plagioclases are saussuritized.

Metagabbro

Metagabbros are exposed especially close to the contact between amphibole bearing quartz-diorite and metadiabase in amphibole bearing quartz-diorite. They form rounded, clipsoidal or potato-like shapes around the Kisecik gold veins, and occur as thin veins cutting the amphibole bearing quartz-diorite in short distances. Elipsoidal metagabbros show well-developed exfoliation. The diameters of rounded metagabbros reach up to 1 to 1.5 m. Metagabbro occurrences, hard, strong and dark colored, arc easily recognizable in light colored, feldspar rich amphibole bearing quartz-diorite which is quite friable due to alteration.

Metagabbro contains medium grained clinopyroxenes, plagioclases and orthopyroxenes. Clinopyroxenes are amphibolized anduralitized(actinolitization-tremolization)as chessboard like (Plate I, fig.3) Orthopyroxenes, less common, are replaced by talc and serpentine along its cracks, borders and cleavages. Some phlogopite was also developed together with talc. Actinolite is partly altered to chlorite.

On the other hand, metagabbro comprises rare or trace amount of oxide and sulphide minerals. Magnetite, hematite (product ofmartitization),ilmeniteand chromite are oxide minerals. Magnetite is fine grained and idiomorph to sub idiomorph and along the borders is partly replaced by hematite. Ilmenites have small grains and lamellaes and are replaced by rutilc and sphene along its borders. Chromites occur as very fine, idiomorph grains in orthopyroxenes. Sulphide minerals are observed within or together with actinolite -tremolite and especially chlorite bearing parts of the rock. The sulphide minerals arc pyrite, chalcopyrite, millerite, pyrolite, sphalerite, chalcocite and covellite.

Fine pyrite crystals arc idiomorphic to subidiomorphic. Millerite can be identified in the stcatized and serpentinized parts of orthopyroxenes in metagabbro. Xenomorphic fine chalcopyrite crystals are replaced by chalcocite and covellite along its borders. Pyrotite occurs as intergrowths with chalcopyrite or inclusions in pyrites. Sphalerite is also fine grained and intergrowths with chalcopyrite.

Miocene deposits

Middle Miocene deposits exposed around Kisecik village rest partly either on Eocene deposits or on ophiolites by a basal conglomerate (Alpan, 1985). This unit is generally light colored but in some parts contains red to brown gravels. Most of the gravels comprised by partly or totaly serpentinized harzburgite. Conglomeratic levels grade up to sandstones, which arc in turn, overlain by sandy-marly limestones. Marls with sandstone lenses overlie the limestones and grade up into gypsifcrous levels.

Quaternary deposits

These deposits are characterized by old terraces, talus material and alluvials. There types of deposits are found at Kisecik stream. Both Miocene conglomerates and Quaternary deposits contain small amounts of detrital gold grains (Molly, 1961; Alpan. 1985).

GOLD VEINS

Primer gold deposits of Kisecik are composed of two different types of ore veins, named Kızıltepe and Deliklikaya Tepe veins. Kızıltepe ore veins arc usually enriched in ore minerals and have higher gold contents. In contrast, Deliklikaya Tepe veins are poor in ore minerals with relatively low gold contents . Therefore, the latter seems not have an economic importance.

At Kızıltepe district, the lower elevations of the most southern vein of Çağatay* and Dikmen mines and Doğan Ocak part look like Deliklikaya Tepe veins. On the other hand. Pamuk-1 and Pamuk-2 mines in Kisecik stream, Küçük Rasim and Kıraç Ali mines (veins) show some similarities to Kızıltepe veins in respect to their ore mineral contents (Fig.2).

Kızıltepe and similar veins

The most important, of the Kızıltepe veins is the one that along which are driven Hakkı-1. Aslan, Ali-1, Sait-1, Rıfat and Atakan Oğuz adits. The vein strikes N 70°W and dips 80-85° to the north. Another thin and short vein trends parallel to this vein and is located 50 m. to the north. in whicn-Hakkı-2. Ali-2 and Sait-2 adits were driven. South of this thin vein, each

The name of (Çağatay used here is taken from the mining engineer of Yurttaşlar Company Mr. Rıfat Çağatay.

50 m. away from it, two parallel short and thin veins are situated and Çağatay, Dikmen, Hüseyin and Bekir adits were driven in them. The vein located in opposite side of these veins in which Küçük Rasim mine was opened extends approximately in the same direction. The vein was intented to be intersected by MTA-1 drillhole but this aim failed. The thickness of the vein is 0.5-0.6 m. A 15 m. long adit was driven along its strike. Pamuk-1 Pamuk-2 veins, located in Kisecik stream, are close to each other and strike N 70°E and dip 75° to the NW. The thicknesses of these veins vary between 6.2 to 0.4 meters. They are rich in chlorite, calcite and pyrite.

Kıraç Ali mine is a short vein 3 to 4 m. in length with a.maximum thickness of 0.25 m. situated in a zone where faults crossing each other with different strikes. This vein extends in a large trench opened by a huge excavation activity. It strikes N 35°E and dips 50° to the NW. According to Aydal (1989) this vein, rich in hydrothermal quartz, chlorite and ore minerals, has the highest gold value among all other Kisecik gold veins. He reports that the gold content of this vein is 156 gr/t. The gold analysis of a sample taken from the same vein by the authors of this paper showed a very low gold grade (Table 1).

Table 1- Chemical analyses of Kızıltepe and Deliklikaya Tepe veins

Elements / *Veins*	*Sample no*	*Atomic Abs. and ICP*		*Optic spectrographic Semi-quantitative analyses*							
		Au grit	*Ag grit*	*% As*	*% Sb*	*% Cu*	*% Zn*	*% Ni*	*% Co*	*% Bi*	*% Te*
Deliklikaya T. Vein -4	AÇK-1	0.46	2.2	nd	nd	0.07	0.1	0.007	0.007	nd	nd
Deliklikaya T. Vein -4	AÇK-2	0.2	nd	nd	nd	0.03	nd	nd	nd	nd	nd
Deliklikaya T. Vein -4	AÇK-3*	0.53	nd	nd	nd	0.008	nd	nd	nd	nd	nd
Altun-2	AÇK-4	0.096	nd	nd	nd	0.004	nd	nd	nd	nd	nd
Damar-1**	AÇK-5	nd	nd	nd	nd	0.007	nd	nd	nd	nd	nd
Damar-1	AÇK-6	0.252	nd	nd	nd	0.007	nd	nd	nd	nd	nd
Altun-3	AÇK-7*	0.14	nd	nd	nd	0.009	nd	nd	nd	nd	nd
Fuat Ocak (Sil. zone)	AÇK-8	nd	nd	>1	nd	0.007	nd	nd	nd	nd	nd
Fuat Ocak** (Lim. zone)	AÇK-9	4.91	22.0	>1	nd	0.1	nd	nd	nd	nd	nd
Doğan Ocak (Alt. Dia.)	AÇK-15	nd	nd	nd	nd	0.007	nd	nd	nd	nd	nd
Doğan Ocak (Quartz ve.)	AÇK-16	0.38	nd	>1	nd	0.007	nd	nd	nd	nd	nd
Doğan Ocak** (Lim. zone)	AÇK-17	0.82	nd	1	nd	0.007	nd	nd	nd	nd	nd
Celalettin-2	AÇK-18	0.21	nd	nd	nd	0.007	nd	nd	nd	nd	nd
Ayvaz-2 (from pile)	AÇK-10*	1.16	3.1	0.25	nd	0.008	nd	nd	nd	nd	nd
Ayvaz-2 (adit entrance)	AÇK-11*	1.37	0.95	0.5	nd	0.015	nd	nd	0.004	nd	nd
Kıraç Ali Ocak	AÇK-14*	0.46	nd	nd	nd	0.008	nd	nd	nd	nd	nd
SK-2B Drill (45-46 m.)	AÇK-19*	nd	nd	nd	nd	nd	nd	nd	nd	nd	nd
Dedection Limits		0.040	0.5	0.4	0.02	0.0004	0.1	0.004	0.002	0.002	0.2

* Analyses are made in Canada and Saudi Arabia. The average of both analyses are shown in the table.

** The samples are collected from gold suspected places.

sil. = Silicified; lim. = Limonitized; dia. = diabase; ve. = vein; nd = not dedected

Kızıltepe ore veins show pinches and swells along their strikes and dips. Metadiabase fragments, completely silicificd, chloritized, sericitized, carbonatized and argillized occur in between mineralized stringers of the veins which locally splays out. Hydrothermal quartz and fault clays accompany to these minerals. Halloysite, illite and montmorillonite are determined as the clay minerals of fault using the XRD and DTA methods. Halloysite and illite are the most abundant clay minerals. The thicknesses of the veins which are generally very poor in ore minerals reach up to 1.5 to 2 m. The maximum total thickness of massive ore, which is important for gold, in this zone is 15 to 20 cm.

Mineralogy of Kızıltepe veins

The minerals of Kızıltepe gold bearing ore veins are arsenopyrite, pyrite, chalcopyrite, sphalerite, marcasite, pyrolite, valleriite, cubanite, native gold, tetradimite, galenite, cinnabar, neodigenite, chalcocite, covellite , malachite, azurite, siderite, ankerite, scorodite and copper vitriol. Gangue minerals arc represented by quartz chlorite, calcite, dolomite, clay minerals, muscovite, sericite and sphene.

Arsenopyrite. - This is by far the most abundant mineral in the investigated ore samples. Arsenopyrite is coarse grained and shows cataclastic structure. Pyrite, quartz, chalcopyrite and sphalerite fill cavities and cataclastic cracks of rhombic and prismatic arsenopyrite crystals. Dimension of the longest prismatic arsenopyrite grain is 3x1.2 mm. Parallel cleavages on some arsenopyrite grains arc locally clearly observed. Arsenopyrite in which pyrite and other mineral veinlets occur is the oldest sulphide mineral, and shows star (winnings. It also contains idiomorphic quartz and rutile, anatase, magnetite and hematiteinclusions.

The result of microprobe analyses, carried out on arsenopyrite crystals, arc given in Table 2. As it is easily seen from the table, arsenopyrite contains high amount of Co besides its main constituents of Fe, As and S. Those Co rich arsenopyrite crystals generally occur next to native gold or sometimes in the same part of the rock with it.

Table 2- Microprobe analyses of Kisecik arsenopyrites

Elements	*Points, % wt*				*Average*
	1	*2*	*3*	*4*	*% wt*
Fe	34.96	35.69	35.08	30.63	34.09
S	19.80	19.12	19.91	20.53	19.84
As	44.48	43.36	42.72	42.28	43.21
Sc	0.10	0.37	0.33	0.28	0.27
Cu	0.29	0.98	0.39	0.69	0.59
Co	0.04		0.30	4.44	1.20
Ni		-	-	0.25	0.06
Au		-	0.64	-	0.16
Total	99.67	99.52	99.37	99.10	99.42

Pyrite. - Pyrite is also one of the most abundant ore minerals observed. Pyrites arc characterized by different origins and ages. Primary ones arc idiomorphic to hipidiomorphic. Some of them arc corroded by later minerals and hence occur as skeletons. Primary pyrites up to 3 mm. are generally coarse grained. The interstices and cracks of the cataclastic pyrites are filled by chalcopyrite and quartz and are replaced by marcasite along their rims and cataclastic cracks. In addition, mostly xenomorphic and rarely vein type pyrites are also present as infillings in interstices and cracks of old quartz grains.

Some other main part of pyrite results as pscudomorphs alter parallel, lamellar hegzagonal pyrotite (Plate I, fig. 4). Such of pyrites increase in amount at the lower parts of the veins. They are generally observed as growths within or together with very fine grained marcasite. The pyrites, formed as pseudomorphs of hegzagonal, lamellar pyrotite show in some parts radial textures. According to Ramdohr (1975), pyrotite is replaced by a mid-product which later turns to pyrite.

A small amount of pyrite is observed as tiny gel structured forms in chalcopyrite. Beside this type of pyrite, a very young type envelopes sphalerite and chalcopyrite as thin layers and veinlets and sometimes cuts them.

Sphalerite, chalcopyrite, quartz and calcite grains intruded into pyrite and corroded rutile, anatase, sphene, magnetite, chlorite, quartz, hematite and arsenopyrite inclusions are observed in pyrites. In some idioblastic textured pyrites, quartz and chlorite are more abundant. The starlets of sphalerite in pyrites indicate that the pyrites replace chalcopyrite and include sphalerite exsolutions. Microprobe analyses were carried out on idiomorphic pyrites. It was determined that the pyrites comprise trace amounts of Co (0.09%), Ni (0.07%), As (0.08%), Sc (0.35%) and Cu (0.054%), in addition to their main Fe and S contents.

Chalcopyrite. - Chalcopyrite is also very abundant among the ore minerals. The amount of chalcopyrite increases especially towards the upper levels of ore veins. Most of them are allotriomorphic and intergrown crystal associations. A small amount of chalcopyrite occurs as exsolutions in sphalerites. In some places, excellent sphalerite exsolution starlets can be observed (Plate I, fig. 5). Ramdohr (1975) points out that sphalerite starlets in chalcopyrite arc very good indicators for high temperature formation of chalcopyrite.Chalcopyrites include inclusions of small pyrite, arsenopyrite, sphalerite, quartz, chlorite, hematite, magnetite, rutile, anatase and sphene grains. Chalcopyrites show oleander leaf-like or parallel lamellar twinning. According to Ramdohr (1975), this feature also stresses formation of chalcopyrite from high temperature hydrothermal solutions. In some places, weak cataclastic chalcopyrite replaces arsenopyrite and pyrite very clearly. Locally, chalcopyrite replaces also prismatic hegzagonal pyrotite lamellae as pseudomorphs and takes its shape and place. In some places, prismatic sphalerite grains extending in two different directions occur in chalcopyrite. Microprobe analyses of chalcopyrite show that it contains Cu (33.38%), Fe (30.84%), and S (34.42%) as main constituents and Zn (0.16%), Co (0.07%), Ni (0.02%), As (0.32%) and Sc (0.12%) in trace amounts.

Sphalerite. - Sphalerite is one of the widely observed main minerals. It is mainly coarse grained, hypidiomorphic and rarely idiomorphic reddish to brownish and sometimes yellowish internal reflections indicate high FeS contents for sphalerite. Microprobe analyses on two sphalerite grains displayed their high Fe content (Table 3). According to the analytical result, the formula of sphalerite is $(Zn_{0.81} Fe_{0.23}) S_{1.03}$. Ramdohr (1975) points out that these kinds of sphalerites form from high temperature solutions. However, sufficient FeS containing solution should be present in that environment as the case for Kisecik ore veins. Some of the sphalerite crystals show well developed parallel twin lamellae and cleavages.

Table 3- Microprobe analyses of Kisecik sphalerites

Elements	*Points, % wt*		*A* *Average % wt*	*B* *Atomic Weight*	*A/B*
	1	*2*			
Zn	53.66	52.75	53.20	65	0.81
S	31.98	33.97	32.98	32	1.03
Fe	13.36	12.34	12.85	56	0.23
Cu	0.94	0.19	0.57	63.5	0.009
Sc	0.28	0.32	0.30	79	0.004
As	0.16	0.22	0.19	75	0.003
Total	100.38	99.79	100.09		

Sphalerite crystals are distinguished into two different types as one with chalcopyrite exsolutions and the other devoid of them. Usually, coarse grained sphalerite crystals contain mainly chalcopyrite and rarely pyrotite and valleriite exsolutions. These are located and aligned parallel to the zoning and certain crystals graphic directions of sphalerite crystals (Plate I, fig. 6). Locally, pyrotite and chalcopyrite exsolutions show myrmekitic growths in sphalerite. Sometimes, valleriite is associated with these growths.

Sphalerite replaces some parts of arsenopyrite, pyrite, quartz and fills the spaces and cataclastic cracks of them. Locally, sphalerite very clearly replaces chalcopyrite on the other hand spaces and cataclastic cracks of sphalerite are filled by younger quartz, calcite, dolomite and chalcopyrite. Besides these fillings, thin pyrite veinlets cut the sphalerite grains.

Marcasite. - Marcasite increases in amount at the lower elevations of ore veins and is formed as a result of conversion of pyrotite to semi product of marcasite-pyrite. In addition, idiomorphic and subidiomorphic pyrite crystals are locally replaced by marcasite along their rims and cataclastic fractures. Primary prismatic marcasite crystals are also observed. Some marcasite crystals show parallel lamellae-twinning.

Loellingite. - Idiomorphic and hypidiomorphic locllingite crystals are found in small amounts in polished ore sections. Locllingite appears softer in hardness and whiter in color when compared with yellowish arsenopyrite. The results of microprobe analyses from two different points in loellingite are given in Table 4. Loellingite forms a solid solution with saffiorite. The formula of loellingite is $(Fe_{0.36}\ Co_{0.13})\ (As_{0.90}\ S_{0.05}) = (Fe_{0.72}\ Co_{0.26})\ As_2$.

Table 4- Microprobe analyses of cobalt-rich loellingite

Elements	*Points, % wt*		*A* *Average % wt*	*B* *Atomic Weight*	*A/B*
		2			
Fe	20.28	20.13	20.21	56	0.36
S	1.69	1.71	1.70	32	0.05
As	67.39	67.19	67.29	75	0.90
Cu	0.70	0.81	0.76	63.5	0.01
Co	7.37	7.41	7.39	59	0.13
Ni	0.93	0.89	0.91	59	0.02
Au	0.56	0.37	0.47	197	0.002
Total	98.62	98.51	98.73		

Pyrotite. - Pyrotite is observed in very small amount within pyrite, chalcopyrite, arsenopyrite, sphalerite and quartz crystals. It occurs, additionally, together with chalcopyrite and valleriite as exsolutions in sphalerite. Hegzagonal pyrotite, which is more abundant at the lower elevations of ore veins, is completely replaced by semi-product and pyrite. Replacement to semi-product is characterized by the bird eye texture.

Valleriite. - Very small amount of valleriite, together with chalcopyrite and pyrotite are found in sphalerite as exsolutions (Plate I, fig. 7). Moreover, second generation valleriite exsolutions are observable in the exsolutions and inclusions of chalcopyrite in sphalerite. The crystals of this generation show extentions and arrangements due to the different lines in chal-

copyrite. Valleriite results from the ore solutions within the temperature range of 250-300°C and is used as geothermometer mineral (Borchert, 1934).

Cubanite. - This mineral is found very rarely and in very small amounts and is observed as thin parallel exsolution lamellae in chalcopyrite (Plate I, fig. 8). Some lamellae cut each other. Cubanite also crystallizes from the ore solutions of 300-350°C and is used as geothermometer mineral like valleriite (Borchert, 1934).

Native gold. - Native gold is observed only in 8 of 57 polished sections from Kızıltepe and similar ore veins. The names of adits from which the native gold bearing samples collected, their mineral paragenesis, the minerals hosting the native gold and the number and sizes of grains measured from one polished section are given in Table 5.

Table 5- Mineral paragenesis, number and size of gold grains and associated minerals of auriferous minerals

Adit name and Sample no.	*Paragenesis*	*Native gold bearing mineral or mineral contacts*	*Observed grain number*	*Grain size (m)*
Hakkı- 2 (AÇ-5)	Arsenopyrite, chalcopyrite, pyrite, sphalerite, pyrotite, hematite, covellite, marcasite, gold, quartz, sericite	Chalcopyrite	7	18x13, 13x9, 6x4, 1x2, 15x2, 2x4, 3x6
		Arsenopyrite	5	22x17, 28x11, 80x15, 12x11, 8x4
		At contact between arsenopyrite and chalcopyrite. The latter cuts the former.	2	17x2, 18x9
		Sphalerite	1	2x4
Çağatay (AÇ-9)	Chalcopyrite, pyrite, arsenopyrite, pyrotite, marcasite, limonite, neodigenite, sphalerite, covellite, malachite, scorodite, quartz	Limonite (originated from chalcopyrite)	2	6x3, 1.5x2
Çağatay (AÇ-10)	Chalcopyrite, pyrite, arsenopyrite, pyrotite, marcasite, limonite, neodigenite, covellite, chalcosite, malachite, azurite, scorodite, quartz	Limonite (originated from chalcopyrite)	1	120x4
		Scorodite	1	2x12
Çağatay (AÇ-11)	Arsenopyrite, chalcoyprite, covellite, malachite, pyrite, marcasite, sphalerite, digenite, tetradimite, pyrotite, quartz	Arsenopyrite	9	17x11, 30x5, 50x45, 10x7, 62x13, 30x14, 12x9, 14x9, 16x13
		In chalcopyrite veinlet cutting arsenopyrite	10	70x6, 22x6, 45x8, 11x8, 45x8, 12x7, 64x7, 4x3, 2x3, 20x12
		Chalcopyrite	4	7x5, 10x10, 14x10, 13x4
Ali-1 (AÇ-18)	Arsenopyrite, chalcoyprite, sphalerite, pyrite, pyrotite quartz, calcite, sericite	Arsenopyrite	1	11x9
Ali-2 (AÇ-21)	Pyrite, sphalerite, chalcopyrite, arsenopyrite, pyrotite, hematite, limonite, quartz, calcite, chlorite, valleriite	At contact between chalcopyrite and arsenopyrite. The former cuts the latter.	1	30x4
		At contact of chalcopyrite, arsenopyrite, quartz	1	32x7
		Between sphalerite and chalcopyrite	1	9x6
Ali-2 (AÇ-22)	Sphalerite, chalcopyrite, arsenopyrite, pyrite, marcasite, quartz, calcite, chlorite	Inbetween quartz, arsenopyrite, chalcopyrite	1	62x45
		Between quartz & chalcopy.	1	40x30
		Sphalerite	1	16x12
Rıfat (AÇ-29)	Pyrite, sphalerite, chalcopyrite, arsenopyrite, pyrotite, valleriite, marcasite, calcite, ankerite, siderite, chlorite, quartz	Arsenopyrite	1	18x4

Native gold grains are generally very small xenomorphic, sometimes drop-like, rounded and spherulic. They are observed in chalcopyrite, arsenopyrite , sphalerite, limonite, scorodite and quartz or at the double or triple contacts of these minerals (Table 5) (Plate II, fig. 1, 2, 3, 4). Very thin and uncontinuous native gold veinlets are found at the contact of arsenopyrite and chalcopyrite, which cut across the cataclastic arsenopyrite crystals (Plate II, fig. 5, 6). Native gold is precipitated at the contact between chalcopyrite and arsenopyrite. The largest grains are found in these veinlets.

Native gold grains are usually and closely related with chalcopyrite and arsenopyrite , as it is clearly seen from Table 5. Native gold is contemporaneous with chalcopyrite but younger than arsenopyrite at the investigated samples of Kiziltepe ore veins. The ones which are rich in chalcopyrite and arsenopyrite, are also rich in native gold. However, sometimes some samples rich in these two minerals contain no native gold. The number of gold grains decrease toward the lower elevations with the abundance of pyrite, chlorite and calcite. Moreover, no native gold is observed in the polished sections rich in arsenopyrite and pyrite. Therefore, native gold grains in Kızıltepe ore veins characterize a heterogeneous distribution. This kind of distribution is also seen in the chemical analyses of the samples, which contain abundant or rare gold grains (Tables 5 and 6).

Table 6- Gold, silver and other element analyses of Kızıltepe and similar massive ore samples

Sample no.	*Adit name*	*Microscopic investigation*	*Atomic absorbsiyon and ICP*		*Optic spectrographic semi-quantitative analyses*							
			Au gr/t	*Ag gr/t*	*% As*	*% Sb*	*% Cu*	*% Zn*	*% Ni*	*% Co*	*% Bi*	*% Te*
AÇ-5	Hakkı-2	+	20.8	39.2	>1	nd	>1	1	nd	0.03	nd	nd
AÇ-7	Hakkı-2	+	17.5	21.6	>1	nd	>1	>1	nd	0.03	nd	nd
AÇ-10	Çağatay	+	19.3	56.0	1	nd	>1	0.2	nd	0.003	nd	nd
AÇ-11	Çağatay	+	96.0	34.8	>1	nd	>1	0.4	nd	0.07	nd	nd
AÇ-14	Aslan	-	3.3	15.9	>1	nd	>1	0.3	nd	0.004	nd	nd
AÇ-18	Ali-1	+	20.0	19.6	>1	0.04	>1	>1	0.004	0.04	nd	nd
AÇ-22	Ali-2	+	8.3	5.0	0.7	nd	0.3	1	nd	nd	nd	nd
AÇ-27	Rıfat	-	2.3	nd	1	nd	0.7	>1	nd	nd	nd	nd
AÇ-29	Rıfat	+	1.0	5.0	1	nd	>1	1	nd	0.003	nd	nd
AÇ-68	Kıraç Ali*		1.24	4.8	>1	nd	0.3	>1	nd	nd	nd	nd
AÇ-69	Kıraç Ali**		2.98	8.4	>1	nd	0.3	>1	0.004	nd	nd	nd
Dedection limits			0.04	0.5	0.4	0.02	0.0004	0.1	0.004	0.002	0.002	0.2

+, Present; -, Not present; nd= not dedected.

* Taken from limonitized zone.

** Taken from silicified zone.

No silver mineral except tellurobismuthite + hessite solid solution crystals are observed in the polished sections of Kızıltepe ore vein samples. Dedection of silver in the analyses and its increasing of contents parallel to gold indicate that some of silver occur in the solid solution with gold (Table 1,6). This feature is also clearly observed during the microscopic investigation. The color of native gold grains rich in silver is lighter than the ones rich in gold with their light white-yellow color. These kind of grains are generally observed in different but sometimes in the same polished section. The microprobe analyses of gold grains in the same polished section verify the microscopic observations (Table 7). The silver and trace amounts of Cu (1.53%), Pt (0.74%) and Co (0.22%) were analysed in these gold grains and are given in Table 7.

Table 7- Microprobe analyses of Kisecik golds

Elements	*Points, % wt*				*Average*
	1	*2*	*3*	*4*	*% wt*
Au	73.70	76.56	79.80	97.20	81.82
Ag	20.10	18.25	16.50	1.00	13.96
Cu	1.80	2.32	1.20	0.80	1.53
Pt	0.80	1.16	0.80	0.20	0.74
Co	0.90	-	-	-	0.22
Ni	-	-	-	-	-
Fe	2.70	1.71	1.70	0.80	1.73
Total	100.00	100.00	100.00	100.00	100.00

Tellurobismuthite. - As very fine grains and in small amounts, this mineral is found only in one sample. The largest tellurobismuthite grains are only 30-40 microns. They are rounded, drop-like and lath-like. The smallest size of tellurobismuthite grains in chalcopyrite are 2-3 microns. The unambigous determination of tellurobismuthite is quite difficult because of its fineness. The mineral considered as Te-Bi mineral resulting from the microscopic investigation is also analysed by using the microprobe method. The existence of tellurobismuthite is proven (Table 8) in that way. The formula of tellurobismuthite is as follows : $Bi_{0.23}\ Te_{0.36} = Bi_2Te_3$.

Tellurobismuthite + hessite solid solution mineral. - Trace amount tellurobismuthite + hessite solid solution minerals arc observed as small grains and intergrowths with tellurobismuthite. The results of microprobe analyses from two measurement points in this mineral are shown at Table 9. According to the analytical results, the formula of the mineral is $(Bi_{0.18}\ Ag_{0.12})\ Te_{0.35} = Bi_3Ag_2Te_{5.5} = Ag_2Te + 3/2Bi_2Te_3$. This expression suggests that a solid solution mineral which has one molecule hessite and one and a half molecule of tellurobismulhite. This mineral might be a new and an unnamed mineral.

Table 8- Microprobe analyses of Kisecik tellurobismuthites

Elements	*Points, % wt*						*A Average % wt*	*B Atomic weight*	*A/B*
	1	*2*	*3*	*4*	*5*	*6*			
Bi	45.83	46.84	47.02	46.95	45.33	50.76	47.12	209	0.23
Te	45.45	47.44	47.57	46.49	44.76	43.31	45.84	128	0.36
Fe	0.88	0.88	0.86	1.21	1.18	1.18	1.03	56	0.02
S	0.27	0.23	0.14	0.13	0.27	0.15	0.20	32	0.006
As	5.86	2.92	2.93	3.08	1.58	1.38	2.96	75	0.04
Se	-	-	-	-	-	-	-	79	-
Ag	0.41	0.33	0.23	0.31	2.43	1.56	0.88	108	0.008
Cu	1.25	1.31	1.18	1.71	1.56	1.55	1.43	63.5	0.02
Ni	0.06	0.05	0.08	0.10	0.08	0.10	0.08	59	0.001
Total	100.01	100.00	100.01	99.98	97.19	99.89	99.54		

Table 9- Microprobe analyses of tellurobismuthite + hessite solid solution mineral

Elements	Points, % wt				A	B	A/B
	1	2	3	4	Average % wt	Atomic weight	
Te	44.99	45.58	43.93	43.06	44.39	128	0.35
Bi	38.47	40.18	38.94	36.93	38.63	209	0.18
Fe	0.82	1.05	0.74	0.79	0.85	56	0.02
S	0.10	-	-	0.13	0.06	32	0.002
As	2.25	0.92	1.60	0.93	1.43	75	0.02
Se	-	-	-	-	-	79	-
Ag	12.68	10.92	14.12	14.57	13.07	108	0.12
Cu	0.59	1.27	0.79	0.93	0.90	63.5	0.014
Ni	0.11	0.08	0.08	0.08	0.09	59	0.001
Total	100.01	100.00	100.20	97.42	99.42		

Galenite. - Galenile is very rare and is observed only in two sections including various sizes. Coarse grained galenile show cleavage fracture spaces. They locally form small idiomorph crystals in sphalerite. In addition, some xenomorph grains of galenite fill the open spaces between quartz crystals.

Cinnabar. - Cinnabar is observed in small amounts in highly chloritized, silicified and carbonitized metadiabase due to hydrothermal alteration. It forms fine grained, xenomorph and intergrown crystal associations both in host rock and ore veins. Cinnabar is found in ankerite-siderite, pyrite and small amount of chalcopyrite disseminations bearing metadiabase.

Neodigenite. - Small amount of neodigenite is observed as veinlets cutting chalcopyrite and sphalerite. Neodigenite is replaced by covellite along its border as a result of weathering.

Chalcocite. - Trace amount of chalcocite is formed by weathering along its borders, cleavages and fractures which is later replaced by covellite. Chalcocite is associated with covellite and limonite.

Covellite. - Small amount of covellite is found as fracture and open space fillings and as thin belts around sphalerite grains. Additionally, chalcopyrite is replaced by small amount of covellite + limonite or chalcocile + covellite + limonite along its borders, cleavages and cataclastic fractures.

Hematite. - Hematite is rare and is found in different types. The most abundant type of hematite shows radial - spherulic, kidneylike or grapelike shapes and concentric textures (Plate II, fig. 7). This type of hematite is observed at the lower elevations of Kızıltepe ore veins and fills the spaces and fractures in between pyrite crystals. Sometimes, they intersect chalcopyrite grains as veinlets. Locally, observing magnetite relicts in gel textures of hematites point out that they are formed by the martitization processes of magnetites with the same textures.

In addition, some hematite occurrences arc found with rough surfaces forming small prismatic crystals or crystal associations in chalcopyrite and pyrite. Quartz crystals with concentric or kidneylike textures are colored to red by some submicroscopic hematites. Sometimes, hematite forms very thin rods and needles in concentric and radial-spherulic carbonate minerals such as ankerite and siderite.

Magnetite. - Magnetite is observed in small amounts and as relicts in gel textured hematites. They also occur as thin veinlets cutting chalcopyrite. Fine grained, radial-spherulic magnetite rods are generally found at the lower elevations of veins. These magnetite rods called as mushketovite (Plate II, fig.8) which occurs in contact type of ore deposits (Ramdohr, 1975). In addition, some magnetite is formed by intergrowings within pyrite which are occured by the replacement of pyrotite under the underground water level. According to Ramdohr (1975), the conversion of pyrotite to pyrite + magnetite can be formulated as follows:

$$6FeS + 2O_2 = 3FeS_2 + Fe_3O_4$$

Rutile + anatase. - Trace amounts of rutile + anatase are observed as fine crystals. The iron contents of the ilmenites in metadiabases has been lost by hydrothermal alteration and hence rutile and anatase are formed as ilmenite pseudomorphs. Because of the derivation from host rock, rutile and anatase, generally as skeletons, rods and xenomorph grains are located as inclusions into all other hydrothermally originated minerals. They are usually found in highly chloritized, serialized and silicified parts of host rock. The largest crystal of rutile observed in pyrite sizes 100x50 microns. The cracks of cataclastic rutilcs are generally filled by younger ore and ganguc minerals.

Some part of rutile has lattice shapes formed by hydrothermal alteration of ilmeno-magnetites. As a result of this alteration, the iron content and magnetite parts of ilmeno-magnetites are driven away from the crystal lattices and rutile lattices occur as the remaining mineral. Also, needle-like rutile crystals are observed. Rutile and anatase grains are replaced by sphene along their borders and cleavages.

İlmenite. - Trace amount of ilmenite are observed as relicts in rutile crystals. Prismatic, skeleton shaped and xenomorph ilmenite grains are determined in sections which arc replaced by trace amounts of rutile, anatase and sphene along their borders.

Chromite. - Small crystals of chromite occur in trace amounts. The largest crystal size is 40x35 micron. Chromite is also derived from diabase like ilmenite, rutile and anatase.

Tenorite. - Small amount of tenorite together with goethite are observed at the cracks and spaces of one polished section. Tenorites here are in the shapes of concentric, kidneylike and grapelike.

Limonite. - Limonites are the weathering products of iron bearing sulphidic minerals, primarily the products of chalcopyrilc and pyritc. Limonilcs are located partly as pseudomorphs of sulphidic minerals and partly as open space fillings. The former minerals sometimes contain the relicts of pyrite, chalcopyrite and arscnopyrite. The cataclastic structures of pyrites and arsenopyrites facilitate their replacement to limonite. Open space filling limonites show concentric, kidneylike and grapelikc textures. Goethite and lepidocrocite modifications of limonites are generally grown side by side or as intergrowths.

A small part of goethites are the weathering products of ankerites and siderites. Sometimes, needles of goethites occur as radial-spherulic textures. Very small amount of limonite are also observed in the cracks of hematites.

Malachite. - Some malachite is found in the cracks and open spaces of ore veins and in old production adits. Malachite is observed together with limonite and other secondary minerals. The malachite occured in the cracks and open spaces show radial and spherulic textures. They are surrounded by gocthite.

Azurite. - Very small amount of azurite is observed together with malachite and other ore minerals as intergrowihs. Azurite is occured in the cracks and open spaces similar to malachite.

Siderite + ankerite. - They are in small amounts and show gradation to each other. Because of their usual co-existence, they are investigated together. Siderite and ankerite are sorhewhat darker than the carbonates like calcite and dolomite. Locally, siderite and ankerite are colored in red by iron oxides and hydroxides. Their open spaces and cracks are filled by idiomorphic quartz and opaque minerals. Additionally, they are observed together with chlorite crystal associations especially at chlorite-rich parts of rocks. Siderite and ankerite are replaced by limonite along the borders and cleavages. During this process, some calcite are liberated. The replacement of limonites from siderites and ankerites are developed from outward to inward as radial-spherulic and concentric textures. Some siderite crystals are entirely replaced by goethite. In some places, siderite and ankerite pseudomorphically replace hegzagonal pyrotite lamellae or pseudomorph pyrites after hegzagonal pyrotite lamellae.

Scorodite. - Scorodite is observed very rarely. They sometimes pseudomorphically replace arsenopyrites along their borders, cracks and cleavages and sometimes occur as cracks and open space fillings. Some arsenopyrite relicts are observable in scorodites after arsenopyrite pseudomorphs.

Copper-vitriol. - Very small amount of copper-vitriol arc recognized especially together with clay and other secondary copper minerals. Like other secondary minerals, copper-vitriol fills the cracks and open spaces.

Quartz. - Quartz is one of most abundant gangue minerals. These hydrothermally originated quartz crystals are in different ages. Some of them are idiomorphic to subidiomorphic, zoned and coarse grained. The largest crystal size is 3-4 mm. Quartz lodes composed of small and xenomorphic crystals in different ages cut those old quartz crystals and primary ore minerals. Old quartz, crystals show generally cataclastic structures. Chlorites, sericites, ore minerals and calcites are observed in the cracks and open spaces of old quartz crystals. Zoned quartz are locally replaced by chalcopyrite corresponding to this structure. Microcrystalline quartz occurrences which are colored in red by submicroscopic hematites show kidneylike-grapelike textures, and they fill the cracks and open spaces. Those are the youngest quartz crystals.

Chlorite. - Chlorite are observed as crystal associations in between quartzs and ore minerals. Chlorites are the most abundant mineral after quartzs. The rate of chlorites increase especially at lower elevations of ore veins. Some crystal associations developed in open spaces show radial-spherulic textures. These chlorite crystal associations which form inclusions between ore minerals are intersected by quartz and carbonate veins.

Calcite + dolomite. - The abundance of these minerals increase at lower elevations of Kızıltepe ore veins and at the contacts of amphibole bearing quartz-diorite and metadiabase. Additionally, very small amounts of calcite and dolomite are observed at the upper levels of ore veins. Coarse grained calcite and dolomite are usually idiomorphic and subidiomorphic and show pressure twinnings. However, calcite and dolomites which fill the open spaces and cataclastic cracks of quartz and ore minerals are smaller and xenomorphic. Bending and folding of pressure twinnings in calcites and dolomites point out that they are faced continuous pressure after their occurrences. Between the hydrothermally originated calcite and dolomite crystals, locally concentric spheroidal shaped, fine grained calcite occurrences which are colored by limonite are observed.

Clay minerals. - Locally abundant fault clay are found together with ore veins. Some cracks and open space filling clay minerals are investigated by XRD and DTA methods. Halloysite, illite and montmorillonite are determined as clay minerals. Halloysite is the most abundant among them.

Muscovite + sericite . - These minerals arc the rarest ones among the other gangue minerals. Muscovite fills the open spaces between quartz crystals as coarse grains. The open spaces and cleavages of muscovite crystals are sometimes filled by goethite. In addition, very small amount of phlogopite crystals and crystal associations arc observed between the quartz crystals. Sericites as small crystals arc generally found in between quartz crystals.

Sphene. - Sphene is very rare and found in trace amounts. They occur generally as small grains. Sphene is formed by the replacement of titan minerals like rutile and anatase. Sphene grains sometimes contain the relicts of the above mentioned minerals.

Deliklikaya Tepe and similar veins

At Deliklikaya Tepe district veins arc poor in ore minerals and sometimes lying parallel to each other but their lengths and thicknesses generally vary by showing different strikes and dips (Fig. 2). Deliklikaya Tepe vein, belonging to this group, strikes N 80°E and dips almost vertically. The thickness of this vein at the road trench is approximately 0.4 meters. Celalettin-1, 2 and 3 veins which are parallel to Deliklikaya Tepe vein, strike N 80° E and dips 87° to the south. The die tance between Celalettin-1 and Celalettin-2 is approximately 20 meters and the distance between Celalettin-2 and Celalettin-3 is approximately 3 meters. The thicknesses of the veins at the road trench are 0.5, 0.3 and 1.0 meters, respectively. Another vein in metadiabase located nearly 40 km. northwest of Celalettin-3 vein contains disseminated pyrite, chalcopyrite, and secondary copper minerals and it strikes N 65° W. The thicknesses of eight veins, numbered from Altun-1 to Altun-8 veins vary between 1 and 1.5 meters, these parallel veins strike N 50° W. The vein in which Fuat Ocak was opened strikes N 60° W and dips 70° to the south. An alteration zone 8-10 meter in width is observed. Eight thin veins are found in this zone enriched in quartz, clay minerals and limonite and their thicknesses are about 0.2-0.3 meters.

At the west side of Deliklikaya Tepe a vein which strikes N 30° E and additional two veins in 0.7-0.8 meter thicknesses strike N 60° W and N 40° W and dip 75° to the north and 80° to the south, respectively. A 15 meter adit, called as Ayvaz Ocak is driven at the lower elevations of another vein which is close to Fuat Ocak. This vein strikes N 70° E and dips 82° to the northwest.

Additionally, some veins similar to Deliklikaya Tepe veins which are poor in are minerals outcrop at Kızıltepe district. Doğan Ocak is a big trench opened for such kind of a vein. Doğan Ocak is located in altered metadiabase zone which has 4-5 meter thicknesses. A lot of quartz veins which consist of clay minerals and limonite occur in Doğan Ocak. The strike of this vein is N 70° E and its dip is 82° to the northwest.

Quartz veins of Deliklikaya Tepe are composed of hydrothermal quartz, strongly affected fault breccia, metadiabase particules and small amount of ore minerals which are located in faults and fractures, occured during the emplacement of amphibole bearing quartz-diorite into metadiabase. Metadiabase particules in veins are silicified, chloritized, carbonitized, sericitized and kaolinized. As a result of this alteration, the intersertal textures of metadiabases have become undescribable.

The quartzs of quartz veins of Deliklikaya Tepe are derived generally from the remaining quartzs after amphibole bearing quartz-diorite occurences and partly from the hydrothermal alteration of metadiabase.

The open spaces of partly idiomorphic quartz crystals are filled by sericite, locally muscovite, phlogopite, clay minerals, chlorite and calcite. Hydrothermal quartzs are in different ages. The first generation quartzs which fill the faults are broken by later movements of faults. The open spaces and cataclastic cracks of there quartz minerals are filled by a younger generation of quartz and calcite. The spaces and cracks of some older quartz minerals are partly filled by ore minerals.

Ore minerals of Deliklikaya Tepe veins

Main ore minerals of Deliklikaya Tepe veins are arsenopyrite, pyrite, chalcopyrite, sphalerite, marcasite. galenite, pyrotite, valleriite, hematite, rutile, anatase, chromite, limonite, covellite, tenorite, malachite, scorodite and copper-vitriol.

Arsenopyrite. - Small amount of arsenopyrite forms disseminations in quartz veins. Sericite and quartz inclusions are observed in idiomorphic arsenopyrite crystals. Arsenopyrite is replaced by scorodite along its borders and cataclastic cracks. Sometimes, a thin belt of covellite is improved at the contact between scorodite and arsenopyrite. The largest arsenopyrite crystal size at Deliklikaya Tepe veins is 1.5x0.3 mm. Prismatic arsenopyrite grains are the oldest sulphide minerals. For this reason, arsenopyrite is replaced by quartz, calcite, sphalerite and chalcopyrite along its borders and cataclastic cracks.

Pyrite. - Small amount of pyrite occur as idiorpprphic and hypidiomorphic crystals in various sizes. They form disseminations and veinlets in ore bearing quartz veins. These kind of pyrites are generally fine grained. The largest grain size is 1.5x1 mm. Quartz, sericite, chlorite and rutile inclusions are observed in pyrite. Idiomorph to hypidiomorph pyrite crystals sometimes accompanied by chalcopyrite and sphalerite intersect altered metadiabase particules in ore bearing quartz veins as

veinlets. Most of the pyrite is partly or totally altered to pseudomorph limonite. Limonilization is developed along the borders, cataclastic cracks and cleavages of pyrites.

Chalcopyrite. - Small amount of chalcopyrite is rarely observed. Xenomorph and fine grained chalcoyprite crystals fill the open spaces between arsenopyritc, pyrite and quartz crystals. Chalcopyrites include inclusions of quartz, chlorite and rutile grains. Sometimes, chalcopyrites envelope pyrite crystals as thin belts. Most of the chalcopyrites are replaced by chalcosite+covellite+limonite along their borders.

Sphalerite. - Small amount of sphalerite forms xenomorph to subidiomorph grains between quartz. The largest grain size is 300x250 microns. Some sphalerite grains contain chalcopyrite cxsolutions. Sphalerites reveal yellowish, reddish to brownish internal reflections. Some sphalerite grains are enveloped by covellite belt representing a thin sementation zone.

Marcasite. - Trace amount of marcasites are observed along the borders and cataclastic cracks of some idiomorph pyrites. In this case, pyrite are partly replaced by marcasite.

Valleriite. - Valleriites together with chalcopyrites form cxsolutions in some sphalerite grains. Trace amount of valIcriitc is rarely observed.

Pyrotite. - Trace amount of pyrotile are observed as small inclusions in pyrite and arsenopyrite. Some pyrotite grains form exsolulions in sphalerites. Pyrotite is locally replaced by a semi-product.

Covellite. - Very small amount of covellite occur as fine crystal associations. Sometimes malachite accompanies covellite. Covellite is sometimes located in open spaces and cracks and sometimes envelopes chalcopyrite, arsenopyrite and sphalerite. Covellite, formed by weathering of chalcopyrite, also envelopes limonite and chalcopyrite.

Galenite. - Fine grained galenite is observed in trace amounts between quartz minerals. They are replaced by anglcsite and cerussite along their edges and cleavages.

Rutile + anatase. - Trace amounts of rutile + anatase are found as fine grains. They occur as a result of hydrothermal alteration of ilmenite grains which are located at altered metadiabase rock particules of ore bearing quartz veins. Additionally the lattices of rutile are resulted from the hydrothermal alterations of ilmeno-magnetites in metadiabases.

Iron contents of ilmenite and magnetite parts of ilmeno-magnetite are moved out from environment during hydrothermal alteration processes. Rutile rarely exhibit prisms or needles. Some rutile grains contain parallel pressure lamellae.

Chromite. - Trace amount of chromite is observed as fine and idiomorphic crystals, some chromite crystals are rarely seen in quartz bearing and altered parts of metadiabase.

Hematite. - Hematite is found in trace amounts occasionally in minute scales. A part of hematite is later generated by martitization of magnetite.

Tenorite. - Forming as cracks and open-space fillings, trace amount of tenorite occur with limonite and malachite. Partly they show concentric and kidneylike-grapelike textures. Tenorite intergrowths with goethite.

Limonite. - Rarely, two different modifications of limonite is observed together with each other. Goethite modification is much more than lepidocrosite modification. Three types of limonite are found at the veins of Deliklikaya Tepe. One of them is limonite pseudomorph of sulphidic ore mineral such as pyrite, chalcopyrite and arsenopyrite. Limonite, in addition to, forms veinlets filling cracks and open spaces. Limonite veins are generally scattered in the rock. Another kind of limonite colors the clayey and scricitic parts of ore bearing quartz veins.

Malachite. - Malachite is rarely or in trace amounts observed at the cracks and spaces of some samples. Malachite is generally associated with covellite and limonite. It forms small and partly idiomorph crystals at the spaces of rocks.

Scorodite. - Very small amount of scorodite is found partly as pseudomorph after arsenopyrite and partly as cracks and open space fillings. Some arsenopyrite relicts are observed in scorodites formed as pscudomorphs after arscnopyrites.

Copper-vitriol. - Trace amount of copper-vitriol is observed at cracks and open spaces of rocks associated with clay minerals. They form as micro crystal associations.

CHEMICAL ANALYSES

Two kinds of samples have been collected for the mineralogical investigations and chemical analyses from the ore veins of Deliklikaya Tepe. Detailed mineralogical investigations were performed on the polished sections of the samples and no gold was found. For the chemical analyses of gold, two different type of samples were taken from the ore of Deliklikaya Tepe and similar veins. Based on his experience, Ali Küpeli, the geologist of Yurttaşlar Company, compiled some samples from limonite and gold rich parts of veins. The MTA crew tried to collect the representative channel samples from the same veins. Gold and silver analyses were performed partly in MTA General Directorate Laboratory and partly in Geological Survey Laboratory in Ottawa, Canada and Dhahran University Laboratory in Saudi Arabia using the methods of AAS and ICP. At the same time, optic spectrographic semi quantitative analyses of As, Sb, Cu, Zn, Ni, Co, Bi and Te were carried out on the same samples. The analytical results are given in Table 1. As it is clearly seen from this table, apart from one sample, all samples from Deliklikaya Tepe and similar veins contain relatively low gold values. With these grades, the veins of Deliklikaya Tepe are economically unimportant.

DISCUSSION AND CONCLUSIONS

Intrusive rock provided SiO_2 rich solutions that consequently brought about gold bearing ore veins of Kisecik has the composition of amphibole bearing quartz-diorite. Tekeli and Erendil (1986), described this rock as isotropic gabbro. An intense hydrothermal alteration developed mainly in the form of silicification and chloritization as a result of intrusion amphibole bearing quartz-diorite into metadiabase. The alteration which decreases in intensity from the contact of these rocks downward is also reported by Tekeli and Erendil (1986). It is due perhaps that these researchers located a plagiogranite, resulted from solutions of last differentiation products, at the contact of amphibole bearing quartz-diorite with metadiabase in their columnar section, since they did not assume that gabbro could generate such kind of alteration. However, such a plagiogranite does not occur in the Kisecik gold field. In this case, here we favor a more acidic source rock as amphibole bearing quartz-diorite for the hydrothermal alteration rather than isotropic gabbro.

The contact of amphibole bearing quarlz-diorite, metadiabase xenoliths in amphibole bearing quartz-diorite and metagabbro concretions show various degrees of actinolitization-tremolitization, epidotization and biotitization. In addition, amphibole bearing quartz-diorite is scapolitized, metadiabase phlogopitized, and gabbro steatized and serpentinized. All these changes are the products of a contact metamorphism at epidote-amphibolite facies which caused by intrusion of amphibole bearing quartz-diorite into metadiabase. The contact metamorphism at the contact of amphibole bearing quartz-diorite with metadiabase decrease downward in intensity and grades into regional metamorphism of green schist facies characterized by silicification, chloritization, carbonatization and sericitization. Some of quartz, calcite and dolomite observed resulted from hydrothermal alteration of metadiabase and some too is highly likely formed from solution left over after crystallization of amphibole bearing quartz-diorite. Magnetite, magnetite portion of ilmeno-magnetite and Fe-compound of ilmenite were leached in the areas of intense hydrothermal alteration. This "Fe" was possibly employed in the composition of mainly sulphide minerals and rarely of Fe-bearing minerals.

Prismatic magnetites (mushketovites) are observed as hematite pseudomorphs along the lower parts of Kızıltepe ore vein. According to Ramdohr (1975), this type of magnetite occurs only in contact type mineralizations.

Three different mineral groups with respect to their origins are defined in the Kisecik gold bearing ore veins. Trace amount of ilmeno-magnetite, ilmenite, rutile, anatase, sphene and chromite were derived from diabase and were subjected to hydrothermal alterations. Arsenopyrite, pyrite, chalcopyrite, sphalerite, pyrotite loellingite, valleriite, cubanite, native gold, tellurobismuthile, tellurobismuthite-hessite solid solution mineral, galenite, cinnabar, neodigenite, magnetite, some hematite, some marcasite, quartz, calcite, dolomite, siderite, ankerite, muscovite and sericite which form the Kisecik ore are all primary minerals and arc resulted from hydrothermal solutions. The surficial weathering of these minerals brought about secondary minerals such as limonite, scorodite, chalcocite, covellite, malachite, azurite, tenorite and copper-vitriol.

Cubanite and valleriite among primary minerals arc the minerals of good geologic thermometer. According to Borchcrt (1934), cubanite exsolutions in chalcopyrite and sphalerite occur at temperatures between 300° and 350°C; valleriite, on the other hand, at 200°-300°C. Chalcopyrite and sphalerite hosting these minerals and native gold contemporaneous with chalcopyrite are formed at these temperatures. Sphalerite starlets and olcandar-leaf twinning in chalcopyrilc suggest that ore is formed by high-temperature solutions (Ramdohr. 1975). The reason that sphalerite shows dark brown-reddish internal reflection is because this mineral contains high amount of FeS in its, crystal lattice. This is only possible at higher temperatures according to Ramdohr (1975). Nevertheless, as is the case for Kisecik mineralization, adequate FeS should be available during the crystallization of sphalerite.

As is well-known, ophiolitic rocks, from the point of geochemistry, are enriched with respect to Cr, Pt, Ni, Co, Cu, Fe, Ti and V, but devoid of As (Schnciderhöhn, 1958; Turekian and Wedepohl, 1961; Turekian, 1972).Cu-mineralization is, similary, depleted in As (Çağatay, 1968; 1977; Çağatay et al., 1982). However, Kisecik ore veins are enriched in As. This, in turn, brings about arscnopyrite and its origin as a subject of discussion. On the other hand, Cu-mineralizations related to magmatic activities created by crustal meltings comprise con. iderable amount of As-minerals (Altun, 1984). Therefore, the authors consider amphibole bearing quartz-diorite which mobilized the ore as a product of crustal melting out of ophiolites and a rock which intruded in ophiolites. Amphibole bearing quartz-diorite is highly likely a product of a magmatic activity connected to the geological events developed subsequent to ophiolite emplacement.

Kisecik gold bearing ore veins arc classified into two very distinct groups in this study. These are "Kızıltepe and similar ones" and "Deliklikaya Tepe and similar ones". The most significant veins of gold deposits are the currently mined southeastern-veins (Fig. 2). Although gold content locally occurs at high amounts in the massive ores of the veins (Tables 1 and 6). The average gold content of samples collected at various elevations of the veins is generally below 5 ppm. The average gold and silver contents of a representative sample pooled from the sample loaded to a truck for ore dressing tests at the Department of Mineral Analyses and Technology of MTA arc 4.7 ppm and 8 ppm respectively (Ulu, E. personnel communications). The analytical results of selected 2300 ton massive ore, shipped to Kütahya-Gümüşköy facilities of Etibank for gold extraction tests and was also analysed for its gold content, revealed 4 ppm Au on the average (Personnel of Yurttaşlar Company and of KiUahya-Giimiis.koy facilities Personnel communications). 3 kg gold, with almost complete fineness was yielded from 2300 ton ore at Kütahya-Gümüşköy facilities (Newspapers and TV-news). This amount of gold out of 2300 ton ore corresponds to a gold grade of 1.3 ppm. Deliklikaya Tepe and similar ore veins are rather poor for gold (Table 1).

Most of the Kisecik gold bearing ore veins terminate at the contact of amphibole bearing quartz-diorite with meladiabase. Among these arc also included the most important Kızıltepe veins which arc currently being mined. Field observations do not testify any significant thicknesses and continuation for these veins. Deliklikaya Tepe veins contain ores with non economical grades at their known portions. Due to inadequate reserves and low grades Kisecik gold bearing veins are considered to form a small, insignificant deposit; even an occurrence rather than a deposit.

ACKNOWLEDGEMENTS

The oppurlunity for investigating Kisecik gold occurrence was provided upon the approval of General Directorate of MTA, subsequent to the invitation of chairman of executive committee of Yurttaşlar Company, Rasim Yurttaş. Ferhat Yurttaş arranged accomodalions for us in Hatay and joined us with Ali Küpeli during our field excursion and provided us any kind of help which we needed. We are grateful to owners and personnel of Yurttaşlar Company and members of MTA.

Chemical analyses of samples collected from Kisecik gold occurrence were carried out in Laboratories of MTA, Dhahran University in Saudi Arabia and Geological Survey (Ottawa) of Canada. The analyses of samples sent to Saudi Arabia were carried out by Namık Çağatay and those to Canada by D.R. Boyle. Cemal Göncüoğlu and Evren Yazgan helped in identification and interpretation of some thin sections. Clay minerals were examined by Ali Van using X-ray diffractometu. Ore minerals were analysed by Akif Özcan using Electron microprobe spectrometer. We are thankful to all these technical staff who contributed a lot in realization of this manuscript.

Manuscript received March 15, 1990

REFERENCES

Alpan, T., 1985, Hatay altın aramaları prospeksiyon raporu: MTA Rep., 2008 (unpublished), Ankara.

Altun, Y., 1984, Giresun-Görele ve Tirebolu (Doğu Karadeniz) yöresindeki renkli metal yataklarının karşılaştırmalı cevher mineralojileri ve kökenleri: İst. Üni. Fen. Bil. Enst., Ph. D Dissertation (unpublished) 146 p.

Aslaner, M., 1973, İskenderun-Kırıkhan bölgesindeki ofiyolitlerin jeoloji ve petrografisi : MTA Publ., 150, 78 p., Ankara.

Atan, O.R., 1969, Eğribucak-Karacaören (Hassa)-Ceyhanlı-Dazevleri (Kırıkhan) arasındaki Amanos Dağlarının jeolojisi : MTA Publ., 139, 85p., Ankara.

Aydal, D., 1989, Hatay-Kızıldağ Masifi güneydoğusunda altın zenginleşmeleri: 43. Türkiye Jeoloji Kurultayı Bildiri Özleri p., 9, Ankara.

Blumenthal, M., 1938, Die Grenzzone zwischen syrischer Tafel und Tauridcn in der Gegend des Amanos : Eclog. Geol. Helvet., 31, 381-383.

Borchert, 11., 1934, Über Entmischungen im System Cu-Fe-S und ihre Bedeutung als geologisches Thermometer: Chemie der Erde 9, 145-172,Freiberg.

Çağatay, A., 1968, Erzmikroskopische Untersuchungen des Weiss-Vorkommens bei Ergani Maden, Türkei, und genetische Doming der Kupfererzlagerstaetten von Ergani Maden : N. Jb. Miner, Abh., 109, 1/2, 134-155, Stuttgart.

———, 1977, Güneydoğu Anadolu bakır yatak ve zuhurlarının jeolojik-mineralojik etüdü sonunda elde edilen jenetik bulgular: MTA Bull., 89, 46-70, Ankara.

———; Pehlivanoğlu, II. and Altun, Y., 1982, Küre piritli bakır yataklarının kobalt-altın minaralleri ve yatakların bu metaller açısından ekonomik değeri: MTA Bull.,93/94, 110-117, Ankara.

Çoğulu, H.E., 1973, Hatay-Kızıldağ masifinin oluşumu hakkında yeni buluşlar: Cumhuriyetin 50. Yılı Yerbilimleri Kongresi Bildiri Özetleri, Ankara.

———, 1974, Hatay bölgesinde ultrabazik tektonikler ve tabakalı peridotitler: MTA Bull., 83, 185-193, Ankara.

Dean, W.T. and Krummenacher, R., 1961, Cambrian Trilobites from the Amanos Mountains, Turkey: Paleontology, 4/1, 71-81.

Delaloye, M.; Pişkin, Ö.; Vaugnat, M. and Wagner, J., 1979, Rare Earth Element concentration in mafics from the Kızıldağ ophiolite (Hatay, Turkey): Schwciz. Min. Pet. Mitt., 59,67-73.

———;———; Selçuk, II.;———;and———, 1980a, Geological section through the Hatay ophiolite along the Mediterranean coast. Southern Turkey: Ofiliti, 5 (2/3), 205-216.

———; Do Souza, H.; Wagner, J and Hedley, 1., 1980b, Isotopic ages on ophiolites from the eastern Mediterranean: Panayiotou, A. ed., Int. Symp. on Ophiolites, 292-295,Lefkoşe

Dubertret, L.., 1953, Geologic des roches vertes du NW de la Sync ct du Hatay (Turgie)· Notes Mem. Moyen Orient, 6, 227 p.

Erickson. D.B., 1940, Report on the geology of Hatay (Turkey): MTA Rep., 1118 (unpublished), Ankara.

Molly, U.W., 1955, Hatay'da yapılan altın aramaları hakkında rapor: MTA Rep., 2323 (unpublished), Ankara.

———, 1961, Türkiye'nin batısında altın ve platin aramaları: MTA Rep., 2841 (unpublished), Ankara.

Ramdohr, P., 1975, Die Erzmineralien und ihre Verwachsungen: 4. Aull. Akademie-Verlag, Berlin.

Schnciderhöhn, II., 1958, Die Erzlagertaetten der Erde Band I: Die Erzlagerstactten der Fruhkristallisation: 315 p., Stuttgart

Selçuk, II., 1981, Etude geologique de la partie meridionale du Hatay (Turquie): Ph. D thesis (unpublished), Univ. de Geneve, 116 p.

Strunz, H., 1981, Mineralogische Tabellen: 7. Auflage, Akademie-Verlagi Leipzig, 621 p.

Tekeli, O. and Erendil, M., 1986, Geology and Petrology of the Kızıldağ Ophiolite (Hatay): MTA Bull., 107. 21-38, Ankara.

Turekian, K.K., 1972, Chemistry of the Earth. Holt. Rinehart and Winston, Inc., New York, 132 p.

———and Wedepohl, K.H., 1961, Distribution of the elements in major units of the earths crust: Geolg. Soc. America Bulletin vol. 72, No. 2, 175-192.

Wijkerslooth, P., 1942, Eine montangeologische Reise nach Hatay: MTA Rep.,1085 (unpublished), Ankara.

PLATES

PLATE-I

Fig. 1 - Objective: 5X, Ocular: 10X, + N
Highly sericitized plagioclases (dark gray-black) of amphibole bearing quartz-diorite. Amphiboles have cleavages quartz (in the middle) is white.

Fig. 2 - Objective: 5X. Ocular: 10X, // N
Clinopyroxenes of intersertal textured diabases are replaced by phlogopite (gray). Plagioclase (labrodor) laths (white), opaque minerals (black).

Fig. 3 - Objective: 5X, Ocular: 10X.+N
Highly actinolitized-tremolitized (laths) meta gabbro.
Plagioclases (labrodor) are white.

Fig. 4 - Objective: 32X, Ocular: 10X, in oil
Hegzagonal lamellae of pyrotite are totaly replaced by pyrite (pseudomorph). Quartz as gangue mineral is black.

Fig. 5 - Objective: 32X, Ocular: 10X, in oil
Sphalerite exsolution starlets in chalcopyrite.

Fig. 6 - Objective: 32X. Ocular: 10X, in oil
Chalcopyrite (white) exsolutions in sphalerite are concordant to the zoned structure of sphalerite. Gangue minerals and spaces (black).

Fig. 7 - Objective: 32X, Ocular: 10X, in oil
Big chalcopyrite exsolutions in sphalerite contain second generation vallehite. Spaces (black).

Fig. 8 - Objective: 32X, Ocular: 10X, in oil
Cubanite (gray) lamellae in chalcopyrite (light gray).
Spaces and gangue minerals (black).

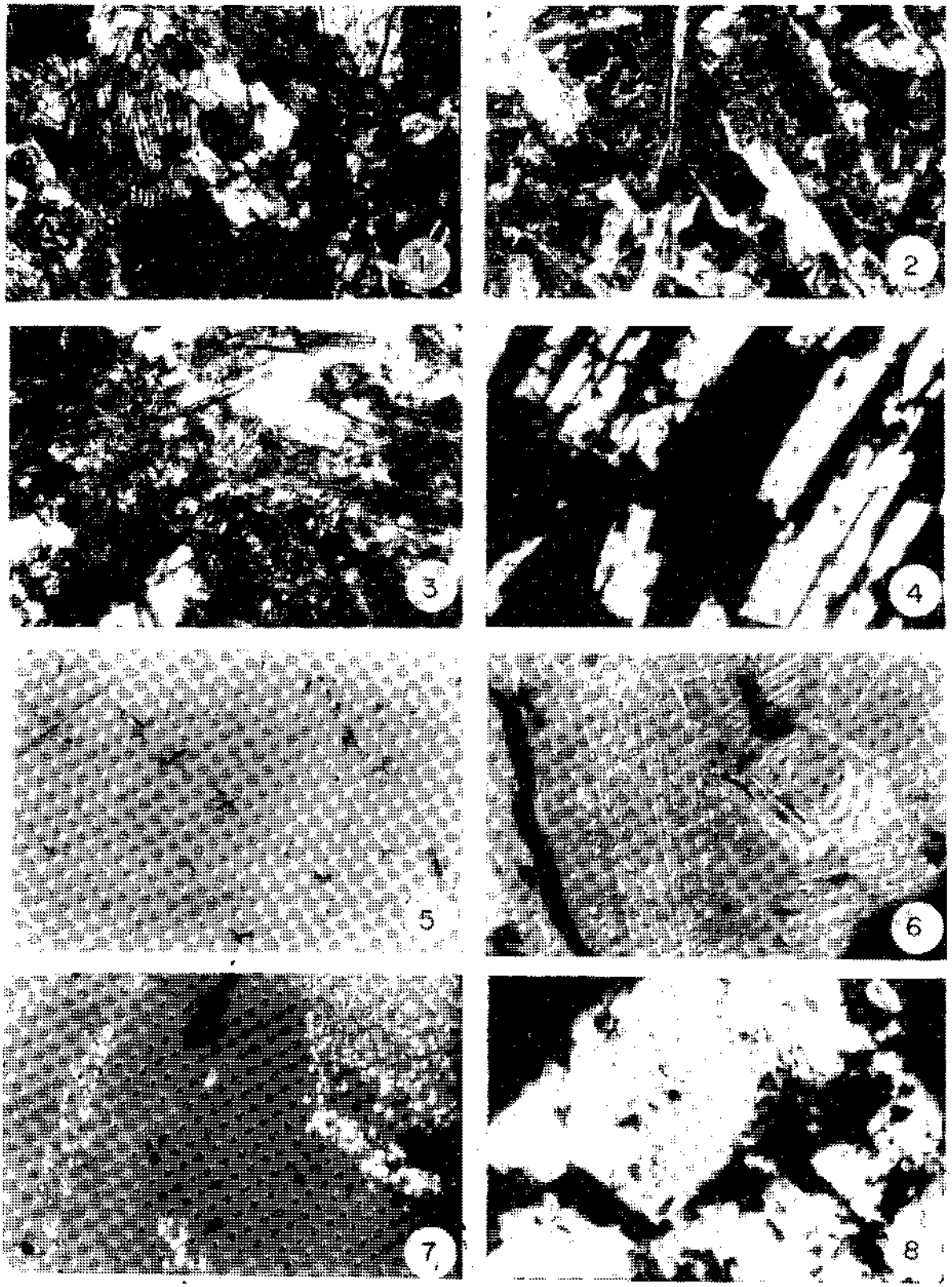
1
2
3
4
5
6
7
8

PLATE-II

Fig. 1 - Objective: 32X, Ocular: 10X, in oil
Native gold (white and scratched); at the contact of chalcopyrite (gray) replacing arsenopyrite (light gray and high relief). Gangue minerals and spaces (black).

Fig. 2 - Objective: 32X, Ocular: 10X, in oil
Native gold (white) in cataclastic arsenopyrite. Cracks are filled by chalcopyrite. Spaces (black).

Fig. 3 - Objective: 32X, Ocular: 10X, in oil
Native gold (white) at the contact of chalcoyprite (stracthed) and quartz (black). Sphalerite (gray), spaces (black).

Fig. 4 - Objective: 32X, Ocular: 10X, in oil
Native gold (white) at sphalerite (dark gray) contact in chalcopyrite (stratched at one edge). Gangue minerals and spaces (black).

Fig. 5 - Objective: 32X, Ocular: 10X, in oil
Native gold (white) in chalcopyrite (gray) vein cutting arsenopyrite (light gray). Gangue minerals and spaces (black).

Fig. 6 - Objective: 32X, Ocular: 10X, in oil
Native gold (white); in chalcopyrite (gray) vein cutting arsenopyrite (light gray), at the contact between chalcopyrite-arsenopyrite and in chalcopyrite. Gangue minerals and spaces (black).

Fig. 7 - Objective: 32X, Ocular: 10X, in oil
Concentric, radial-spheluric textured hematite spheres in dolomite (black).

Fig. 8 - Objective: 32X, Ocular: 10X, in oil
Mushketovites (dark gray) are highly replaced by martitized hematite (gray). Pyrite (white), gangue minerals and spaces (black).

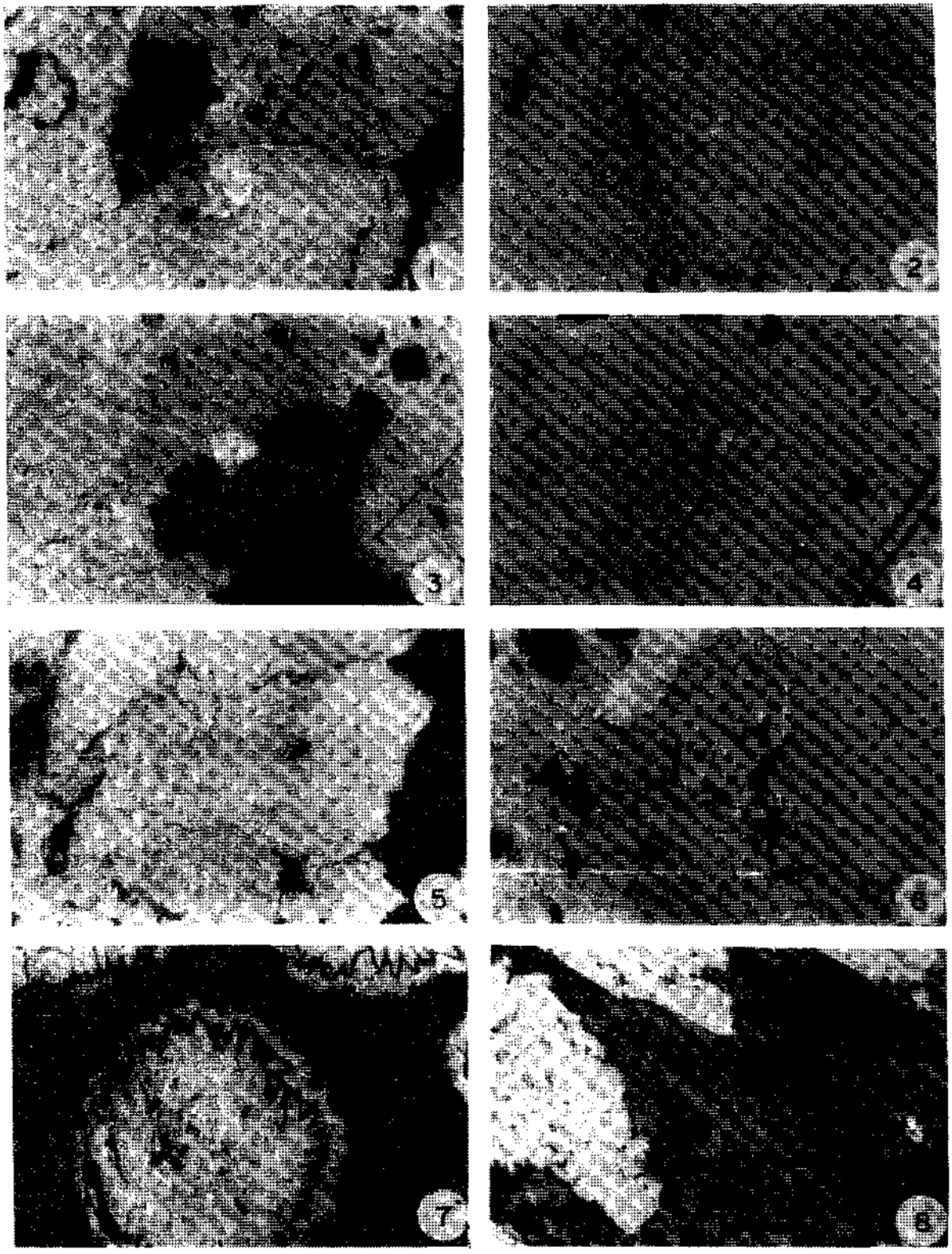
1
2
3
4
5
6
7
8

Mineral Res. Expl. Bull., 112, 39 - 46, 1991

ECONOMIC POTENTIAL OF RESIDUAL DEPOSITS IN PENEPLANATED AREAS IN TURKEY

Kenan TÜFEKÇİ *

ABSTRACT.- Peneplain is a geomorphological unit which is formed in the final stage of the fluvial denudational cycle. The developed peneplains on the bedrocks of containing iron, olivine, pyroxene, feldspar or fcldspalhoids comprise lateritic ore deposits. Besides the bedrock, the formation of this residual deposits arc due to both tropical climate and nonactive tectonic conditions. Today, actual lateritizations has been going on in the climatic bells where tropical climate conditions are dominant in the world. But it isn't impossible to bring up that the lateritization has been lasting under actual climatic influences in Turkey. Paleoclimatological conditions in the geological past arc important for Turkey. For this reason, especially, the cycles of Upper Cretaceous and Lower to Middle Miocene in Turkey are suitable climatic cycles to lateritizations in Turkey, the relics of the oldest relief forms pertaining to Upper Cretaceous and the relics of "Anatolian Peneplain" pertaining to the denudational cycle of the Lower to Middle Miocene may be very interesting for residual ore deposits. When Turkey's tectonic evolution is appraised from this view point: while the Pontides, the Anatolides and Tauridcs in places appear to be the suitable belts, but not the Border Folds region. As a result, it isn't impossible to have enough knowledge about the residual deposits and their peneplanation cycles from the present surveys in Turkey. Consequently, the evolution of the residual deposits isn't known with details yet. For this reason, the prospection of the deposits must be planned by amulti-disciplinerprogramme. Geomorphologically, the extend of the deposits must be mapped and their relations with the geomorphologic units must be explained.

INTRODUCTION

It is a fact which has been slated al many panels on carlhsciences that the future of a country's industry could be secured by providing its required raw material and energy domestically. For this purpose, new natural resource exploration methods and theses are being developed and exploration process is now considered as an interdisciplinary program. That latcritic ore deposits which are the object of this research have not been explored in detail in Turkey, except the Çaldağ (nickel) and Seydişehir (aluminum) areas, makes the prospection of ore deposits more interesting.

Besides the characteristics of bedrock, the factors such as climate, topographic features, and geomorphologic evolution have also an imporiant effect on the formation of the residual ore deposits. The bedrocks containing iron, olivine, pyroxene, feldspar and feldspalhoid minerals are gradually turned into the residual ore deposits by simultaneous formation of peneplancs and a thick leaching zone forms in the peneplanes in tropical climates. However, change in climate or the end of tectonic stability during the peneplanation may change the position of the formed or yet-to-be formed residual ore deposits.

In this paper, the residual ore deposits are investigated geomorphologically and the morphogenetic and morphoclimalic factors affecting the formation of these deposits in Turkey are also reviewed.

CONCEPT OK PENEPLANE AND THE CHARACTERISTICS OK RESIDUAL ORE DEPOSITS FORMING IN PENEPLANES

In order to form residual ore deposits in an area, addition to tropical climate, a period of tectonic stability, that is, a peneplane formation period is required. Therefore, first of all the concept of peneplane and the characteristics of peneplanes should be briefly considered. The term "Peneplain" was first used by Davis in 1889 referring to a nearly fcaturless, gently undulating land surface of considerable area, which presumably has been produced in the penultimate stage of a humid fluvial geomorphic cycle (Erinç 1982). According to Davis, flat areas which are gently undulating and spread over considerable areas are produced as a result of millions of year-long erosion of internally weakened formations (Fig. 1). Peneplane is such that the original topographic relief has been eroded down, the intensity of mass movements is lesser, the streams carry smaller quantity of materials and slow down due to the small quantity of strcamload. These gcomorphologic units, known also as Truncated Plane", are distinguished from denudational planes by their greater size (Ardos. 1971). The residual ore deposits form in this geomorphologie unit, the characteristics of which is briefly discussed above,

Peneplanes may be subjected to tectonic deformation during/after formation. Tectonic movements may rip these units by hundreds of meter deep trenches and cause the laterite deposit, which are in the peneplane, to be eroded and rede-

* Maden Tetkik ve Arama Genel Müdürlüğü. Jeoloji Etütleri Dairesi, Ankara-Turkey.

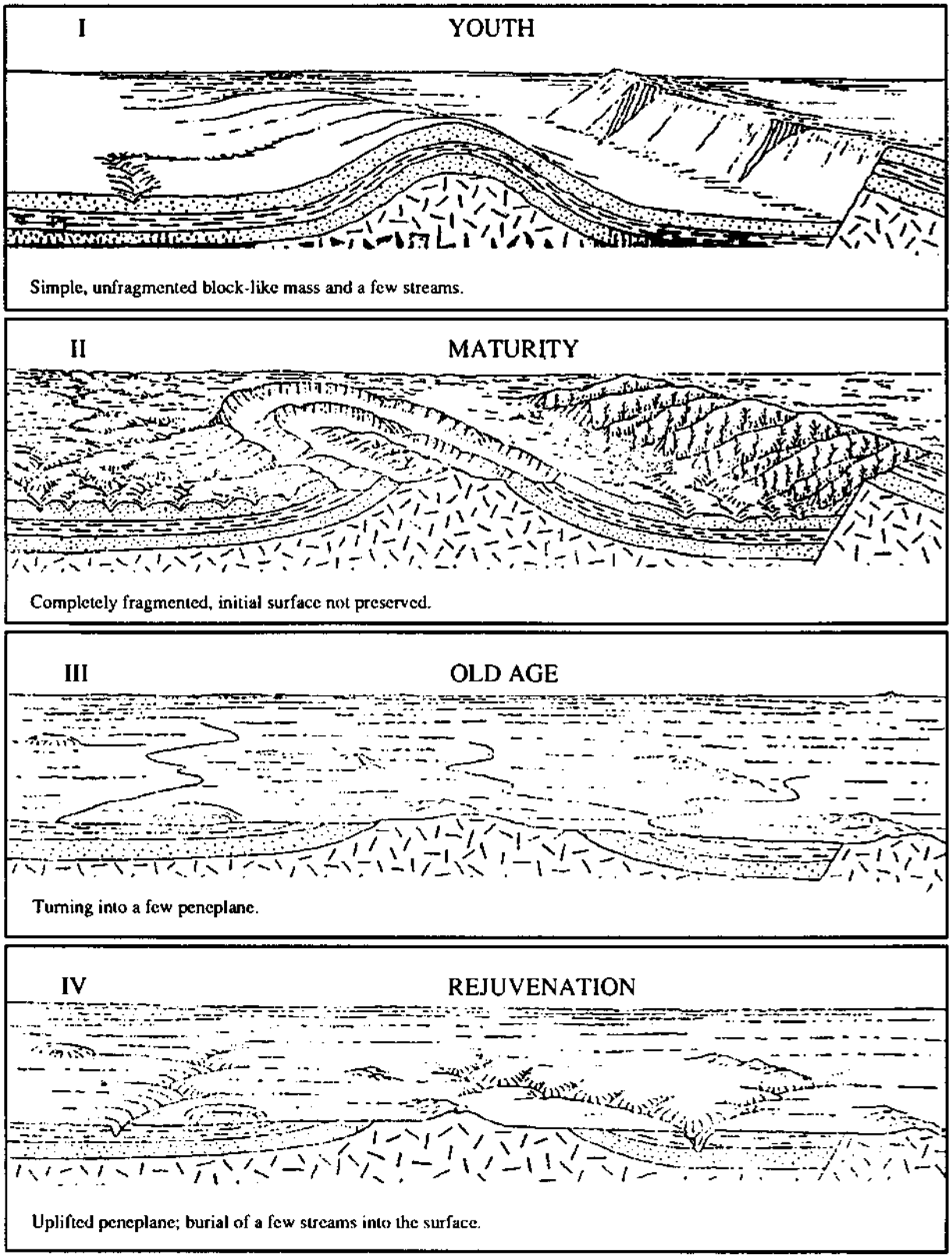

Fig. 1- Stages in geomorphic cycle in a humit area.

posited in various environments. It has been determined that today some of the ancient peneplanes have been folded or depressed, some of them have been eroded down to the sealevel and some others have been fossilized by younger sediments which cover them. For instance, the bauxite deposits in Arkansas formed in pre-Eocene peneplanes and are locally blanketed by the Tertiary claystones and sandstones (Özkoçak, 1980). The bauxite deposits in Şarkikaraağaç-Yalvaç, Akşehir, on the other hand, formed in diabase and were fossilized by the overlying Upper Jurasic limestones (Özkoçak, 1980). As a result of erosion of the sediments covering these fossilized peneplanes, the ancient surfaces can be determined as exhumed surfaces.

Lithology of the rock in which peneplane developes is also important. Although these deposits form in different type of hostrocks in humid climates, for residual iron deposits, especially the ultra-basic rocks with low aluminum content for nickel deposits, dunite, peridotite and pyroxenile, and for the residual bauxite deposits, feldspar or feldspathoid bearing rocks arc important (Özkoçak, 1973, 1980; Cornwall, 1973). The examples to this type of deposits are those; after the sub-oceanic basalt-andesile flow in the Late Oligocene or the Early Miocene in New Caledonia there occured great peridotite emplacement. This ultrabasic massif, dominated by harzburgite, was uplifted above the sea level and peneplanated, over 50 m thick iron laterite blanket formed in it in a tropical climate (Özkoçak, 1980). In the above-mentioned climate, the peneplanes forming in dunites, peridotites and pyroxenite are also suitable for the formation of the residual nickel deposits. Vinogradov (1956) estimated that the average nickel content of these rocks is 0.1-0.3 %. Whereas Golightly (1979) listed the factors necessary for the formation of the residual nickel containing deposits as follows: 1- Mineralogy and tectonic emplacement of peridotite; 2- Climate; 3- Topographic relief; 4- Geomorphologic background. It is a fact that economic residual deposits can be mined in the peridotitic areas which were peneplanated in tropical climates. However, it is necessary to assert that there have been periods of laterite forming conditions in geologic times similar to the actual laterite forming conditions. This type of a period occured in Turkey as well as in the other parts of the world during the Middle Tertiary and Upper Cretaceous. Although the hostrocks vary in type in the formation of the residual bauxite deposits the peneplanes forming in feldspar and feldspar rich rocks are especially suitable.

The relationship between the bauxite residual deposits and hostrocks can be shown on several examples around the world: The deposits forming in nepheline syenites arc found in Arkansas, Brazil, Guinca and Los Islands; the deposits forming in basalts and dolerites (diabases) are in India, Germany, Scotland, Guinea and Cameroon; the deposits forming in metamorphic schists arc in Guyana Ghana, Guinea and Ivory Costs; the deposits forming in sandstones are in Nigeria. Bauxite deposits forming in carbonaceous rocks are found commonly in Spain, France, Italy, Grece, Yugoslavia and Turkey, that is, around the Mediterranean Sea (Özkoçak, 1980).

As can be seen, the formation of the residual deposits is related not only with hostrock but also with the peneplanation processes. Another effect is suitable climate which produces leaching zone in the peneplanes.

RELATIONSHIP BETWEEN THE RESIDUAL DEPOSITS AND CLIMATE

Another factor I mentioned above for forming residual deposits is climate. These deposits form in the morphoclimatic regions which have tropical climate. Persons (1970) showed the relationship between temperature and precipitation for latcrite formation on a plot (Fig. 2). It is seen on the plot that the average temperature and rainfall for the formation of laterite deposits vary between 18.3-30.0 degree centigrade and 50.8-228.6 centimeter, respectively. According to Golightly (1979) annual rainfall is 159-300 cm.

The formation of the laterite deposits still continues in the tropical and subtropical areas, such as Solomon Islands, Philippines, Cuba, Venezuella, Puerto Rico, Dominica, New Caledonia, Australia, India, Brazil, Guatemala, Indonesia, which have economic residual deposits.

The current climate types in Turkey, some of which are the Mediterranean, Black Sea, and continental climates, are not suitable for the formation of the residual deposits. The average temperatures in the sectors with these climates are as such: The average annual temperature from the Mediterranean cost to the Urfa district 18°-19°C, around the Agcan cost 15°-18°C, along the Marmara Sea and the Black Sea 13°-15°C and in the central Anatolia, 11°-13°C. On the other hand, the highest amount of annual rainfall is in the eastern Black Sea region (higher than 2 m). In the western Black Sea region and the western Mediterranean region and around the Hatay district, the annual rainfall is 1-2 m; in the Aegean and Marmara regions and in most of the eastern Anatolia, the annual rainfall is 0.5-1 m.

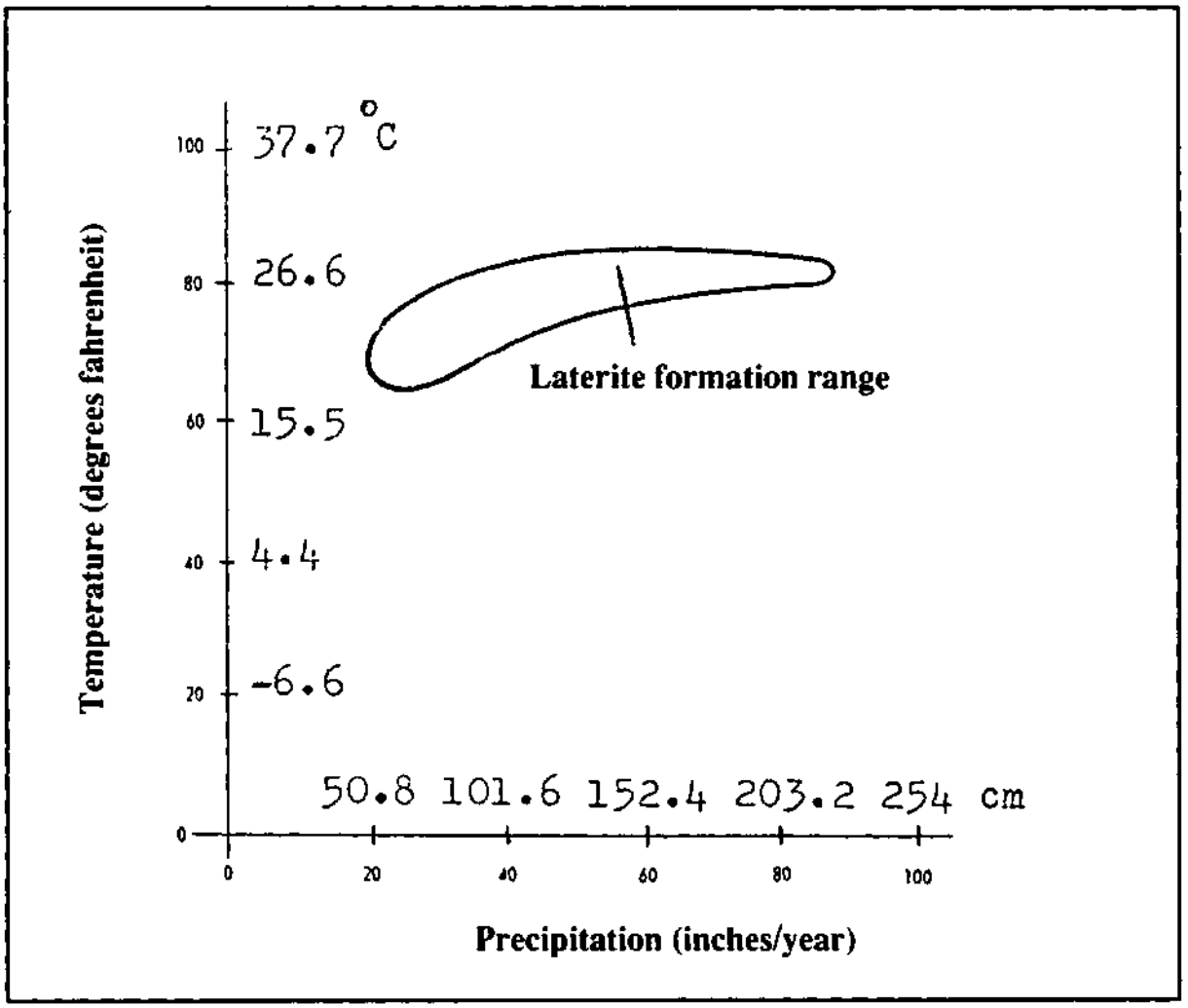

Fig. 2 - Precipitation-temperature relation in laterite formation. Temperatures converted into °C and precipitation values converted into centimeter.

The average temperatures and rainfall in Turkey are lower than the temperatures and rainfall given in Persons (1970). Therefore an actual laterite deposit formation seems not possible in Turkey.

Kurter (1979), who distinguished four effective chemical weathering types in Turkey by using climatic data, pointed out that the eastern Black Sea region has the most intensive chemical weathering. Although the rainfall is quite high in this region temperature is not as high as the tropical regions. Kurter (1970) stated that no part of Turkey has humid tropical conditions. As a result of this, today's climatic conditions have not allowed any lalerite formations in Turkey.

However, besides the actual laterite belt. Riddle Oregon, USA, which formed in laterized plato remnants and the Arkansas bauxite, which formed in a pre-Eocene peneplane and fossilized under the Tertiary sediments (Özkoçak, 1980) are the evidences showing that the necessary climatic conditions were dominant to form residual deposits in North America in the past as it is the case with the actual residual deposits to form residual deposits. In the Mediterranean basin, on the other hand, the nickel laterites in Yugoslavia and Grece have been fossilized by the Cretaceous limestones or Tertiary sediments (Golightly, 1979). In Turkey. 50 m thicklateritic nickel deposits in Çaldağ, Turgutlu (Yıldız, 1977, 1981), the lateritic belt in serpentinitcs around Sivrihisar (Boyalı, 1984; Boyalı and Koç, 1986), the lateritic nickel deposits in Orhaneli, Bursa, although

not very typical (Wilson, 1976), various iron laterites in Erzincan, Sivas, Malatya, Hatay and Ankara (Özkoçak, 1973), the nickel laterite in Frankenstein (Silesia), the allochtonous bauxite deposits in northern Urals, USSR, are the evidences indicating that suitable climatic conditions were also dominant in Asia, Europe and Anatolia in the past as in the North America.

As shown by the examples around the world, it is necessary to know Turkey's paleoclimatic characteristics in order to shed a light on the laterite forming conditions in Turkey. According to the characteristics which have been determined by various authors, while the tropical climate was dominant during the Cretaceous period in the Early Paleocene the climate was warm around the world but later the temperature dropped gradually. In the Eocene, contrary to the Paleocene, the climatic conditions were more evident and around the poles the climate was similar to the temperate climates of today. However, both climate and temperature were higher than the current temperatures of the temperate climates. In the Oligocene, finally, the winters were cooler and the difference between rainy and dry seasons was more evident. The Early and Middle Miocene were periods when a warm humid climate was effective in Turkey for a long time and also an "Anatolian Peneplane" developed in this climatic condition. Contrary to the arid and semi-arid climate in the Upper Miocene, in the Pliocene, a humid-warm climate was effective. During the Early Pleistocene epoch, warm climate withlower humidity was interrupted by short cooler-and-rainy periods.

Consequently, the paleoclimatic data indicate that warm-humid (tropical) climates during the Cretaceous period (specifically the Upper Cretaceous) and the Early-Middle Miocene were the right conditions to form residual deposits in Turkey.

RELATIONSHIP BETWEEN THE TECTONICS AND THE RESIDUAL DEPOSITS IN TURKEY

A relationship between the tectonic activity and the formation of residual deposits in a region should be expected. It is possible to assert that residual deposits form in the rocks in suitable climatic conditions when these rocks are uplifted above the scalevel by tectonic movements. Therefore it is necessary to review briefly the tectonic evolution of Turkey. As it is known, studies have been done for a long time in order to distinguish the tectonic units and determine the tectonic evolution in Turkey (Ketin, 1966). According to the tectonic units of Anatolia which was established by Ketin (1966, 1983), the oldest mountains, the Caledonian and Hercinian massifs, which are located in the Pontides were like islands in the Tethis Sea while the other regions of Anatolia were mostly under the scalevel at the beginning of the Mesozoic Era. The Anatolides developed at the end of the Cretaceous period and were the second in the tectonic evolution. The Torides developed at the end of the Oligocene. The Margin Folds, on the other hand, completed their evolution from the Late Miocene to the Early Pliocene. Therefore it can be asserted that the tectonic-orogenic development in Anatolia was from north to south, and the Pontides, Anatolides, Torides and the Margin Folds developed as mountain bells in this order (Ketin, 1966, 1977, 1983).

As the briefly-reviewed tectonic evolution is assesed regarding the residual deposits it can be asserted that the Ponlidcs, Anatolides and Torides might have been affected by the tropical conditions during the Cretaceous and the Early-Middle Miocene whereas the Margin Folds arc not promising for the development of laterite deposits.

RELATIONSHIP BETWEEN THE EROSION-DEPOSITION PERIOD AND THE RESIDUAL DEPOSITS IN TURKEY

Some regions of Anatolia were uplifted above the scalevel by the tectonic movements that took place from the Upper Cretaceous to the Eocene (Ketin, 1959), however, the actual morphology of Turkey began to form in the Oligocene and completed during the Neogene and Quaternary by internal and external forces (Erol, 1980). However, this process was interrupted by the general tectonic movement and a silence period and also by the changes in the climate. In accordance with this, a geomorphologic evolution occured as erosion and deposition periods lasting from the Late Oligocene to the Pleistocene. According to the principles suggested by Erol (1980, 1983) and the results of the geomorphological studies conducted in the framework of these principles, the erosion-deposition periods that took place in Turkey can be briefly determined as follows:

The oldest geomorphologic remnants belonging to the Upper Cretaceous (DF system).

The Upper Oligocene crosional surfaces (DO systems).

The Lower-Middle Miocene period (D I systems).

The Upper Miocene period (D II systems).

The Pliocene period (D III systems).

The Lowermost Pleistocene period (D IV systems).

The Lower and Upper Pleistocene period.

The Holocene period.

Among these periods, the oldest geomorphologic remnants of the Upper Cretaceous and the crosional surfaces of the Miocene arc significant for the formation of residual deposits. The north and northwest Anatolian mountain ranges were like islands in the Tethis Sea even in Mesozoic, and then, they were raised totally above the scalevel by the tectonic movements in the Oligocene to form that part of Anatolia where the oldest geomorphologic units may be found. The central Anatolian mountain chain, which was subjected to the first intensive orogenic movement at the end of the Cretaceous period and was raised above the scalevel at the end of the Eocene, is an orogenig belt in which relatively younger old-geomorphologic remnants may be found. However, since these units have continuously been eroded since their forming, it is not very probable that these old remnants be preserved. But still, the remnants of the former erosion surfaces in the Cretaceous period have been detected as fossils and some smaller parts of these remnants crop out in some areas where the covering rocks were eroded away (Erol, 1980).

On the other hand, a new erosion-deposition period started over Anatolia by a scries of tectonic movements at the end of the Oligocene and a peneplanc called the Anatolian Peneplanc developed under tropical conditions of this periods. Thus the existence of the remnants of this peneplane has been proven by the geomorphologic studies conducted in various parts of the country (Bilgin, 1969; Atalay, 1977, 1978, 1983; Erol, 1980. 1981, 1983; Kozan et al., 1982; Özgür, 1983; Durukal et al., 1984, 1985; Tonbul, 1986; Tüfekçi, 1987). This erosion-deposition period regarding the laterite deposit is important for Turkey. In this period, the Anatolian Peneplane, which developed under the tropical conditions, was eroded almost down to the scalevel. It is then, possible to assert that a deep leaching zone in this peneplane formed during the crosional period.

As a result, as the erosion-deposition periods are reviewed in respect to the residual deposits in Turkey, the erosion surfaces of the Lower-Middle Miocene (D I systems in Erol, 1980) which started to develope first in Anatolia under the tropical conditions in the Lower-Middle Miocene and were affected by neotectonic movements are significant regarding the formation of the residual deposits. Furthermore, the old geomorphologic remnants of the Upper Cretaceous (DF systems) which arc detected as fossils arc also promising in regard to the residual deposits.

RESULTS

The residual deposits form by peneplanation of the hostrocks containing iron, olivine, pyroxene, feldspar or feldspathoid under the tropical conditions, and by formation of a deep leaching zone in the forming peneplane. This leaching zone is closely related with tectonic stability. In the case that tectonism starts to activate, the residual deposits arc totally or partially eroded and redeposiled in known depression areas to form secondary (allochthonous) deposits. In the world and also in Turkey, the Upper Cretaceous and Lower-Middle Miocene had suitable conditions for the formation of residual deposits. Today, while laterization continues in the tropical bell, actual laterization does not occur in Turkey, for Turkey has no more tropical conditions. On the other hand, the formation of these deposits is also related with tectonic evolution of Turkey. Therefore certain parts of the Pontides where the first and intense orogenic movements occured should be expected to have laterizated under the tropical conditions in the Cretaceous period. During the Lower-Middle Miocene this belt also had the similar climatic conditions. Although the Anatolides and Torides may also be thought to have been affected by the tropical conditions in the Cretaceous period the important role was of the conditions in the Lower-Middle Miocene. The Margin Folds, which were affected by intense orogenic events at the end of the Miocene are not promising for the formation of laterile deposits. In the formation of these deposits; hostrock; climate; topographic features; geomorphologic evolution have significant role. However, there has not been enough information collected in the studies on laterile deposits in Turkey regarding the relationship between the residual deposits and the peneplanation periods and thus the evolution that these deposits have gone through is not known in detail. Therefore, besides the already available methods, the geomorphologic methods should also be

considered, the evolution and relations with the geomorphologic systems should be determined, and the distribution of these deposits should be mapped. It is clear that this type of studies will contribute to the prospection of the primary, secondary and fossil laterite deposits.

ACKNOWLEDGEMENTS

I would like to thank to Prof.Dr. Oğuz Erol for his contributions to this research which was prepared as a Master's seminar and presented in the 12 nd. Geomorphologic Congress.

Manuscript received June 5,1989

REFERENCES

Ardos, M., 1971, I.es surfaces d'erosion et relations avec Les Peneplaines: Jeom. Bull., no. 1.

Atalay, I., 1977, Sultandağları ile Akşehir ve Eber gölleri havzalarının strüktüral, jeomorfolojik ve toprak erozyonu etüdü: A.Ü.Publ. no. 500. Ed. Fak.Publ. no.91, Araştırma Ser. no. 75.

———, 1978, The geology and geomorphology of the Erzurum plain and its surroundings: A.Ü. Publ. no. 543, Ed. Fak.Publ. no. 91, Araştırma Ser. no. 81.

———, 1983, The geomorphology and soil geography ot the Muş plain and its surroundings: E. Ü. Ed. Fak. Publ. no. 24.

Bilgin, T., 1969, Biga yarımadası güneybatı kısmının jeomorfolojisi: İ.Ü. Publ. no. 1433, Cog. Enst. Publ. no. 55.

Boyalı, İ., 1984, Yunusemre - Karaçam - Doğray - Korkun - Karaburun - Dümrek (Mihalıççık, Sivrihisar - Eskişehir) yöresi nikel - kobalt prospeksiyonu: MTA Rep., 7589 (unpublished), Ankara.

———and Koç, İ., 1986, Dinözü - Yarıkçı - Hamidiye - Bahtiyar - Kavak - Beyköy (Mihahççık/Eskişehir) yöresi nikel ve kobalt prospeksiyonu: MTA Rep., 8016 (unpublished), Ankara.

Cornwall, R.H., 1973, Nickel: U.S. Geological Survey Prof, paper, 820.

Durukal, S.; Keçer, M.; Tüfekçi, K.; Durukal, A. and Soylu, C.C, 1984, Şebinkarahisar, Alucra (Giresun) ve Suşehri (Sivas) dolayının jeomorlolojisi: MTA Rep., 7664 (unpublished), Ankara.

———; ———; ———; ———and ———, 1985, The geomorphological relationships between erosion - sedimentation cycles and primary - secondary uranium deposits in Şebinkarahisar (Giresun) region: Jeom. Bull., no. 13.

Erinç, S., 1982. Jeomorfoloji: İ.Ü. Ed.Fak. Publ. no. 2931.

Erol, O., 1980, The Neogenc and Quaternary erosion cycles of Turkey in relation to the erosional surfaces and their correlated sediments: Jeom. Bull., no. 8.

———, 1981, Morphotectonic results of the geomorphological study of the Biga peninsula, Northwestern, Turkey: Bulletin of The Inqua Neotectonic Commision, Number 4, Stockholm.

———, 1983, Neotectonic and Geomorphological Evolution of Turkey: Jeom. Bull., no. 11.

Golightly, J.P., 1979, Nickeliferous laterilcs: A general description. International Laterite Symposium, Newyork.

Ketin, İ., 1959. Türkiye'nin orojenik gelişmesi: MTA Bull., 53, 78-86.

———. 1966, Anadolu'nun tektonik birlikleri. MTA Bull., 66, 20-34.

———, 1977, Türkiye'nin başlıca orojenik olayları ve paleocografik evrimi: MTA Bull., 88, 1-4.

Ketin, İ, 1983, Türkiye jeolojisine genel bir bakış İTÜ Kütüphanesi, 1259.

Kozan, A.T.; Öğdüm, E; Bozbay, E.; Bircan, A.; Keçer, M.; Tüfekçi, K.; Durukal, S.; Durukal, A.; Ozaner, S.and Herece, M., 1982, Burhaniye (Balıkesir) - Menemen (İzmir) arası kıyı bölgesinin jeomorfolojisi: MTA Rep. 7287 (unpublished), Ankara.

Kurter, A., 1979. Türkiye'nin morfoklimatik bölgeleri: İ.Ü. Publ. no. 2585, Coğ.Enst.Publ. no. 106.

Lobeck, A.K., 1939, Geomorphology an introduction to the study of landscape: McGraw Hill Book Company Inc. Newyork.

Özgür, R., 1983, Aydın - Gemerek - Ortaklar Dolayında genç tektoniğe bağlı jeomorfolojik gelişme: MTA Bull., 99/100, 142-147.

Özkoçak, O., 1973, Importance de la geomorphologie pour la recherche des giasement mettaliferes: Jeom.Bull., no. 5.

———, 1980, Sedimanter demir, manganez ve alüminyum yataklarının özellikleri ve oluşum koşulları: MTA Publ., 22.

Persons, S.B., 1970,Laateritegenesis, location, use: monographs in Geoscince, Newyork.

Tonbul, S., 1986, The general geomorphological pacularities and evolution of the western part of the Elazığ district: 10. Türkiye Jeomorfoloji Bilimsel ve Teknik Kurultayı Bildiri Özleri, Ankara.

Tüfekçi, K., 1987, Ilgın gölü dolayının jeomorfolojisi: A.Ü. Fen Bilimleri Ens. Yüksek Lisans Tezi (unpublished).

Vinogradov, A.P., 1956, The regularity of distribution of chemical elements in the earth's crust: Geochemistry (Geokhimia) no.1 (English Hd).

Voloboycv, V.R., 1961, TICSS, 6,:Vol. 20, 1956, Sov.Soil. Science no. 11.

Wilson, H.D.B., 1976, Nickel and chronium associated with ultrabasic rocks in Turkey: MTA Kütüphanesi.

Yıldız, M., 1977, Manisa ili, Turgutlu ilçesi, Çaldağ civarının Ni - Co etüt ve arama raporu: MTA Rep. 6813 (unpublished), Ankara.

———, 1981, Çaldağ nikel yataklarının maden jeolojisi ve ekonomik potansiyeli: Ege Bölgesi Yeraltı Kaynakları Kongresi Bildiri Özleri, İzmir.

PETROGRAPHICAL STUDY OF THE ZINC-LEAD DEPOSITS IN THE BOLKARDAĞ (ULUKIŞLA-NİĞDE) DISTRICT

Sedat TEMUR***

ABSTRACT— In the studied area, the ore are presented both by primary mineralizations which are composed of sulphide minerals and by secondary mineralizations which are composed of oxide and carbonate minerals. In the primary mineralizations the main minerals are pyrite, sphalerite and galena. Also there are pirrotite, arscnopyrite, chalcopyrite, argantite, pyrargirite, magnetite, fahlore, geocronite, freislebenite. boumonite, marcasite, boulangerile, meneginite, skutlerudite, molybdenite, electrum, native Au and native Ag in minor ratios. In primary ore, the common gangue minerals are quartz, calcite and dolomite. In minor ratios, there are barite, siderite, seriate, biotite, muscovite and chlorite. The secondary minerals are smitsonite, anglesite, seruscite, hematite, lepidocrocite, amorph iron hydroxide, gothite, malachite, azurite, hemimorphide and hydrozincite. The main mineralization which occurs within some representative minerals has been realized in four period. These periods can be distinguished by the definite textural and structural features such as exsolution, inclusion, idiomorphism, slit, metasomatose or by the appearance and absence of some minerals.

PETROLOGY OF THE PLIOCENE VOLCANICS AROUND MUŞ SE, ANATOLIA

Ahmet TÜRKECAN*

ABSTRACT— This study has been carried out in the Muş region in southeast Anatolia. It covers particularly the petrography and geochemistry of the Pliocene aged volcanics in the region. In general volcanics are observed as plateau lavas having all properties of alkaline volcanism. Sometimes peralkaline and tholeiitic volcanism can also be observes together with these alkaline volcanics. The major and trace elements of the volcanics show that they are indicative of an intracontinent. The radiometric datings showed that the volcanism which gave the first products of neomagmatism started in the Early Pliocene.

Mineral Res. Expl. Bull., 112,47-58.1991

SHOSHONITIC, MONZONITIC PLUTON NEAR MURMANO, EASTERN CENTRAL TURKEY - A PRELIMINARY NOTE

H.P. ZECK* and Taner ÜNLÜ**

ABSTRACT— The major and trace element composition of three series of samples from the Murmano pluton (Divriği-Sivas), eastern central Turkey, has been investigated in this study. Element distribution patterns as shown in variation diagrams favour the hypothesis that the pluton has a composite character, consisting of a number of intrusive bodies, representing separate magma batches. Earlier geochronological investigations suggest that the Murmano pluton postdates the ophiolite obduction in the area. Mineralogical criteria and the chemical data presented here indicate that the rocks are I-type plutonic rocks which have many characteristics of the calc-alkaline rock series for which current classification diagrams indicate an active subduction zone setting. High total alkalies versus SiO_2, K_2O versus SiO_2, K_2O/Na_2O, Rb, Ba, Al and Fe_2O_3/FeO, and low TiO_2 suggest that the pluton has a shoshonitic character.

INTRODUCTION

The Murmano pluton intrudes the ophiolites of the Inner Tauride suture zone, located between the Kırşehir and Tauride blocks (Fig. 1), and postdates the ophiolite obduction (Zeck and Ünlü, 1988a; 1988b). The pluton bears a composite

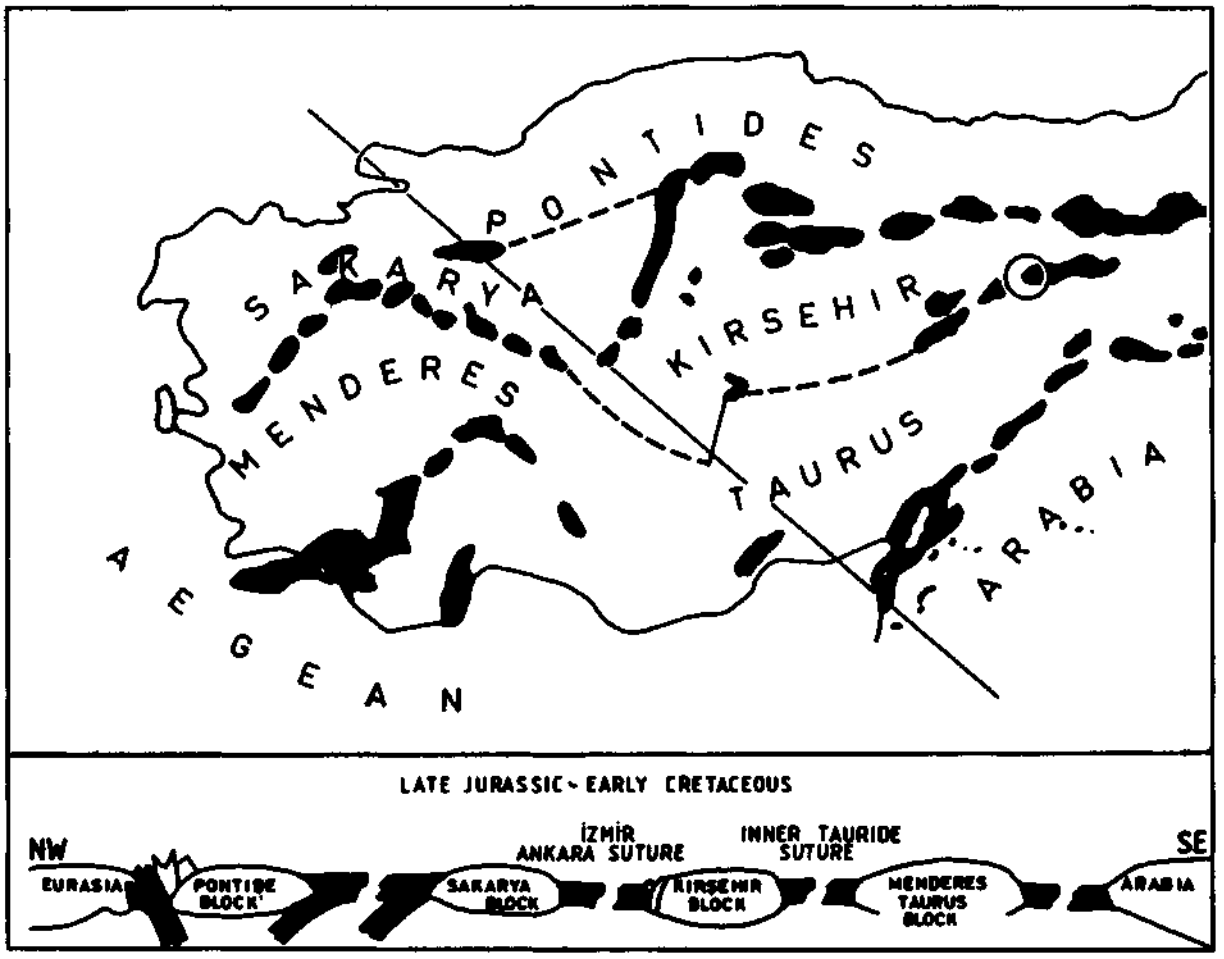

Fig. 1 - Geological sketch map showing the distribution of ophiolite complexes in Turkey. The cross section outlines the proposed plate tectonic model for the Late Jurassic-Early Cretaceous (Şengör and Yılmaz, 1981; Görür et al., 1984; Robertson and Dixon, 1984). Circle indicates location of the area investigated.

* Geological Institute, University of Copenhagen, Denmark.
** Ankara Üniversitesi, Fen Fakültesi, Jeoloji Mühendisliği Bölümü, Ankara- Turkey.

character and at least two magma batches are thought to be involved. In a Nicolaysen diagram these magma batches define parallel isochrons which indicate an intrusion age of 110±5 Ma (Zeck and Ünlü, 1987). The initial $^{87}Sr/^{86}Sr$ ratios for these two isochrons are 0.7069 and 0.7059, respectively, suggesting that two different magmatic sub-systems were involved. An origin of these two magmas by fractional crystallization of the same starting magma seems unrealistic in view of the large difference in initial $^{87}Sr/^{86}Sr$ ratio between the two magmas. More feasible models for the origin of these magmas are, for example, different degrees of crustal assimilation by the same starting magma, mixing of two magmas in different proportions, various proportions of restite/melt mixing in an anatectic setting and anatexis of different source rock complexes. All these models except the last would be expected to give rather simple variation diagrams determined by mixing lines between two compositions.

The present paper focusses on the major and trace element geochemistry of the pluton and the interpretations in Zeck and Ünlü (1987,1988a, 1988b) are verified. The data obtained are used to characterize the plate tectonic setting of the rocks. Chemical variations between the various sub-areas of the pluton are discussed with the aim to further constrain the choice of possible petrogenetic models for the pluton.

GEOLOGICAL SETTING, FIELD RELATIONS AND PETROGRAPHY

The inner Tauride suture zone within which the Murmano pluton is located is characterized by the occurrence of many ophiolite complexes (Fig. 1). The geological map of the area NNW of the town of Divriği which contains the Murmano pluton was made by Koşal (1973). The ophiolite complex in the area studied appears dismembered, consisting mainly of serpentinites. The Murmano pluton is intrusive into the serpentinites (Zeck and Ünlü, 1988a; 1988b).

The Murmano pluton typically consists of massive rocks. An obscure flow foliation has only been observed locally. Interpenetrative foliation or lineations of metamorphic-tectonic origin are absent. Modal compositions vary from quartz syenitic through monzonitic to dioritic (plutonic rock classification and nomenclature is according to Streckeisen, 1976). Monzonite is the predominant rock type in the composite pluton. Some petrography is given here; for more details see Zeck and Ünlü(1987).

The diorites occur mainly in the SW part of the pluton. The rocks are coarse-to medium-grained. Light grey, euhedral-subhedral, 0.5-2 cm. large crystals of plagioclase dominate the hand specimen. Thin sections demonstrate the otherwise obscure mega-crystic nature of the rocks and the presence of a flow foliation, both mainly supported by the plagioclase crystals set in a mm-sized matrix consisting of plagioclase, biotite an clinopyroxene. Plagioclase typically has a composition of An_{60-30} K-feldspar is absent or forms a few rare crystals in the matrix. Biotite forms independent crystals within the plagioclase framework, but also forms crystals surrounding, and probably grown on, crystals of clinopyroxene and opaque material, and, together with amphibole these replace the clinopyroxene to some extent. The colour index is 30-40. LT alteration products amount to 1 -2 vol % of the rocks.

The monzonites are medium-to coarse-grained, have a massive structure and a greyish appearance, somewhat lighter in colour than the diorites. Many of them have clinopyroxene and biotite as major mafic minerals, amphibole being present as minor replacements of clinopyroxene. In others, hornblende (-like amphibole) is the dominant mineral, most sections enclosing remnants of clinopyroxene. In many samples titanite is a rather important mafic mineral (1-2 vol %), rather than an accessory. K-feldspar is perthitic and forms up to 2 cm. large poikilitic crystals enclosing all other components, namely smaller euhedral plagioclase crystals. Plagioclase also forms larger, 1-2 cm. large crystals. LT alteration products form up to c.1 vol % of the rocks.

Within the coarse-to medium-grained, typically plutonic rocks which make up the bulk of the Murmano pluton, fine-grained, in part porphyritic rocks were found which in many cases form dykes with sharp contacts towards the plutonic rocks; in some cases the field relations are somewhat uncertain. Many of these fine-grained rocks show the same mineralogical relations as the plutonic rocks, indicating close genetic relations. Some others show a somewhat different mineralogy, suggesting more complex genetic relations towards the monzonites-diorites.

The fine-grained rocks with a similar mineralogy as the monzonites-diorites comprise micro diorites, micro syenites, and micro quartz syenites. Most rocks are porphyritic with a (very) fine-grained groundmass (f = 50-400 m m.) and pheno-

Table 1- Chemical composition, major and trace elements, of a suite of rocks from the Murmano pluton.

	AREA "A" △							AREA "C" ○								AREA "B" ●								
%	85Z126	85Z127	85Z128	85Z129	85Z130	85Z131	85Z132	85Z134	85Z136	85Z137	85Z138	85Z139	85Z140	85Z142	85Z143	85Z150	85Z151	85Z152	85Z153	85Z154	85Z155	85Z156	85Z157	85Z158	85Z159
SiO_2	52.72	51.55	47.45	60.73	56.44	66.33	60.19	63.01	63.06	63.66	62.65	64.51	64.19	60.34	59.56	64.23	59.59	60.07	59.91	50.99	68.00	59.69	60.20	59.66	59.01
TiO_2	1.05	0.71	0.99	0.52	0.76	0.42	0.80	0.58	0.58	0.54	0.55	0.52	0.52	0.79	0.85	0.54	1.07	0.98	0.82	1.00	0.35	0.99	0.95	1.10	1.07
Al_2O_3	18.92	16.43	18.44	17.01	18.66	15.96	17.41	16.73	17.01	16.51	16.84	16.80	16.67	17.00	17.08	16.60	17.57	17.95	18.17	16.71	15.86	17.60	17.40	17.71	17.57
Fe_2O_3	1.88	1.28	2.83	0.34	0.78	0.36	0.47	1.23	1.21	1.59	1.65	1.38	1.38	1.01	1.70	1.33	2.25	0.40	1.62	0.44	0.80	1.99	1.81	0.52	2.20
FeO	4.42	3.32	5.09	0.52	1.22	0.39	1.05	2.37	2.46	2.17	2.33	2.26	2.14	3.63	3.34	1.90	2.58	1.22	2.19	2.39	0.85	2.05	2.04	1.29	2.64
MnO	0.11	0.10	0.14	0.03	0.04	0.02	0.05	0.06	0.06	0.07	0.06	0.66	0.66	0.09	0.09	0.06	0.06	0.05	0.04	0.06	0.02	0.04	0.05	0.05	0.05
MgO	3.66	6.06	6.88	1.56	3.52	0.76	2.33	1.67	1.67	1.58	1.70	1.49	1.51	2.16	2.36	1.56	1.97	1.91	1.47	4.70	0.50	1.95	1.84	2.03	2.06
CaO	7.40	13.86	11.29	4.20	8.19	2.34	6.12	3.71	3.73	3.39	3.63	3.27	3.46	4.29	4.72	3.55	4.20	6.29	4.04	13.90	2.24	4.59	4.44	6.48	4.69
Na_2O	4.40	3.19	2.96	2.54	6.22	4.15	4.50	4.62	4.58	4.42	4.67	4.56	4.55	4.57	4.38	4.47	4.80	5.08	5.23	5.07	4.17	5.02	4.91	4.97	5.02
K_2O	3.28	1.49	2.09	9.90	1.01	7.09	5.81	4.79	4.61	4.71	4.41	4.74	4.57	4.65	4.66	4.71	5.09	4.97	4.90	0.78	6.39	4.87	5.09	4.90	4.91
P_2O_5	0.46	0.69	0.45	0.20	0.26	0.21	0.31	0.24	0.25	0.23	0.24	0.22	0.23	0.30	0.34	0.23	0.34	0.33	0.27	0.33	0.16	0.35	0.33	0.37	0.36
LOI	1.03	0.98	1.18	2.08	2.46	1.16	0.57	0.67	0.69	0.47	0.66	0.57	0.54	0.72	0.60	0.46	0.49	0.38	0.44	2.89	0.23	0.41	0.36	0.33	0.51
TOT	99.33	99.66	99.79	99.63	99.56	99.19	99.61	99.68	99.91	99.34	99.39	100.98	100.42	99.55	99.68	99.64	100.01	99.63	99.10	99.26	99.57	99.55	99.42	99.41	100.09
ppm																									
Rb	97	43	108	286	33	206	141	169	171	173	157	193	177	160	184	159	154	117	134	29	189	133	143	134	141
Ba	1200	541	1636	1536	248	1042	1107	972	970	886	944	937	920	1053	1101	929	1355	1188	1296	122	757	1349	1406	1266	1237
Pb	8	7	1	1	5	5	7	8	9	5	7	8	7	5	6	5	11	9	7	34	6	3	9	6	7
Sr	555	676	966	242	425	185	346	340	351	323	337	332	334	338	390	328	352	352	337	372	207	366	363	375	364
La	32	51	20	36	19	25	38	57	39	41	42	41	49	32	61	39	31	57	52	23	63	40	41	47	48
Ce	61	70	43	43	41	41	66	66	67	64	73	67	64	60	71	64	58	92	59	47	66	61	68	71	61
Nd	27	35	20	21	22	18	29	27	34	28	29	27	25	29	34	26	27	33	28	24	26	29	31	29	30
Y	23	30	19	25	23	24	27	24	33	26	23	26	25	24	30	25	27	29	25	25	28	30	29	30	28
Th	8	8	4	26	23	24	15	20	20	24	21	23	23	14	22	21	21	23	16	12	43	23	22	18	17
Zr	115	103	57	221	208	190	204	200	183	218	200	206	216	266	289	200	233	236	189	146	262	223	202	239	237
Nb	24	9.8	20	27	32	23	25	24	29	28	25	27	26	27	28	25	29	27	30	15	30	29	28	30	30
Zn	72	31	75	1	7	1	6	12	17	14	18	14	11	19	24	6	8	17	11	107	1	3	9	2	9
Cu	16	5	24	2	8	3	4	2	4	2	2	2	2	2	2	2	2	3	12	22	2	2	2	2	2
Co	47	50	42	34	23	51	42	52	50	66	60	68	73	64	57	68	48	75	60	48	96	58	54	58	53
Ni	38	59	114	32	30	18	30	17	22	17	15	17	18	23	25	15	14	14	14	9	14	18	15	18	13
Sc	11	26	19	5	5	4	7	8	8	7	9	7	6	8	8	6	10	7	8	13	5	9	10	7	9
V	130	121	230	30	43	25	65	56	56	50	53	48	49	80	82	51	82	64	64	126	18	81	77	80	85
Cr	75	154	288	13	10	9	31	20	21	18	21	17	17	35	33	19	17	14	13	22	11	18	18	20	19
Ga	19	13	15	17	12	17	17	15	19	20	15	16	17	17	16	18	18	17	18	18	16	19	16	19	19

crysts of plagioclase, K-feldspar and amphibole, which latter may have replaced earlier magmatic clinopyroxene. LT alteration products are more abundant than in the monzonites-diorites, amounting to c.3-5 vol %. Some more even-grained micro quartz syenites occur and these are very similar to the monzonites.

Of the rocks with deviating mineralogy, two types were recognized. Micro-dioritic rocks with kersantitic character, showing grain sizes of 0.1-3 mm, consist mainly of plagioclase, clinopyroxene, biotite and opaque material. Some olivine occurs and the colour index is c. 45, mainly due to c. 25 vol % of biotite. The alteration products amount to c. 2 vol % of the rock. Scapolite-rich rocks were found in clear cut, 0.5-1 m wide dyke bodies. The rocks consist of c. 50 vol % of scapolite, forming a poikiloblastic matrix enclosing all other components of the rock (clinopyroxene, 30-35 vol %, plagioclase, c. 15 vol %, titanite, amphibole, biotite, carbonate, and chlorite). The rocks are interpreted as sub-volcanic dykes, the glassy or very fine-grained groundmass of which has been completely replaced by scapolite (Zeck and Ünlü, 1987).

GEOCHEMISTRY

Major element analyses were made by X-ray fluorescence analysis of glass discs prepared with a sodium tetraboraie flux, except for Na and Mg which were analysed by atomic absorption and volatiles which were obtained as loss on ignition.

Trace elements were analysed directly on pressed powder pellets by X-ray fluorescence using a Philips PW 1400 and the techniques of Norrish and Chappell (1977). Results were corrected for background interference from tube and sample spectral lines, and for matrix variation (using the major element composition). USGS Standards (G-2, GSP-1, AGV-1, W-l, BCR-1, PCC-1) were used for calibration (Gladney et al., 1983).

The results of the analyses are presented in Table 1, and a number of variation diagrams. Figs. 3-11.

INTERPRETATION AND DISCUSSIONS

A crucial element in the interpretation of the Rb-Sr isotopic systematics of the pluton is the observed composite character of the intrusive body (Zeckrand Ünlü, 1987). This suggestion was based on the study of Rb-Sr isotopic relations in two restricted areas, 3-4 km apart (Fig. 2). In the present paper a new series of samples is introduced, consisting of 9 samples collected along the main road, c. 2-3 km SE of the village of Murmano. The area in the south-western part of the body will be referred to as area "A", that in the southern part as area "B" and the new area along the road as area "C".

A number of selected chemical components have been plotted for these three sample series. In the selection of these components emphasis has been placed on relatively immobile components. The distribution of these components may be expected to give an indication of the original, magmatic relations within the intrusive body. These components will not have been affected, or only to a limited degree, by the post magmatic alterations which were observed in the rocks.

Two major components, TiO_2 and MgO, were plotted in Harker diagrams. The two diagrams (Fig. 3a,b) show rather different relations. TiO_2 shows a separate trend and distribution for area A compared to the other two areas. Areas B and C show the same trend, but the distribution along the trend is different. Considering that the rocks of these two sample series show a very similar mineralogy, indicating a similar level of differentiation, this suggests that also these two sample series may represent different magmatic material. Note the position of sample 85Z154, a heavily scapolitized rock (Zeck and Ünlü, 1987). Apparently the scapolitization process involved a Considerable loss of SiO_2.

MgO shows a well defined common trend for all three sample series. This diagram on its own merit could explain the rocks in the pluton as members of the same differentiation series. The difference between the three series here is mainly one of different distribution along the same trend. The position of the scapolitized sample may suggest that a considerable increase in the MgO percentage has taken place, combined with a SiO_2 decrease.

Sr shows a rather well defined trend (Fig. 3c), when the scapolitized sample is disregarded. In detail, the three areas might possibly define three parallel trends, with C defining the highest, B the intermediate and A the lowest in the Sr-SiO_2 diagram. Scapolitization seems not to affect the Sr content.

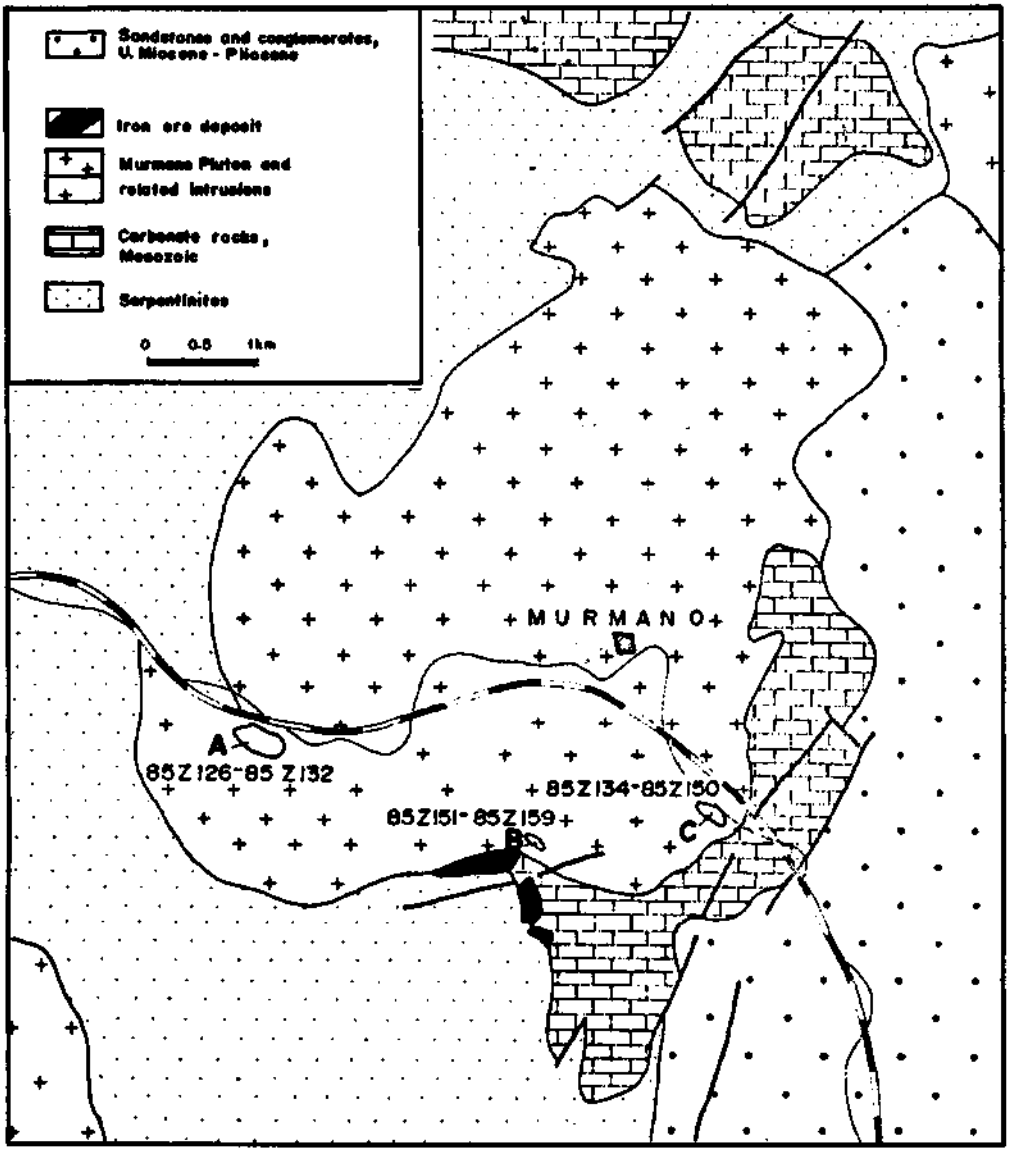

Fig. 2 - Geological map of the area containing the Murmano pluton, Koşal (1973).

Y shows rather complex relations (Fig. 3d). The samples from area A show a distribution which is different from that from the other two areas. Areas B and C show similar patterns. Scapolitization seems to involve a decrease in Y content. The relations for Zr (Fig. 3e) and Nb (Fig. 3f) conform to those for Y.

Ni and Sc show very similar behaviour (Figs. 3g, h). Area A shows clear differences from the other two areas. Areas B and C show considerable similarity. Scapolitization seems hardly to affect Ni and may involve a slight increase in Sc combined with a decrease in SiO2.

K/Rb ratio distribution versus SiO_2 (Fig. 4) shows clear differences between the three areas. The Scapolitization seems to involve a decrease of K/Rb combined with a decrease in SiO2.

Rb/Sr relations (Fig. 5) show systematic differences between the three areas. Scapolitization resulted in a strong Rb depletion, whereas Sr seems hardly affected (Fig. 3c).

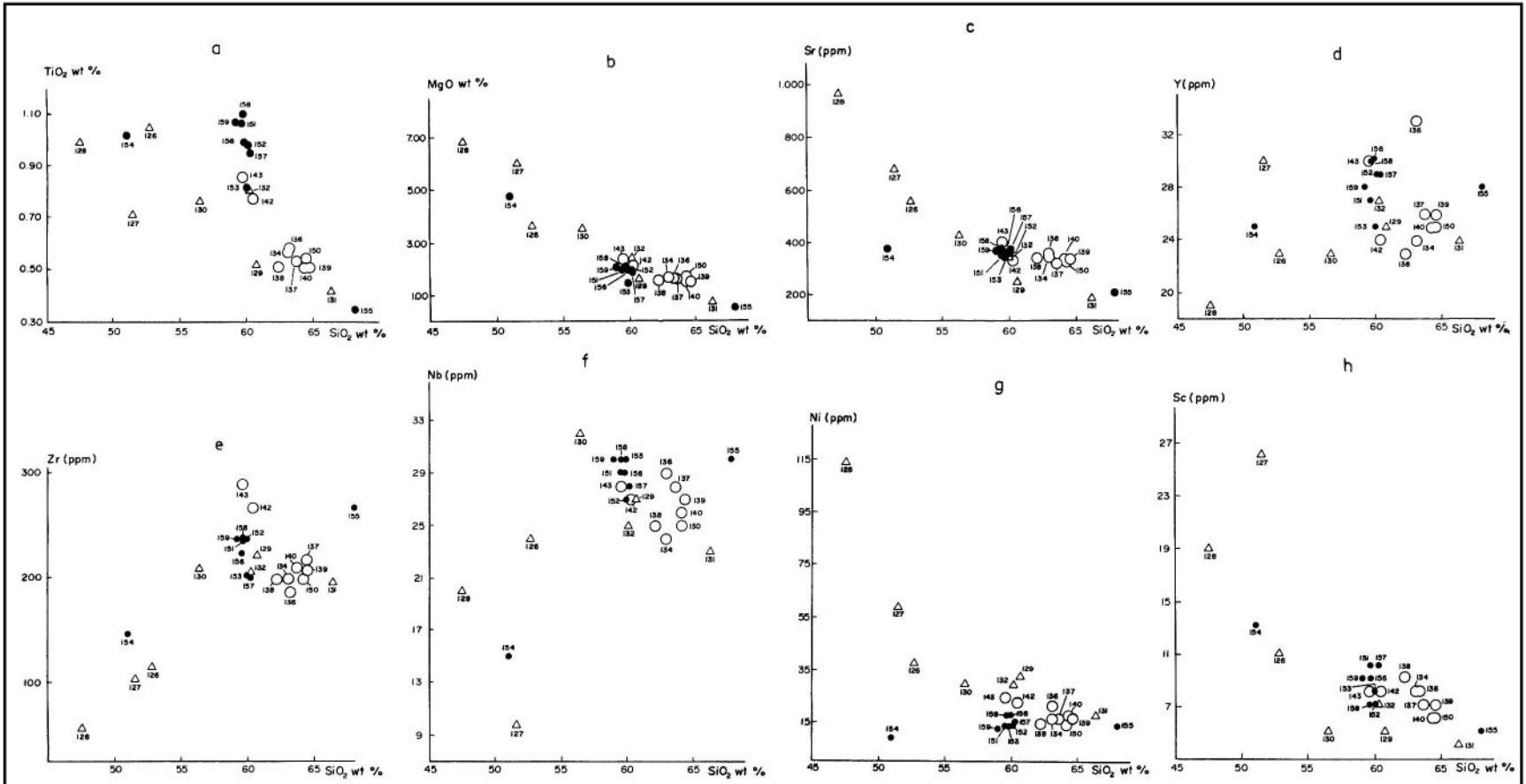

Fig. 3 - Eight Harger diagrams of two components (TiO_2 and MgO) and six trace elements (Sr, Y, Zr, Nb, Ni and Sc). Signatures: triangles-sample series at the south western side of the body (85 Z 126-85 Z 132); closed circles-sample series at the southern side of the body (85 Z 151-159); open circles-sample series along the road, c.2-3 km SE of Murmano (85 Z 134-150)

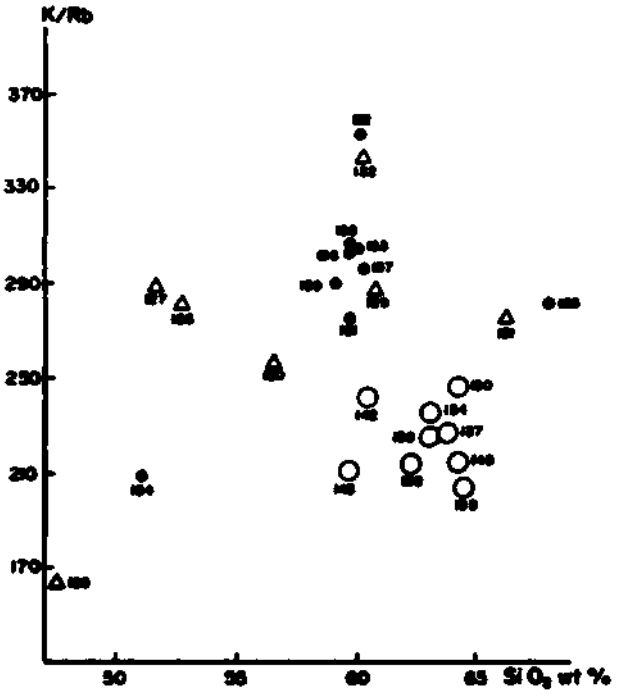

Fig. 4 - K/Rb-SiO_2 diagram. Signatures as in Fig.3.

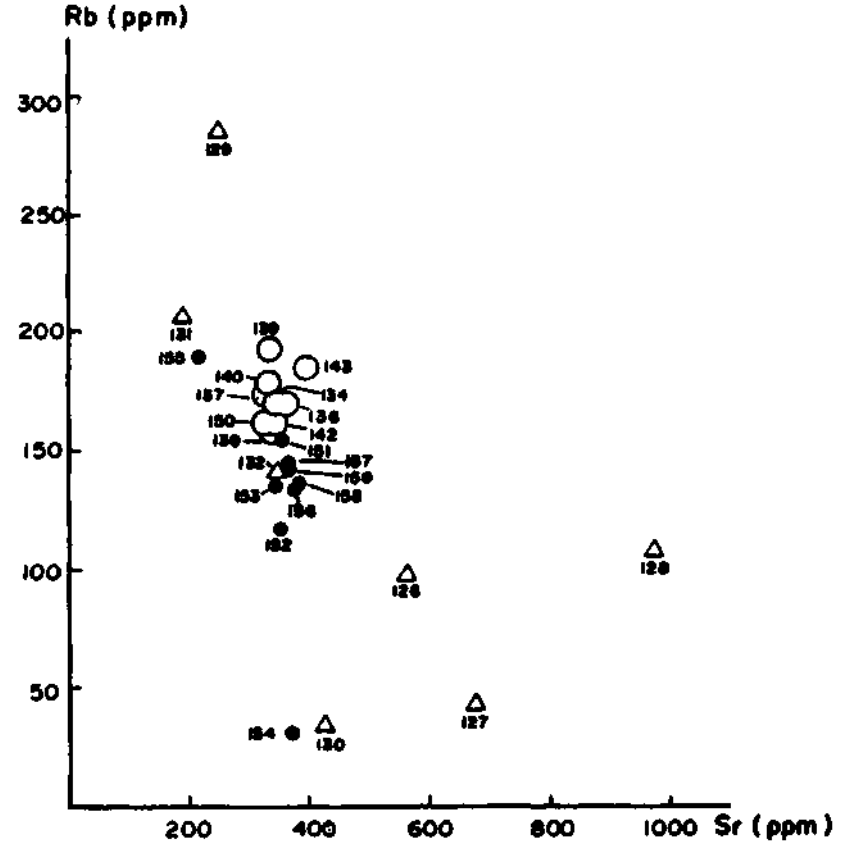

Fig. 5 - Rb-Sr diagram. Signatures as in Fig.3.

The geochemical relations discussed above seem to indicate that there is a clear difference between area A on the one hand and B and C on the other. The differences between B and C are less well defined, but in some of the diagrams, for example K/Rb, differences are suggested. The conclusion on the basis of the available data therefore would be that the hypothesis, that the Murmano pluton consists of a number of separate intrusive phases which represent different batches of magma, is confirmed by the major and trace element geochemistry.

The geochemical character of the intrusion as a whole gives valuable information about its plate tectonic setting. Fig. 6 shows the distribution of 25 samples plotted in the AFM diagram. The pattern is indicative for a calc-alkaline ser-

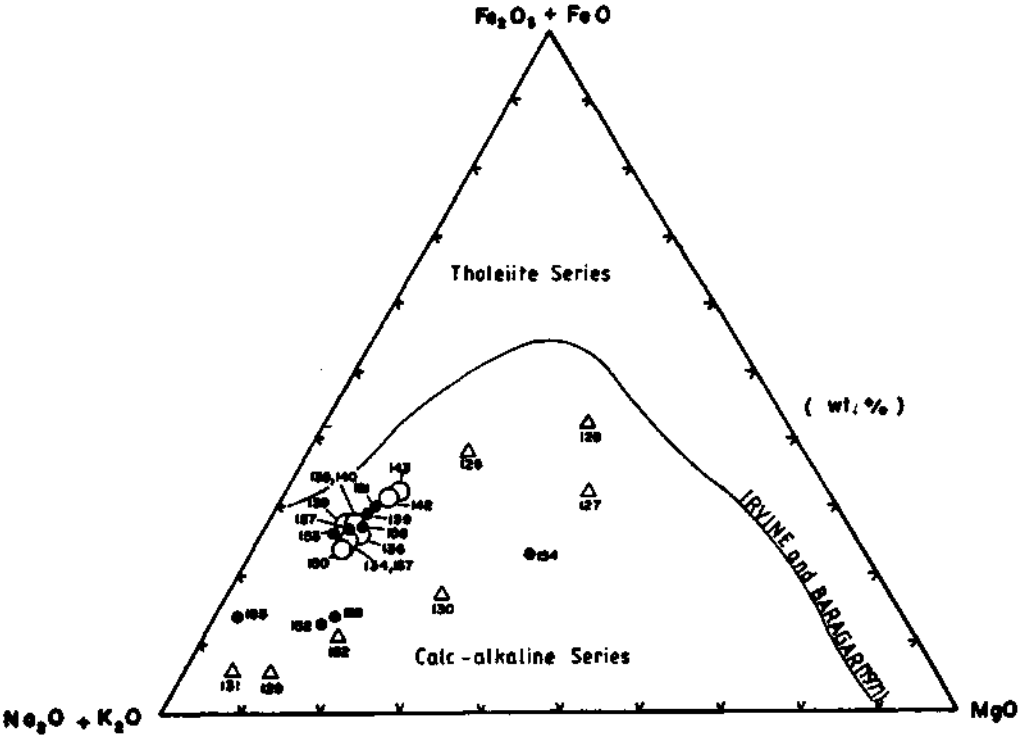

Fig. 6 - AMF diagram. Dividing line after Irvine and Baragar (1971). Signatures as in Fig.3.

ies related to lithosphere subduction (Irvine and Baragar, 1971). Figs. 7a and b support the non-tholeiitic, calc-alkaline nature of the pluton. Earlier investigations (Bayhan, 1980; Bayhan and Baysal, 1982) have indeed classified the Dumluca pluton. which is located only c.1.5 km SW of the Murmano pluton, as calc-alkaline. However, a number of discrimination diagram plots and other geochemical criteria seem to indicate a shoshonitic character for the Murmano pluton studied here. The (Na_2O+K_2O) versus SiO_2 diagram (Irvine and Baragar. 1971; Morrison, 1980), see Fig. 8, suggests a shoshonitic or alkaline rather than a calc-alkaline nature. The K_2O versus SiO_2 diagram (Peccerillo and Taylor, 1976; Morrison, 1980; Rickwood. 1989). see Fig. 9. suggests a shoshonitic rather than a calc-alkaline character. The MgO versus FeO* diagram, see Fig. 10, suggests a shoshonitic rather than a calc-alkaline or alkaline nature for the rock complex. It is noted that this latter diagram demonstrates that the Murmano rock series is decidedly poorer in FeO* than the rocks compiled by Morrison (1980).

The majority of the samples have a SiO_2 content within the range for andesites. With some reservations for the plutonic character of the Murmano rock series, we could therefore apply the criteria given by Bailey (1981) to discriminate between three erogenic settings: oceanic island arc, continental island arc and andean. Eleven of our samples (Table 1) have a SiO_2 content between 59.00 and 62.00, which represents the andesite screening window preferred by Bailey (1981). For these samples K_2O/Na_2O ranges from 0.94 to 1.06 (not counting two outliers at 1.29 and 3.90) with a mean

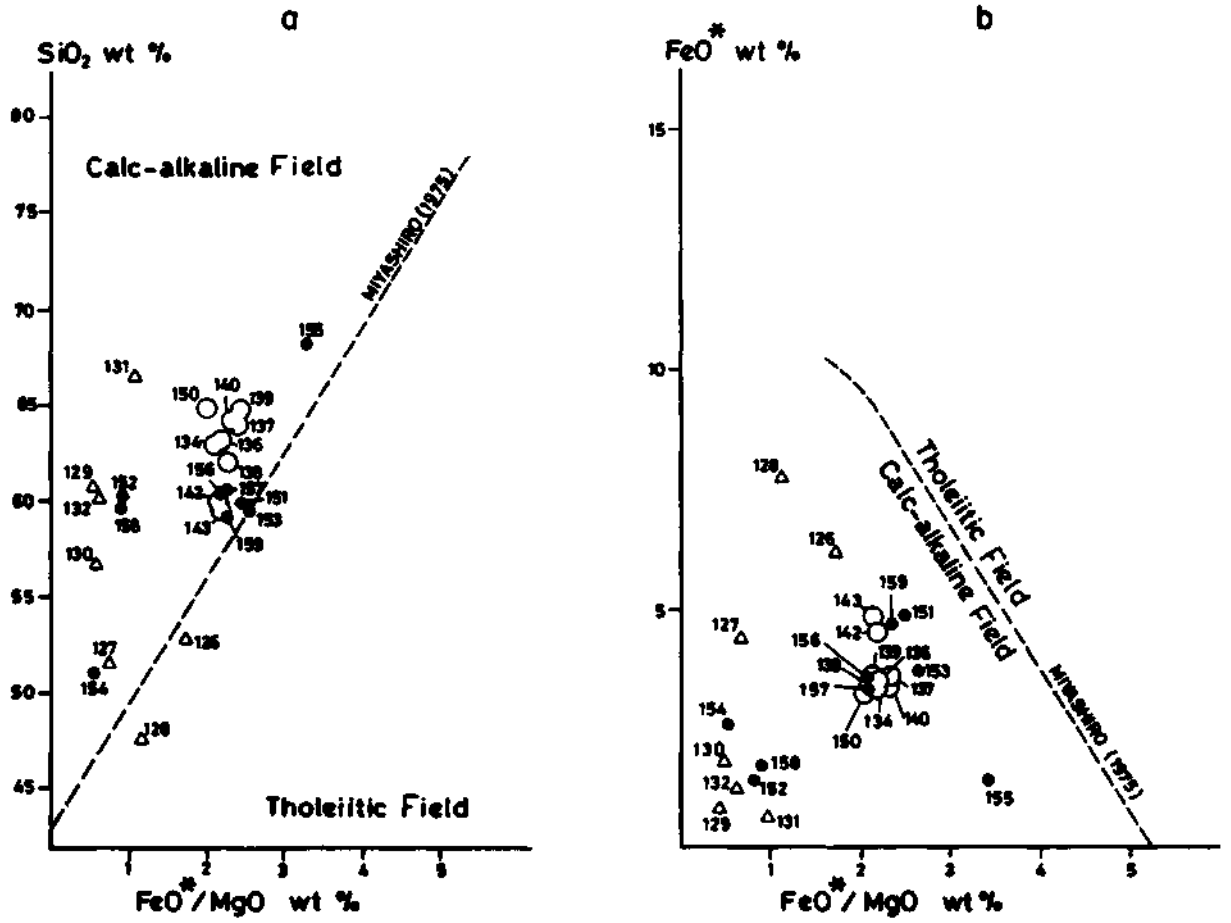

Fig. 7 - a - SiO_2-(FeO*/MgO) and b-FeO*- (FeO*/MgO) diagrams. Dividing lines after Miyashiro (1975). Signatures as in Fig.3.

value of l.(X). which conforms to the value given for shoshonitic andesites. Rb content is high (ranging from 117 to 184 ppm. with a mean value of 144 ppm). and also Ba content is high (ranging from 1053 to 1536, with a mean value of 1263 ppm). which also is in agreement with a shoshonitic character. Sr on the other hand is rather lower (range 338-390, mean 358 ppm). than suggested by Bailey (1981).

A continental island arc setting is suggested by 1) P/La values ranging from 23 to 48, with a mean value of 33, 2) K/La values ranging from 634 to 1363, with a mean of 975, and 3) Zr/Y values ranging from 6.97 to 11.08, with a mean of 8.39. Th contents ranging from 14 to 26, with a mean of 20 ppm. and Ni contents ranging from 13 to 32. with a mean of 20 ppm favour an Andean or continental island arc setting, in that order. La/Y values ranging from 1.15 to 2.08. with a mean value of 1.58 favour an oceanic or continental island arc environment, in that order. It may be concluded that the trace element content seems to favour a continental island arc setting.

Also for granitic rocks geochemical distribution diagrams have been calibrated in order to discriminate between rocks from different geotectonic settings, e.g.. Didier and Lameyre (1969), Chappell and White (1974), Pitcher (1983) and Pearce el al (1984). The diagrams given by Pearce et al. (1984) employ Y. Nb. Rb and SiO_2 contents to discriminate between granitic rocks from within plate settings (WPG), ocean ridge settings (ORG) collision settings (COLG) and volcanic arcs (VAG). The Murniano plutonic rocks consistently plot in the VAG field (Fig. 11a-d). in agreement with the continental island are setting suggested above.

Another system of discriminating between different granitic rock types on the basis of their plate tectonic setting, employs 5 different, types of granitic material. The M-type includes the rare plagiogranites of oceanic island arcs. The

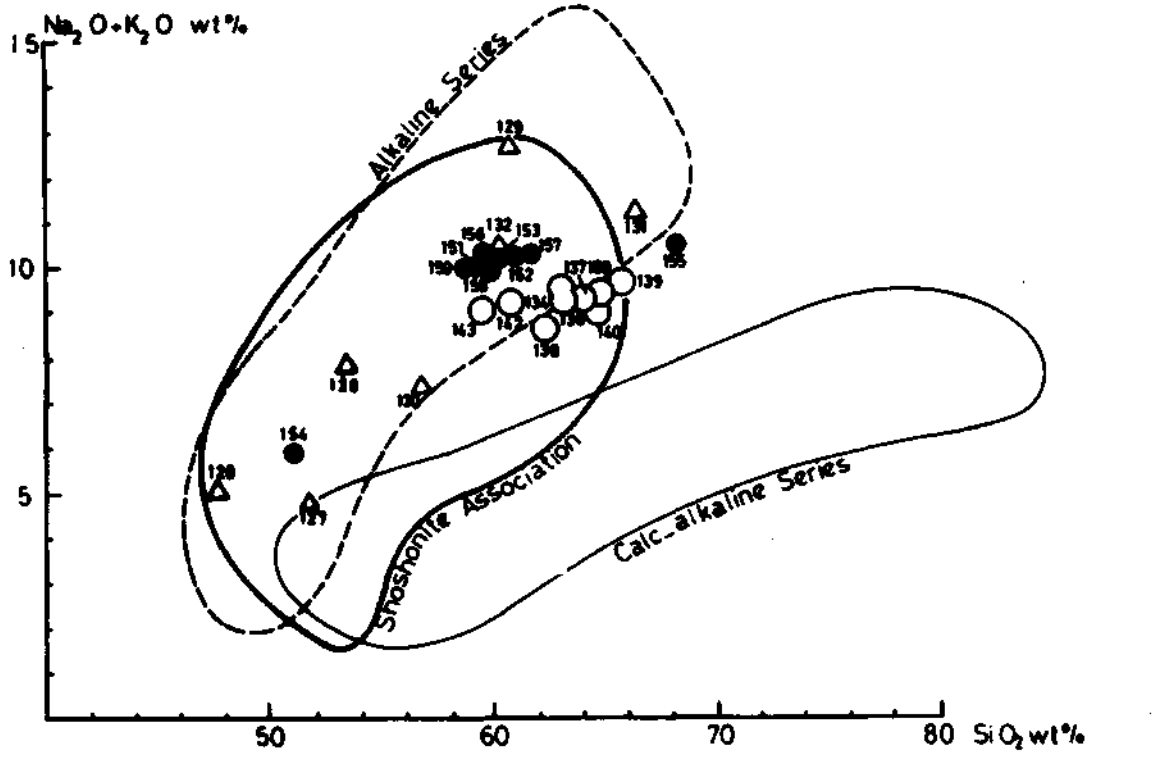

Fig. 8 - (Na_2O+K_2O)-SiO_2 diagram. Fields for calc-alkaline and alkaline series Irvine and Baragar (1971), shoshonite association Morrison (1980). Signatures as in Fig.3.

I_{co}-type (Cordilleran type) is transitional to the M-type and comprises the voluminous gabbro/quartzdiorite/tonalite assemblage of active continental plate edges. The I_{ca}-type (Caledonian type) is different from the Cordilleran type; it represents the granodiorite/granile series of post-orogenic uplift regimes. Clearly separate is the S-type series which incorporates the peraluminous granite assemblage of eucratonic and continental-collision fold belts. Also rather well defined is the so-called A-type (Loiselle and Wones. 1979). which comprises the alcalic granites of both the stabilized fold belts and rifting systems of cratonic areas.

A number of chemical and mineralogical criteria have been put forward to differentiate between the various types of granitic rocks. A major mineralogical criterion is given by the nature of the mafic minerals. In the Murmano pluton, clinopyroxene, hornblende and biotitce are the major mafic minerals. This is common in M-and I-series, and seems to rule out the S-and A-types, which show muscovitc, brown-red biotite, garnet and cordierite, and green biotite, alkali amphiboles and pyroxenes, respectively. The widespread occurrence of titanite favours the I_{co}-type over M-type and I_{ca}-type .

Isotope geochemistry data, such as the initial $^{87}Sr/^{86}Sr$ ratio can also be used to characterize the plate tectonic setting. Initial $^{87}Sr/^{86}Sr$ ratios for the Murmano pluton are between 0.7059 and 0.7069. These values seem to rule out an M-typification for which values < 0.704 are given. For I_{co}- and I_{ca}-types, values of <0.706, and 0.705< <0.709 are given, respectively (Pitcher, 1983). The Murmano values seems to fit the I_{ca} range best.

It is of special interest to note that on the basis of a global compilation, porphyry Cu and Mo mineralisations are connected to this type of granitic rocks. However, in the case of the granitic rocks in the Inner Tauride suture zone, this seems not to have been realized. A special investigation to ascertain this aspect seems warranted.

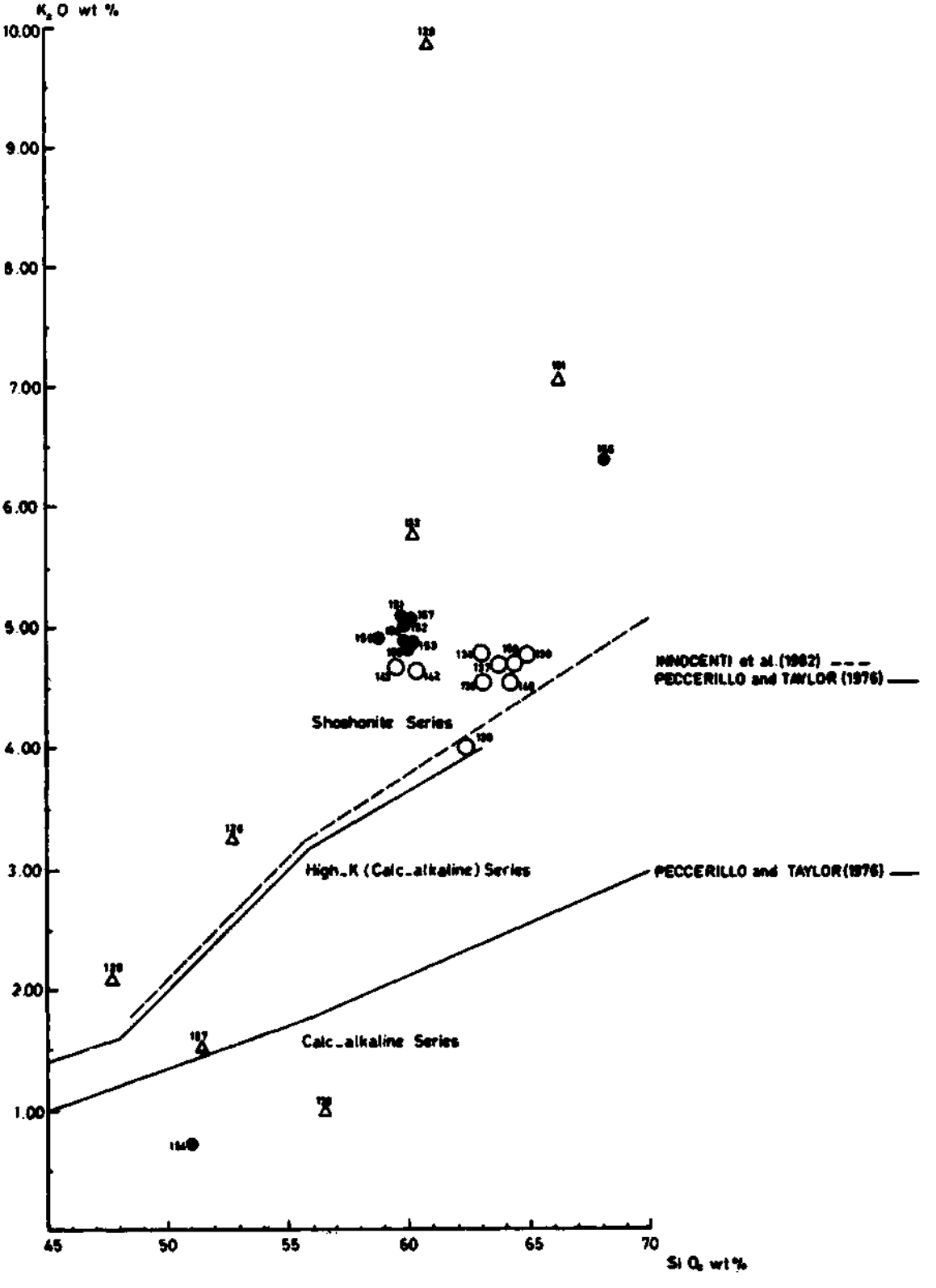

Fig. 9 - K_2O-SiO_2 diagram after Rickwood (1989). Dashed lines Innocenti et al. (1982) and solid lines Peccerillo and Taylor (1976). Signatures as in Fig.3.

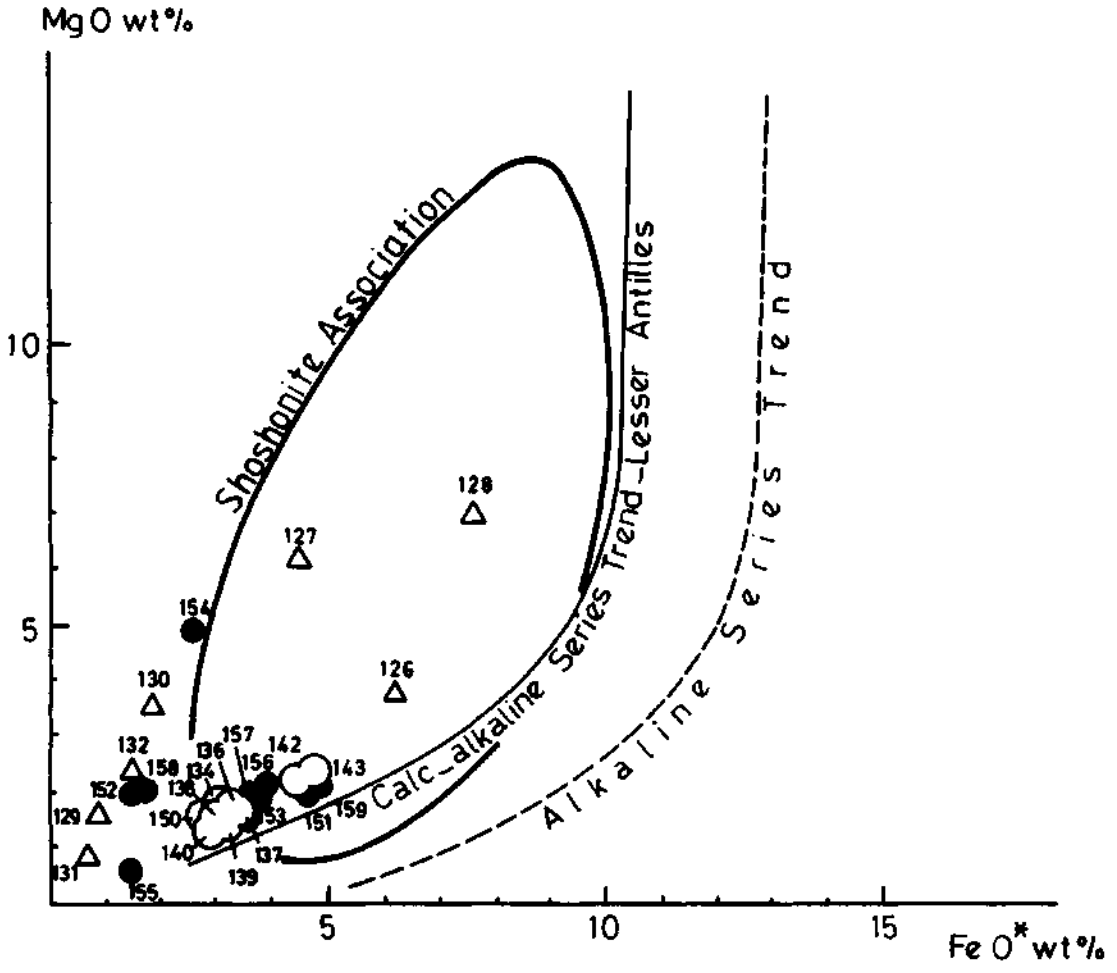

Fig. 10 - MgO-FeO* diagram. For further information, see Morrison (1980). Signatures as in Fig.3.

CONCLUSIONS

The conclusion of the present investigation is that the Murmano pluton is a composite pluton of predominantly monzonitic character. Current literature classifies the closely related Dumluca pluton, located only 1.5 km from the Murmano pluton, as calc-alkaline (Bayhan, 1980; Bayhan and Baysal, 1982). A large number of geochemical classification diagrams suggest a shoshonitic character for the Murmano pluton.

Geochemical plate tectonic discrimination diagrams and other geochemical and mineralogical criteria suggest that the magmatic material from the Murmano pluton has an I-type character and was formed in a continental island arc environment, in connection with an active subduction zone. The geological information (Zeck and Ünlü, 1988a; 1988b) suggests that the subduction took place in the same general period, during which the ophiolite complexes were obducted. As a result the subduction related magmas intruded into the obducted ophiolite series.

ACKNOWLEDGEMENTS

Major element analyses were made at the Greenland Geological Survey in Copenhagen by Ib Sorensen, and trace element analyses at the Institute for Petrology of Copenhagen University by John Bailey. The authors wish to acknowledge the mentioned persons.

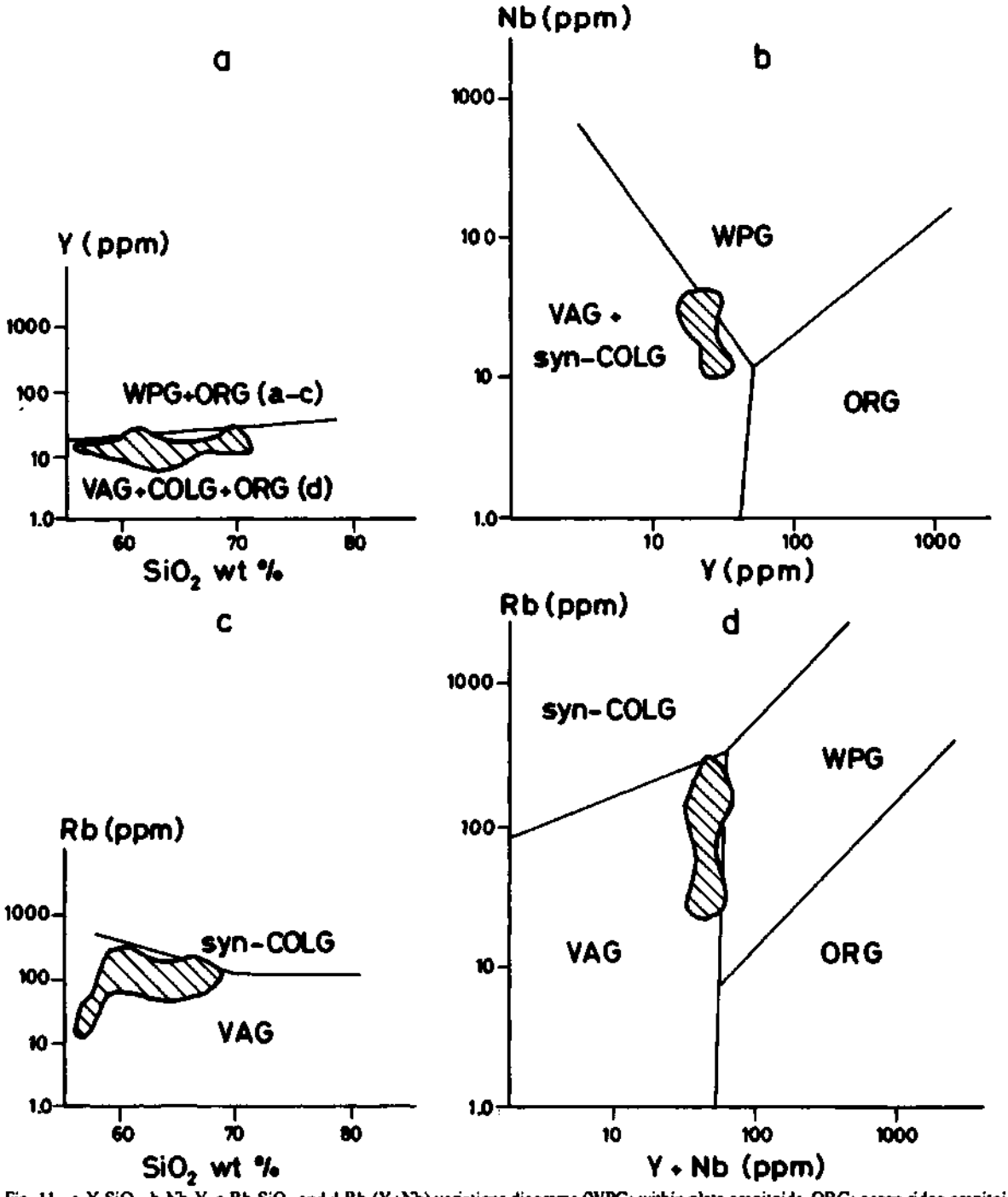

Fig. 11 - a-Y-SiO_2, b-Nb-Y, c-Rb-SiO_2 and d-Rb-(Y+Nb) variations diagrams (WPG: within plate granitoids, ORG: ocean ridge granitoids, VAG: volcanic arc granitoids, COLG: collision granitoids). For further information, Pearce et al. (1984).

The authors want to express their gratitude to MTA and TDÇİ, Ankara, and the Research Council of Denmark for supporting the field investigations (SNF-grants to HPZ, j. nr. 81 - 4717 and 81-5697) and the X-ray fluorescence equipment at the Institute of Petrology at Copenhagen University. Additional support was given by the Ministries of Education of Turkey and Denmark.

Manuscript received May 17,1989

REFERENCES

Bailey, J.C., 1981, Geochemical criteria for a refined tectonic discrimination of erogenic andesites: Chem. Geol., 32, 139-154.

Bayhan, H., 1980, Güneş-Soğucak (Divriği/Sivas) yöresinin jeolojik, mineralojik, petrografik-petrolojik ve melalojenik incelenmesi: Doktora Çalışması, Hacettepe Üniversitesi, Yerbilimleri Enstitüsü, 188, Ankara.

———, and Baysal, O., 1982, Güneş-Soğucak (Divriği/Sivas) Yöresinin petrografik-petrolojik incelenmesi: Türkiye Jeol. Kur. Bull., 25, 1-13, Ankara.

Chappel. B.W. and White, A.J.R., 1974, Two contrasting granite types: Pacific Geology, 8, 173-174.

Didier, J. and Lameyre, J., 1969, Les granites de Massif Central francais: etude comparee des leucogranites el granodiorites: Contrib. Mineral. Petr., 24, 219-238.

Görür, N.; Oktay, F.G.; Seymen, İ. and Şengör, A.M.C., 1984, Paleotcctonic evolution of the Tuzgölü basin complex, central Turkey: sedimentary record of a Neo-Tethyan closure: Dixon, J.E. and Robertson, A.H.F., ed., The geological evolution of the eastern Mediterranean, Blackwell, Oxford, 467-482.

Gladncy, E.S.; Bums, C.E. and Roelandts, I., 1983, 1982 compilation of elemental concentrations in eleven United States Geological Survey rock standards: Geostandards Newsletter 7, 3-226.

Innocenti, F.; Manetti, P.; Mazzuoli, R.; Pasquarc, G. and Villari, L, 1982, Anatolia and north-western Iran: Thorpe, R.S., cd., Andesites, Wiley, Chichester, 327-349.

Irvine, T.N. and Baragar, W.R.A., 1971, A guide to the chemical classification of the common volcanic rocks: Can. Jour. Earth Sci., 8, 523-548.

Koşal,C., 1973, Divriği A-B-C demir yataklarının jeolojisi ve oluşumu üzerinde çalışmalar: MTA Bull., 81, 1-22, Ankara.

Loiselle, M.C. and Woncs, D.R., 1979, Characteristics of anorogenic granites: Abstr. Geol. Soc. Am. Ann. Meeting 1979, 539.

Miyashiro, A., 1975, Classification, characteristics and origin of ophiolites: J.Geology, 83, 249-281.

Morrison, G.W., 1980, Characteristics and tectonic selling of the shoshonite rock association: Lilhos, 13, 97-108.

Norrish, K. and Chappel, B.W., 1977, X-ray fluorescence spectrometry: Zussman, J., ed., Physical Methods in determinative Mineralogy, 2nd ed., Academic Press, 201-272, London.

Pearce,J.A.; Harris, N.B.W. and Tindle, A.G., 1984, Trace element discrimination diagrams for the tectonic interpretation of granitic rocks: J. Petrology, 25, 956-983.

Peccerillo, R. and Taylor, S.R., 1976, Geochemistry of Eocene calc-alkaline volcanic rocks from the Kastamonu area. Northern Turkey: Contrib. Mineral. Petrol., 58, 63-81.

Pitcher, W.S., 1983, Granite type and tectonic environment: Hsu, K., ed., Mountain Building Processes, Academic Press, 19-40. London.

Rickwood, P.C., 1989, Boundary lines within petrologic diagrams which use oxides of major and minor elements: Lithos, 22,247-263.

Robertson, A.H.F. and Dixon, J.E., 1984, Introduction: aspects of the geological evolution of the eastern Mediterranean: Dixon, J.E. and Robertson, A.H.F., ed., The geological evolution of the eastern Mediterranean, Blackwell, Oxford, 1-74.

Şengör, A.M.C. and Yılmaz., Y., 1981, Tethyan evolution of Turkey: a plate tectonic approach: Tectonophysics, 75, 181-241.

Streckciscn, A.H., 1976, To each plutonic rock its proper name: Earth Sci. Rev., 12, 1-33.

Zeck, H.P. and Ünlü, T., 1987, Parallel whole rock isochrons from a composite, monzonitic pluton, Alpine belt. Central Anatolia, Turkey: N. Jb. Mineral. Mh., 1987, 193-204.

———and———, 1988a, Alpine ophiolite obduction before 110 ± 5 Ma ago, Taurus Belt, eastern central Turkey: Tectonophysics, 145, 55-62.

———and———, 1988b, Murmano plutonunun yaşı ve ofiyolitle olan ilişkisi (Divriği/Sivas): MTA Bull., 108, 82-97, Ankara.

PETROLOGY OF AKÇATAŞ GRANITE (NEVŞEHİR) IN THE MIDDLE ANATOLIAN MASSIVE

Ş.Nihal AYDIN**

ABSTRACT— Akçataş granite is located in the northwest of Nevşehir. Granites, orthodase granites, orthoclase granite with oligoclase, granodiorites, quartzdiorites, diorite (albitized), syenites, monzonites, quartzmonzonite, monzodiorite and altered plutonic rocks (granites and/or orthoclase granites) are identified in pluton. The enclaves are sparsely observed in granites and granodiorites. Abyssal rocks are determined as granite aplite, granite porphyre, diorite porphyrite (albitized). Field and microscobik studies show that magma has become differentiated twice, has generally assimilated the pieces of adjacent sedimentary rocks, intruded not deeper than the top level of the mesozone, genesis of enclaves are identical with plutonic rocks and hydrothermal stage was effective.

Mineral Res. Expl. Bull., 112, 59-64,1991

THE DISCUSSION OF SCHRODINGER WAVE EQUATION ON THE CONCEPT OF POINT MASS PAIRS

Sırrı KAVLAKOĞLU *

ABSTRACT— As it is known, the light emission has both of wave and quantum nature. Because of the latter, it can be handled as a point mass in the case of necessity. The wave properties of the light are investigated by Maxwell wave equations and the point mass properties by Schrödinger wave equation. The purpose of the paper is to show that these two properties of the light can be treated by a single equation system. To realize this aim, "Extended Maxwell Equation System" is proposed and it is shown that, this system, under acceptable limitations, comprises both electromagnetic wave equations and the scalar wave equation from which Schrödinger wave equation can be derived. Thus it is revealed that the symetry which is present between electric field vector and magnetic field vector in the "Extended Maxwell Equation System", also exists between wave front surface normals of y and φ of two scalar Schrödinger wave equation. Since, the coefficients of Schrödinger wave equation pair can be different, it is possible to assume the existence of two different mass points, associated to these two wave front surface which arc perpendicular to each other.

INTRODUCTION

Maxwell equation system provides most effective means to investigate the electromagnetic fields (Straton, 1941). The investigation of the electromagnetic wave properties of the light could be done with these equations (Bateman, 1955).

But, the direct investigation of the "light-quantum" properties of the light cannot be done with Maxwell equation systems. Only, after introducing the concepts of singular points, singular curves, the investigation of the electron model of the light is done with Maxwell equation systems (Bateman, 1955).

As it is known, "pointmass-wave" properties of the light are investigated by using Schrödinger "wave-equation" (Sommerfeld. 1928).

Events of the light comprise of "pointmass-wave" events as well as electromagnetic wave events. Therefore, it is thought to be interesting to investigate all the events of light within the framework of one equation system. Maxwell equation system is considered a good approach to realise this aim.

As the first step, it has been shown that Maxwell equation system's can be extented by using Helmholtz theorem (Phillips, 1933). Secondly, it has been shown that scalar wave function of the extension term, satisfies Schrödinger wave equation. Since the coefficients of Schrödinger equation pair can have different values, there must be two point mass, differing from each other, connected to two orthogonal surfaces. Therefore, in any light emission event, point mass pair concept has to be a concept which should be considered seriously.

Thus, it has become possible to investigate an electromagnetic wave event together with the associated pointmass-wave event by using proposed extented Maxwell equation system. In this way , it has been proved trial Maxwell symetry between electric field intensity vector and magnetic field intensity vector exist, also, exists between the wave surface normals of y and φ of the scalar wave equations of the system.

Therefore a concept of seperate pointmass related to the two orthogonal surface, y and φ may be accepted.

THEORY

EXTENDED MAXWELL EQUATION SYSTEM

Maxwell equation system (Bateman, 1955) is:

$$\nabla X E = -\frac{1}{C}\frac{\partial H}{\partial t} \qquad \nabla . H = 0$$

$$\nabla X H = \frac{1}{C}\frac{\partial E}{\partial t} \qquad \nabla . E = 0 \qquad (1)$$

E : vector of electric field intensity
H : vector of magnetic field intensity
C : velocity of light
t : time

E and H are assumed as

$$E = E_0 (x, y, z) e^{i\omega t}$$
$$H = H_0 (x, y, z) e^{i\omega t} \qquad (2)$$

Here, (ω) is angular velocity, (x,y,z) are cartesion coordinates. According to Hclmoltz theorem, a vector F can be ex pressed as the sum of one selonoidal and one irrotalional vectors as:

$$F = -\nabla\Psi + \nabla X A \qquad (3)$$

Scalar (ψ) and vectorial (A) functions arc the functions of time as.

$$\Psi = \Psi_0 (x, y, z) e^{i\omega t} \qquad A = A_0 (x, y, z) e^{i\omega t}$$

Mathematically, according to the Helmoltz theorem, the following equation of

$$\frac{1}{C}\frac{\partial E}{\partial t} = \nabla X H$$

can be written as

$$\frac{1}{C}\frac{\partial E}{\partial t} = -\nabla\psi + \nabla X H \qquad (4)$$

or as

$$\frac{1}{C}\frac{\partial}{\partial t}\left(E - i\frac{C}{\omega}\nabla\psi\right) = \nabla X H \qquad (5)$$

Let's assume

$$S = E - i\frac{C}{\omega}\nabla\Psi$$

Under this situation, a modified, mathematically extented for of Maxwell equation system (1) is defined as

$$\nabla XS = -\frac{1}{C}\frac{\partial H}{\partial t} \qquad \nabla.H = 0$$

$$\nabla XH = \frac{1}{C}\frac{\partial S}{\partial t} \qquad \nabla.S = 0 \qquad (6)$$

In the paper, the Equation system (6) is called "Extented Maxwell Equation System".

PHYSICAL MEANING MAXWELL EQUATION SYSTEM

The following wave equations, can be written easily, from equations (6), as

$$\nabla^2 S - \frac{1}{C^2}\frac{\partial^2 S}{\partial t^2} = 0$$

$$\nabla^2 H - \frac{1}{C^2}\frac{\partial^2 H}{\partial t^2} = 0 \qquad (7)$$

From them

$$\nabla^2 S_0 + \frac{\omega^2}{C^2} S_0 = 0 \qquad (8)$$

$$\nabla^2 H_0 + \frac{\omega^2}{C^2} H_0 = 0 \qquad (9)$$

differential equations can be written.

Since

$$S_0 = E_0 - i\frac{C}{\omega}\nabla\Psi_0$$

(E_0, Ψ_0 are reel), and substituting it in (8), it is got

$$\nabla^2\left(E_0 - i\frac{C}{\omega}\nabla\psi_0\right) + \frac{\omega^2}{C^2}\left[\nabla^2(\nabla\psi_0) + \frac{\omega^2}{C^2}\nabla\psi_0\right] = 0$$

By separating reel and imaginary terms in this equation the following differential equation is got.

$$\nabla^2 E_0 + \frac{\omega^2}{C^2} E_0 - i\frac{C}{\omega}\left[\nabla^2(\nabla\psi_0) + \frac{\omega^2}{C^2}\nabla\psi_0\right] = 0 \qquad (10)$$

To find the solution, these are written as

$$\nabla^2 E_0 + \frac{\omega^2}{C^2} E_0 = 0$$

$$\nabla^2 (\nabla\psi_0) + \frac{\omega^2}{C^2}\nabla\Psi_0 = 0$$

are written.

Therefore the solution of the equation system (6), is reduced to the solution of the following three differential equations.

$$\nabla^2 E + \frac{\omega^2}{C^2} E = 0 \qquad (11)$$

$$\nabla^2 H + \frac{\omega^2}{C^2} = 0 \qquad (12)$$

$$\nabla^2 (\nabla\psi) + \frac{\omega^2}{C^2} \nabla\psi = 0 \qquad (13)$$

Equation (13) is the part of the "Extented Maxwell Equation Eystem".

Because of (11) and (12) equations, (1) and (6) equations systems have all the properties of the electromagnetic wave propagation. Additionally, (6) equation system contains a scalar (ψ) function.

To reveal the properties of (ψ), (13) differential equation is written as:

$$\nabla\left(\nabla^2 \psi + \frac{\omega^2}{C^2} \psi \right) = 0$$

From this,

$$\nabla^2 \psi + \frac{\omega^2}{C^2} \psi = l$$

(l) is an integration constant.

The latter equation can also be written as:

$$\nabla^2 \psi + \left(\frac{\omega^2}{C^2} - \frac{l}{\psi} \right) \psi = 0 \qquad (14)$$

Let's assume l≠0 and,

$$\frac{\omega^2}{C^2} - \frac{l}{\psi} = \frac{\omega^2}{a^2} \qquad (15)$$

Under this situation the equation (14) will be transformed into the form of,

$$\nabla^2 \psi + \frac{\omega^2}{a^2} \psi = 0 \qquad (16)$$

"a" is the phase velocity and because of (15), it is the function of position,

Let's put $\frac{\omega}{a} = k, \frac{C}{a} = n$ and $k = k_0 n$

Here, (k) is wave number, (n) is the refractive index of the space.

Then, the equation (16) becomes as,

$$\nabla^2 \psi + n^2 k_0^2 \psi = 0 \qquad (17)$$

To investigate the properties (n^2), let's assume

$$\psi = B\, e^{ik_0 T}$$

where (B) and (T) are the functions of (x,y,z) cartesian coordinates. In this case

$$\left(\frac{\partial T}{\partial x}\right)^2 + \left(\frac{\partial T}{\partial y}\right)^2 + \left(\frac{\partial T}{\partial z}\right)^2 = \Delta T_1$$

This is Hamilton differential equation (Sommerfeld, 1928).

Here $\Delta T_1 = n^2$

On the other hand, ΔT_1 is

$$\Delta T_1 = 2m \mid e - U(x,y,z) \mid$$

Here, m, point mass; e, energy constant and U is potential energy.

Then differential equation becomes,

$$\nabla^2 \psi + 2m(e-U) k_0^2 \psi = 0$$

or

$$\nabla^2 \psi + 2m(e-U)\left(\frac{2\pi}{h}\right)^2 \psi = 0$$

where (h) is Planck's constant (Sommerfeld, 1928). This is the well-known Schrödinger's wave equation.

As, it has been shown, the (ψ) function in the equation (6) justifies Schrödinger wave equation.

Therefore, it becomes possible to investigate all the light events comprising of wave, pointmass-wave characteristics of the light, by using "Extended Maxwell Equation System".

On the other hand, if the similar operations are done in the $\frac{1}{C}\frac{\partial H}{\partial t}$ field, one wave front (ψ) function orthogonal to wave front function (ψ) will be specified. Consequently, it will be possible to infer the presence of two different mass points associated with these functions.

Manuxcript received May 11, 1990

REFERENCES

Bateman, H.,1955, The Mathematical Analysis of Electrical and Optical Wave-Motion: Cambridge University Press.

Phillips, H.B., 1933. Vector Analysis: Cambridge.

Sommerfeld, A., 1928, Wave Mechanics: E.P. Button and Company Inc., New-York.

Straton, J.A., 1941, Elektromagnetik theory: McGraw-Hill Book Company, Inc., New York.

REMOVAL OF ELECTROMAGNETIC COUPLING EFFECT FROM IP PHASE DATA

İlyas ÇAĞLAR***

ABSTRACT— Since the electromagnetic (EM) coupling effect causes spurious anomalies on induced polarization (IP) pseudo-section phase data collected over metallic sulphide mineralization area, it is difficult to evaluate and to interpret as truely of these data. Coupling removal process by dividing (DAKG) IP pseudo-section data has been developed for to remove this effect on raw phase data. In this process theoretical earth model considered as has continuously varying conductivity. Apparent resistivity and EM coupling computations have been made by using mathematical expressions based on this earth model. DAKG process is applied to the real IP phase field data given by recent works in which used the "Quadratic Extrapolation" (QE) and "Complex Resistivity Interactive" (CRI) techniques. The extension of mineralization zone, is described as agrees with the results of QE and CRI techniques by interpreting of pseudo-section decoupled phase data obtained from DAKG process. Hence, it is seen that the DAKG was an useful process like QE and CRI on removing of EM coupling.

Mineral Res. Expl. Bull., 112, 65-70,1991

CIDEINA, A NEW FORAMINIFERAL GENUS FROM THE MAASTRICHTIAN LIMESTONE OF THE CIDE REGION (NORTH TURKEY)

Ercüment SİREL*

ABSTRACT. - In 1973,a discoidal foraminifera was described and figured as *Cuvillierina sözerii* by the present author from the Maastrichtian of Cide region, NE of Zonguldak, Northern Turkey. In this paper, *Cuvillierina sözerii* is reviewed on well preserved and abundant materials of this species from the type locality. In the light of the obtained new generic features, *C. sözerii* is transfered to the genus *Cideina* n. gen., as well as the complex rotaliid genus *Cideina* with orbitoidal character is described, figured and discussed. Key words: Systematic, Foraminifera (Lepidorbitoididae), Maastrichtian, Turkey (Cide, NE of Zonguldak).

INTRODUCTION

In this paper, the stratigraphy of the Cide region (Fig. 1,2) and the description of *Cideina* n. gen. (type species *Cuvillierina sözerii* Sirel, 1973) from the same area have been presented.

The first paleontological study on the larger Upper Cretaceous foraminiferas was carried out by Ami (1932) from the Ereğli region, SW of Zonguldak, W Black Sea. A new species of *Siderolites* as *Siderolites heracleae* was reported by Ami from the Kepesköy tepe, 6 km. east of Ereğli, of the Upper Turonian to Middle Campanian. However, Ami's species could be

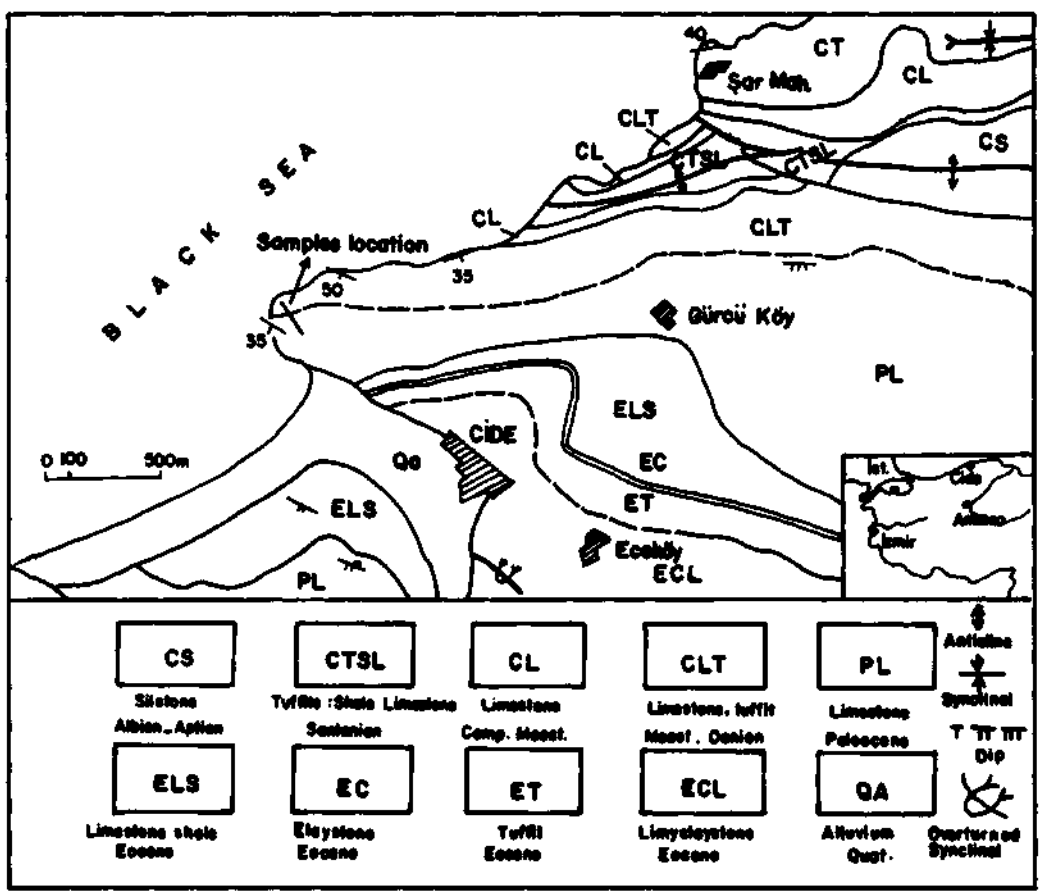

Fig. 1 - Geological map of Cide region (mapped by Ş.Uysal; B.Erdoğan and F.Şaroğlu).

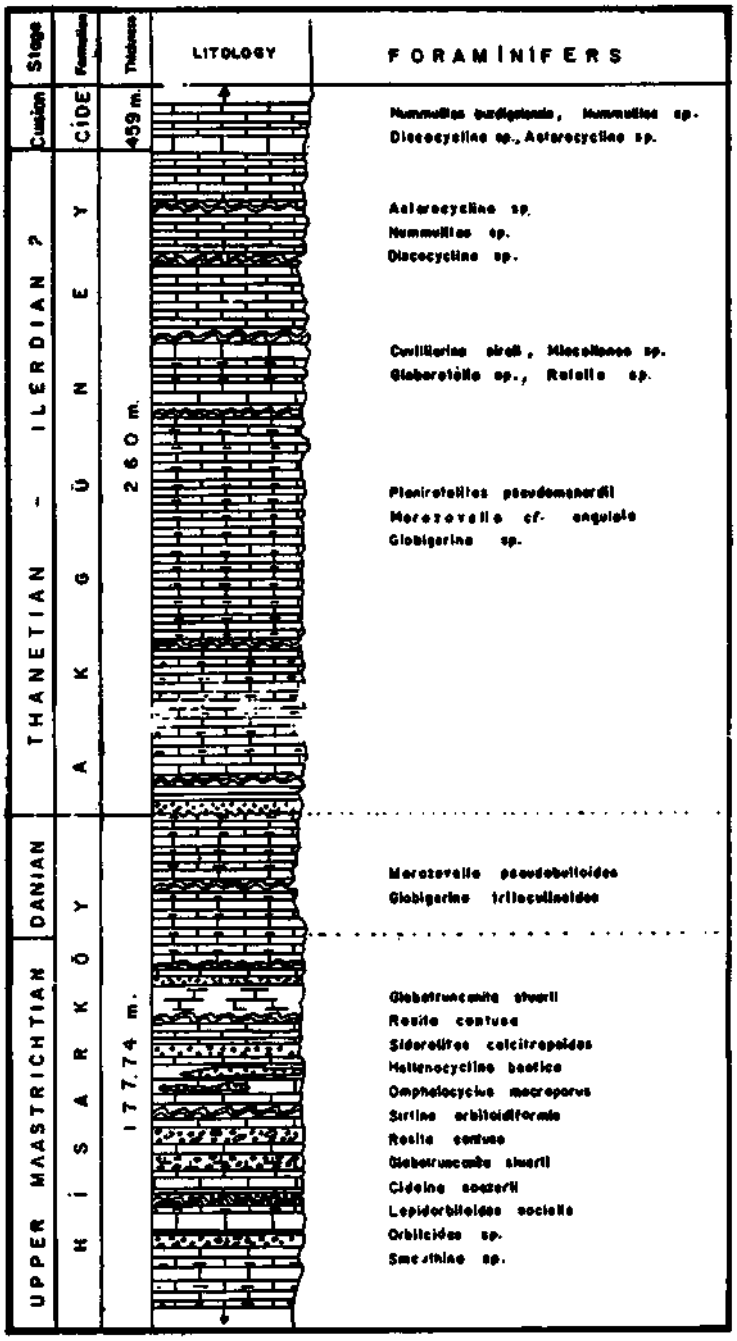

Fig.2- The section measured from the type locality of the *Cideina* n.gen.

identical with *Pseudosiderolites vidali (* Douville). Unfortunately, it was not reported any paleontological study on the larger foraminiferas of the investigated area until 1973. In 1973, the discoidal foraminifera from the Maastrichtian of the Cide region was described and figured as *Cuvillierina sözerii* by Sirel and this species is retained in genus *Cuvillierina* on the basis of its coiling and external omemantation. The recent study on-this discoidal complex foraminifera from the specimens collected from the same locality following second visit by the author, have shown that observed new remarkable orbitoidal characters are present. In the light of the new diagnostic characters, *Cuvillierina sözerii* was transfered to the genus *Cideina* n. gen..

Due to the hardness of the studied samples. It was not possible to obtain free individuals. The present study is based only on selected random thin sections.

All the thin sections bearing this new foraminiferal genus figured in this paper are deposited at the Museum d' Histoire naturelle, Geneva, Switzerland.

STRATIGRAPHY

A project on the Northern Anatolian Fault zone was carried out during 1970-71 by the Geological Mapping Department of the Mineral Research and Exploration Institute of Turkey. The geological map (1:50 000 scale) of the Cide-Kurucas.ile region was made and the several new lithostratigraphic units were established by Akyol et al. (1974) from the West Black Sea region. Mesozoic-Tertiary biostratigraphy of the Cide area was investigated as a part of this project by the present author (Sirel, 1973).

In the Cide region, the following lithostratigraphic units of the Aptian-Albian, Coniacian-Santonian, Campanian-Maastrichtian, Maasthchtian-Danian, Paleocene (Thanetian-Ilerdian?) and Eocene (Cuisian) ages crop out (Fig.l). They were named by Akyol et al (1974).

Ulus **formation** (CS)

This formation is composed of siltstone, alternating sandy shale, rare sandy limestone intercalations near basal parts; alternation of calcareous claystone and sandstone is dominant between Kurucaşile and Cide town. It is very thick, about 3000 m in places. It contains *Hypacanthoplites* aff. *jacobi* (Collet), *Procheloniceras* cf. *amadei (* Hohenegger). Aptian-Albian ages are designated by this fauna.

Kurucaşile formation

This unit is most widespread in the Black Sea region and composed of the following seven members: Çaydere clayey limestone member, Baldıran tuffite member, Songet limestone member, Unaz limestone member, Yeniceköy tuffit member, Cambu agglomerate-lava Member and Kumbos Tuffite-calcareous shale member. The following two members of the Kurucas.ile Fm. crop out in the Cide region.

*Yeniceköy tuffite member (CTSL).*_ Basaltic tuff alternating with tuffite, both gray-green to brown-green; rare intercalations of thinly bedded, light purple, pink, silicified limestone. Thickness varies very much, 780 m. thickness measured. The unit contains *Dicarinella concavata* (Brotzen), *Marginotruncana coranata* (Bolli) designate Coniacian- Santonian.

*Unaz limestone member (CL).*_ This member composed of clayey limestone, mostly pink, rarely green thin bedded; rare intercalations of tuffite and sandstone, avarage thickness of the member is 140 m. From the lower part of the member the following foraminiferas have been obtained indicating Campanian age: *Globolruncanita elevata* (Brotzen) and *Globotruncana linneiana* (d'Otbigny). The upper part of the unit yielded the following globotruncanid species indicating Campanian-Maastrichtian: *Globotruncana area* (Cushman) and *Globolruncana rozetta* (Carsey).

Hisarköy formation (CLT)

The unit is composed of light gray limestone, thick bedded; green and dark red siltstone, thin bedded tuffit intercalations mainly in the upper part; to the eastern part; pebbly appearance due to the large-sized intraclasts; chert nodules in the upper part. The examined limestone with new genus *Cideina* described in this paper yielded the following associations of the foraminifcral species indicating an Upper Maastrichtian age: *Siderolites calcitrapoides* Lamarck, *Sirtina orbitoidiformis* Bronnimann & Wirz, *Omphalocyclus macroporus* (Lamarck), *Hellenocyclina beotica* Reichel, *Lepidorbitoides* sp., *Orbitoides* sp., *Navarella* sp., *Globotruncanita stuarti* (De Lapparent), *Rosita contusa* (Cushman). The formation continues upward conformably with clayey limestone beds containing primitive globorotaliid species : *Morozovella pseudobulloides* (Plummer), *Globigerina triloculinoides* Plummer. According to these foraminiferal species, Danian age has been assumed for the Upper part of the Hisarköy formation.

Akgüney formation (PL)

The formation is composed of thinly bedded clayey limestone intercalations; *Planirotalites pseudomenardii* (Bolli), *Morozovella* cf. *angulata* (White), *Cuvillierina sireli* İnan, *Miscellanea* sp., designate Thanetian age. The following foraminiferal species have been found in the upper part of the formation: *Nummulites* sp., *Discocyclina* sp., according to these species, Ilerdian? age has been assumed for the upper part of the unit. This unit overlies uncomformably Hisarköy formation.

Cide formation (ELS, EC, ET, ECL)

This unit is composed of limestone, shale, claystone, tuffit and limy claystone; *Nummulites burdigalensis* (de la Hame), *Discocyclina* sp. indicate Cuisian age for the unit.

SYSTEMATIC DESCRIPTION

Order : Foraminiferida Eichwald, 1830
Superfamily : Orbitoidacea Schwager, 18/6
Family : Lepidorbitoididae Vaughan, 1933
Genus : *Cideina* n.gen.
Type species : *Cuvillierina. sözerii* Sirel, 1973

Derivation of name: Cide, a town in the west Black Sea region, N Turkey.

Diagnosis : Test large, discoidal to low conical with broadly rounded peripheral margin, small sized spherical protoconch followed by few whorls of trochospirally arranged small chambers of early stage, later nearly planispiral and involute with rapidly expanding whorl, test wall calcareous, finely perforate of radially fibrous calcite during the early ontogeny, being calcareous, coarsely perforate in the late ontogeny; weakly thickened pillars extending from the early chambers to the umbilical side of the test, between pillars there appear to be thin umbilical vertical canals; the dorsal side covered by four, may be more, layers of lateral chambers interspersed by relatively thin pillars, lateral chambers connect with each other by primitive stolons; septal flap well developed and enclosing intraseptal canals, divergent canals and vacuoles present over chambers of outer whorl, dimorphism not observed.

Cideina soezerii (Sirel), 1973

(Plate I, fig. 1-12, Plate II, fig. 1-9)

1973 *Cuvillierina sözerii* Sirel, p. 69, Plate I, fig. 1-6; Plate II, fig. 1-4.

Holotype: Nearly axial section (89-09), illustrated by Plate I, fig. 9.

Depository: Holotype and figured types are deposited at the Museum d'Histoire Naturelle, Geneva, Switzerland.

Material: 52 specimens in random sections, exclusively from the type locality.

Type locality: Cide town, NE of Zonguldak, N Turkey.

Type level: Upper Maastrichtian.

DESCRIPTION

Test is free, discoidal, to low conical; periphery is broadly rounded; the central part of the discoidal shell is slightly inflated compared to the periphery of the test (Plate I, fig. 1, 2, 5, 6, 8, 9). The test wall is calcareous, finely perforated of radially fibrous calcite in early stage, becoming calcareous, coarsely perforated with large vacuoles in the last spiral (Plate I, fig. 1,2, 5, 6, 8, 9,11; Plate n, fig. 1, 5, 7, 8). The superficial sections clearly shows that both sides of the shell are covered by reticulate ornemantations related to divergent canals (Plate I; fig. 12).

Dimensions.- Eight typical specimens have the following measurements.

Table 1

Specimens	*Shape and diameter of proloculus*	*Diameter (mm)*	*Thickness of central part (mm)*	*Thickness of periphery (mm)*	*Diameter of the early stage (mm)*	*Number of the early stage chambers*	*Number of adult chambers*
89-01	-	3.00	0.60	0.38-0.55	1.12	-	-
89-05	-	2.00	0.62	0.42-0.48	0.62	-	-
89-09	-	2.67	0.67	0.40-0.50	0.99	-	-
89-11	-	-	0.73	-	0.65	-	-
89-13	50 µ	1.80	-	-	0.70	24-25	14
89-16	60 µ	3.00	-	-	0.72	23	12
89-17	-	2.05	-	-	0.45	-	13
89-18	25 µ	2.09	-	-	0.85	28-30	-

Internal characters. - In the course of the ontogeny the early involute asymetric spiral (trochospiral coiling) is followed by completely planispiral involute, thickened adult spiral with complex structure related to canal system and vacuoles (Plate I, fig. 1,2, 5, 8, 9,11). The monolocular spheric embryo is enveloped by 23-30 small chambers of the early ontogeny (Plate I, fig. 1-6, 8-11). The weakly thickened conical pillars are extending from the trochospiral chambers to the surface of the test indicating the ventral side of the shell; there are thin vertical canals between the pillars (Plate I, fig.1, 3, 9, 11). The sizes of the trochospiral early chambers gradually increase from the first whorl to the last one (Plate II, fig. 1-8). Later mature chambers are very different in size and shape; they are arranged in completely planispiral involute thickened last spiral (Plate II, fig. 1-8). The last 3-4 adult chambers being very characteristic, become larger and reach to 4-8 times of the sizes of the early chambers (Plate II, fig. 1,4, 5, 8). The spiral thickness begins to increase from the first whorl and reaches its maximum at the last whorl. The thickened last spiral is characterized by the presence of the divergent canals and large vacuoles (Plate I, fig. 1, 3, 8,10; Plate II, fig.1, 3, 5). In the first 1-2 whorls of the early stage, the spire interval gradually increase but, at the last whorl, it suddenly becomes wider as operculinid pattern (Plate II, fig. 1-8). Some equatorial sections of this form (Plate II, fig. 1,4-8) suggest the existence of the septal flap in the adult chambers. A similar septal flap can be observed in *Daviesina tenuis* (Tambareau) (Caus& Hottinger & Tambareau, 1980, fig. A.B.E-G; Plate IV, fig.3,6). The dorsal side of the test is covered by four, may be more, layers of lateral chambers interspersed by relatively thin pillars (Plate I, fig.1,3,5-11). This is a similar corresponding structure in *Sirtina orbitoidiformis* Bronnimann and Wirz, 1952, fig. 4a; the lateral chambers are connected with each other by the primitive stolons. The early and the adult chambers communications are made by a slit form intercameral foramen, at the base of the septum (Plate II, fig. 1,7).

REMARKS

The here described new rotaliid genus with complex structure resembles in some of its internal features orbitoidal foraminiferas: on the dorsal side of *Cideina n.*gen. occur layers of lateral chambers as known from the typical orbitoids, on the other hand, the existence of the early spiral stage with umbilical pillars suggests to the typical rotaliid members. Because of the presence of the rotaliid and orbitoid characters, this new genus has been placed in Lepidorbitoididae Vaughan. However, it will be suitable to establish the new family within the super family *Orbitoidacea* for the genera *Sirtina. Cideina* even *Orbitokathina.*

Rotaliid genus with orbitoidal character, Sırtina was first, described from the Maastrichtian of Iran and Libya by Bronnimann & Wirz (1962). It is spirally arranged rotaliid form with well developed umbilical pillars. Most remarkable is the presence of the orbitoidal lateral chambers on the dorsal side of the shell. *Sırtina,* in which the spire is trochoid in the early stage and planispiral-involute in the adult. This new genus resembles *Sırtina* by its spiral stages and having orbitoidal lateral chambers on the dorsal side. But, *Cideina* n.gen.clearly differs from *Sırtina* in having thickened last spiral with the divergent canals and large vacuoles. In addition, the wall of the last spiral in new genus, is built with coarsely perforated calcite whereas *Sırtina* has finely perforated calcareous wall.

Lenticular rotaliid genus with orbitoidal character, *Arnaudietla* was first described by Douville (1907) from the Campanian of France. This monotypic genus has characteristicly two to five spirally arranged primary chambers, well developed lateral chambers on both sides of the test, no equatorial chambers. Whereas, in the *Cideina* lateral chambers occur on the dorsal side only, and trochospirally arranged primary chambers with pillars arc visible in a short series of 1-2 whorls in the new genus (Plate I, fig. 1, 2, 8, 9,11).

Cideina n.gen. differs from *Cuvillierina* Debourle (1955) in possesing lateral orbitoidal chambers on the dorsal side; in addition, there is superficial differences between the two genera: the external surface of the *Cuvillierina* is covered by reticulate ornamentation with chevron pattern whereas, new genus has irregular reticulate ornamentation on the external surface.

The lenticular, bilaterally symmetrical planispiral enrolled genus *Pseudosiderolites* (type species *Siderolites vidali* Douville) was established by Smout (1955). This genus is abundant arround the type locality of *Cideina* n.gen. and throughout Black Sea region; it occurs in the neritic limestone and associated with *Arnaudiella* sp., *Orbitoides tissoti* Schlumberger and *Helicorbitoides* n.sp.. The new genus *Cideina* is easyly distinguished from the Campanian genus *Pseudosiderolites* by having orbitoidal lateral chambers on the dorsal side of the test.

Stratigraphic occurence. Cideina soezerii occurs in light gray hard limestone near the Cidc town (Fig.l). It is associated with rich foraminiferal species of the Upper Maastrichlian: *Siderolites calcilrapoides, Sırtina orbitoidiformis, Omphalocyclus macroporus, Hellenocyclina beotica, Lepidorbitoides* sp., *Navarella* sp., *Rosila coniusa, Globotruncanita stuarti.*

Manuscript received May. 30,1990

REFERENCES

Akyol, Z. & Erdoğan, B. & Göger, E. & Güner, Y. & Şaroğlu, F. & Şentürk, İ. & Uysal, Ş., 1974, Geologic map of the Cide-Kurucaşile region: MTA Publ., Geological map of Turkey (1:50 000) quadrangle series.

Ami, P., 1932, Eine neue *Siderolites* spezies *(S.heracleae)* (aus dem) Senon von Ereğli an der kleinasiatischen Schwarzmeerküste und versuch einer Bereinigung der Gattung: Eclogae Geol. Helv., vol. 25, pp. 204.

Bronnimann, P. & Wirz, A., 1962, New Maastrichlian Rotaliids from Iran and Libya: Eclogac Geol. Helv., vol. 55, no.2, pp. 519-528.

Caus, E. & Hollinger, L. & Tambareau, Y., 1980, Plissement du "Septal flap" et systeme de canaux chez *Daviesina,* foraminiferes Paleocenes: Eclogae Geol. Helv., vol. 73, no. 3, pp. 1045-1069.

Debourle, A., 1955, *Cuvillierina eocenica,* nouveau genre et nouvelle especes de foraminifere de I'Yprdsien d'Aquitaine: (a) Soc. Geol. de France, Comples Rendus Somm. no. 2, pp. 19.

Douville, H., 1906, Evolution el enchainement des foraminiferes: Bull. Soc. Geol.. France, vol. 4, no. 6, pp., 588-602.

Sirel, E., 1973, Description of a new *Cuvillierina* species from the Maastrichtian of Cide (Northern Turkey). Bull, of the Geol. Soc. of Turkey, vol. 16, no. 2, pp. 69-76.

Smout, A.H., 1955, Rectification of the Rotaliidae (Foraminifera) and two new Cretaceous forms resembling *Elphidium:* Washington Acad. Sci. Jour., vol. 45, no. 7, pp. 201-210.

PLATES

PLATE -1

Cideina soezerii (Sirel)

Maastrichtian

Cide town, N Turkey

Fig. 1 - Subaxial section (89-01), showing trochospiral stage with pillars and the vacuoles in the last spiral, X29.

Fig. 2 - Axial section (89-02), showing both stage of growth, X26.

Fig. 3 - Subaxial section (89-03), showing layers of lateral chambers on the dorsal side and vacuoles in the last spiral, X31.

Fig. 4 -Oblique section (89-04), inclined to the equatorial plane, X39.

Fig. 5- Subaxial section (89-05) showing both growth stage and lateral chambers, X40.

Fig. 6 - Subaxial section (89-06), X 29.

Fig. 7 - Oblique section (89-07), showing the layers of lateral chambers, X40.

Fig. 8 - Axial section (89-08), slightly oblique, showing both growth stage and lateral chambers, X28.

Fig. 9 - Axial section (89-09) holotype, both growth stage, lateral chambers intersperced thin pillar and vacuoles, X30.

Fig. 10 - Axial section (89-10), slightly oblique, showing lateral chambers intersperced thin pillars, X42.

Fig. 11 - Axial section (89-11), showing involute trochospiral stage with pillars and lateral chambers with basal stolons, X42.

Fig. 12 - Superficial section (89-12), showing irregular reticulate ornemantation and pores, X39.

1

2

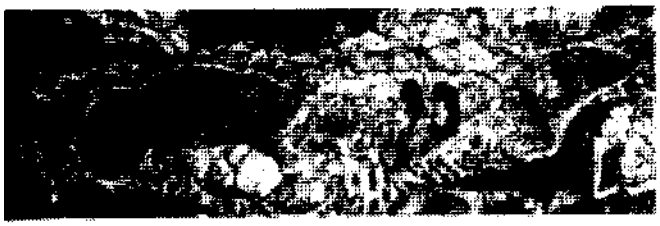

3

4

5

6

7

8

9

10

11

12

PLATE - II

Cideina soezerii (Sirel)

Maastrichtian

Cide town, N Turkey

Fig. 1- Equatorial section (89-13), showing vacuoles in the thickened last spiral, X33.

Fig. 2 - Subequatorial section (89-14), slightly oblique, X20.

Fig. 3 - Approximately equatorial section (89-15), X25.

Fig. 4 - Equatorial section (89-16), showing "septal flap"in the last spiral, X26.

Fig. 5 - Equatorial section (89-01), showing large vacuoles and "septal flap", X57.

Fig. 6 - Oblique section (89-13), inclined to equatorial plane, showing "septal flap", X39.

Fig. 7 - Equatorial section (89-17), showing "septal flap"in the last spiral, X36.

Fig. 8 - Incomplete equatorial section (89-18), X27.

Fig. 9 - Oblique section (89-19), inclined to axial plane, X42.

1

2

3

4

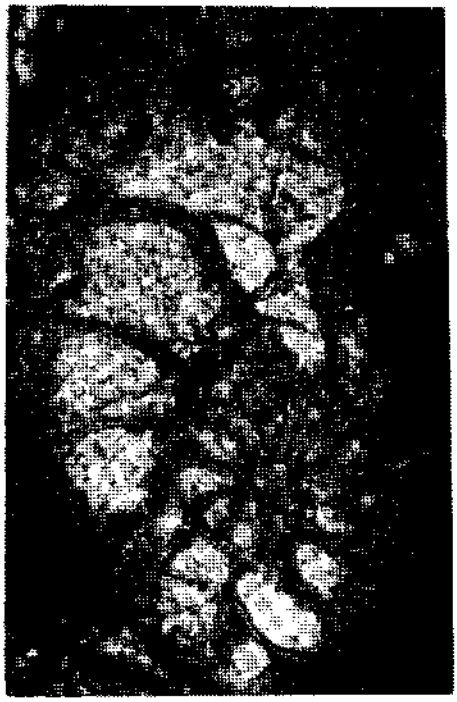

5

6

7

8

9

Mineral Res. ExPlate Bull., 112. 71-76. 1991

PRESENCE OF *NUMMULITES FABIANII* (PREVER) GROUP *(Nummulites* ex gr. *fabianii)* AND ASSOCIATED FORAMINIFERS IN THE ELAZIĞ REGION

Niyazi AVŞAR*

ABSTRACT— The presence of *Nummulites* ex gr. *fabianii* has been indicated in the Eocene sediments, and the stratigraphy of the region is briefly given. The rock units of Paleozoic, Mesozoic and Cenozoic ages crop out in the region. The Paleozoic sequence is composed of metamorphic rocks. This unit is tectonically underlain by the Mesozoic sequence formed of magmatic rocks. The Paleozoic and Mesozoic rocks arc unconformably overlain by the sandstone and algal limestones of the Upper Lutetian age. Algal limestone contain genera of the Foraminifcra such as *Nummulites perforatus* (Montfort). *Assilina spira* (de Roissy), *Alveolina fusiformis* Sowerby, *Alveolina elongata* d'Orbigny, *Fabiania cassis* (Oppenheim) and *Chapmanina gassinensis* (Silvestri). The Priabonian sequence conformably overlies the sandstone and algal limestones of the Upper Lutetian age. It is composed of the alternating sandstone and clay and limestones. The Priabonian sequence is characterized by the species of Foraminifera such as *Nummulites fabianii* (Prever), *Nummulites* ex gr. *fabianii, Nummulites striatus* (Bruguicrc), *Chapmanina gassinensis* (Silvestri), *Asterigerina rotula* (Kaufmarm), *Linderina brugesi* Schlumberger, *Eorupertia magna* (Le Calvez). *Halkyardia minima* (Liebus) and *Praernapydionina huberi* Henson. The Upper Miocene sequence unconformably overlies the limestone of the Phabonian age, and it is composed of volcanic rocks.

INTRODUCTION

The investigated area is located around the Üçtepe, Körpe, Çatalharman and Egopköy 15 km NW of Elazığ province (Eastern Anatolia) (Fig. 1).

The geology of this area was studied by numerous researchers (Ketin, 1946; Tolun, 1955; Kipman, 1976; Tuna, 1979; Naz, 1979; Bingöl, 1984; Turan, 1984; Özkul, 1982; Asutay, 1985). In the eastern part of studied area, in Palu region, the presence of the marine Oligocene has been determined by Sirel et al. (1975).

The purpose of this study is to reveal the presence *of Nummulites* ex *gr. fabianii* in the Elazığ region which is known all over the world up to now but which could not be included within any group between *Nummulites fabianii* (Prever) and *Nummulites intermediums* (d'Archiac) and to give briefly the stratigraphy and the associated foraminifers of the region.

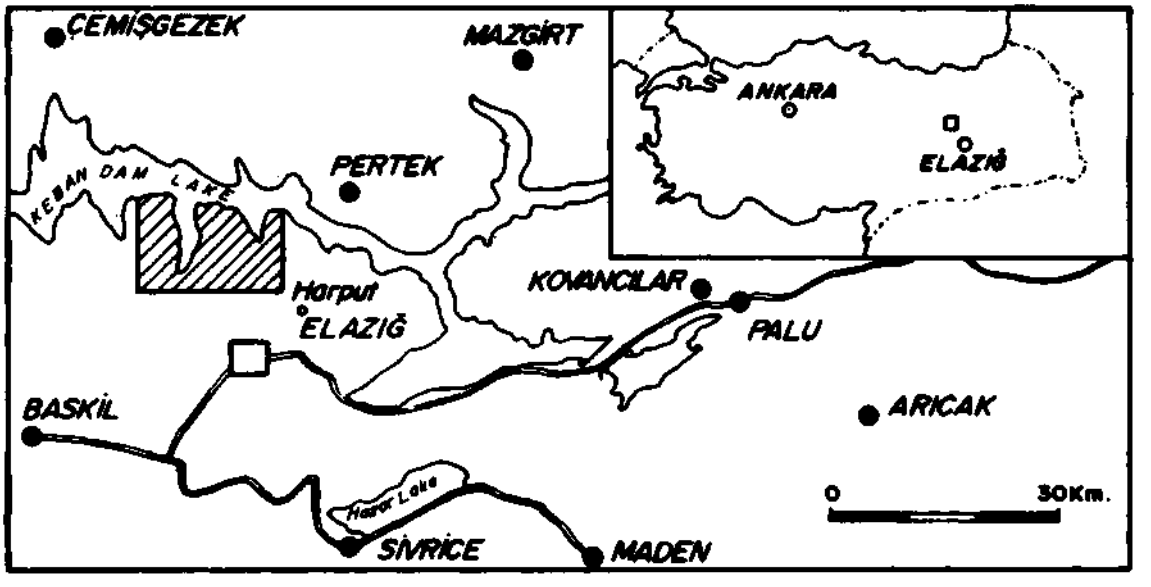

Fig. 1- Location map of the study area.

STRATIGRAPHY

Paleozoic

The Paleozoic sequence is composed of metamorphic rocks such as crystallized limestone, calcschist, marble, metaconglomerate and calcphyllite. These metamorphic sequences are tectonically thrusted over the Mesozoic units, and their primary relation is not known.

Mesozoic

This sequence is represented by granite, granodiorite, gabbro, diabase, basalt, agglomerate, tuff, volcanic sandstone and limestone. This magmatic unit is unconformably overlain by the younger sedimentary and volcanic rocks.

Eocene

Upper Lutetian: The Paleozoic and the Mesozoic rocks are unconformably overlain by the Upper Lutetian sediments. It consists of conglomerates which are various colored, medium to thick bedded sandstone and algal limestones. Algal limestones contain genera of Foraminifera such as *Nummulites perforates* (Montfort), *Assilina spira* (de Roissy), *Alveolina fusiformis* Sowerby, *Alveolina elongata* d'Orbigny, *Fabiania cassis* (Oppenheim), *Chapmanina gassinensis* (Silvestri) and *Silvestriella tetraedra* (Gümbel).

Priabonian: The Priabonian sediments conformably overlie the sandstone and algal limestones of the Upper Lutetian age. It is composed of the alternating sandstone and clay and limestones which are white yellow and beige colored fossiliferous and regularly bedded. The Priabonian sequence is characterized by the species of Foraminifera such as *Nummulites fabianii* (Prever). *Nummulites* ex gr. *fabianii, Nummulites striatus* (Bruguiere), *Asterigerina rotula* (Kaufmann), *Eorupertia magna* (Le Calvez), *Halkyardia minima* (Liebus), *Linderina brugesi* Schlumberger and *Praerhapydionina huberi* Henson.

Miocene

Upper Miocene: This unit unconformably overlies the limestones of the Priabonian age and the older units. It generally consists of basalt, tuff, agglomerate, limestone and sandstone.

SYSTEMATIC DESCRIPTION

In this chapter, the description *of Nummulites* ex gr. *fabianii* which belongs to *Nummulites fabianii* (Prever) group, found in the Priabonian and associated foraminifers is given below.

(Plate I, figs. 1-10; Plate II, figs. 1-9)

Form A: Test small, slightly inflated lenticular, with a rounded margin. The surface is covered by a reticulum generally arranged in two different ways. Its mesh is rectangular shaped on the margin and near the margin, and it has a reticulum towards the center of test. Diameter is 4.2-5.1 mm. and its thickness is 2.3-3.2 mm.

In the equatorial section, the dimension of the first chamber is about 263 microns in sphacrical and protococh 288x361 microns, deutroconch 175x350 microns in oval. The spiral lamina is growing progressively until the end of the penultimate whorl.

Septa are rectilinear, slightly recurved and slightly inclined to the spiral lamina of the previous whorl. The chambers are subquadrate or slightly longer than higher in the early whorls, but later become decisively rectangular and towards the last whorls the chambers are 3-4 times longer than higher.

Form B: Test lenticular, with a sharp margin, and it has a slightly swollen in the center. Its diameter is 8-10.6 mm. and thickness is 1.4-3 mm. In the equatorial section, the first chamber is very small. Other characteristics are the same as the macrospheric form.

Distribution and associated foraminifers

The *Nummulites* ex gr. *fabianii* is found in the limestone of the Priabonian with *Nummulites fabianii* (Prever), *Nummulites striatus* (Bruguiere), *Sphaerogypsina globulus* (Reuss), *Linderina brugesi* Schlumberger, *Chapmanina gassinensis* (Silvestri), *Asterigerina rotula* (Kaufmann), *Eorupertia magna* (Le Calvez), *Halkyardia minima* (Liebus), *Praerhapydionina huberi* Henson, *Rotalia* sp., *Austrolrillina* sp., *Peneroplis* sp., and *Planorbulina* sp. in the Körpe, Egopköy and Çatalharman measured stratigraphic sections (Fig. 2), (Plate II, III).

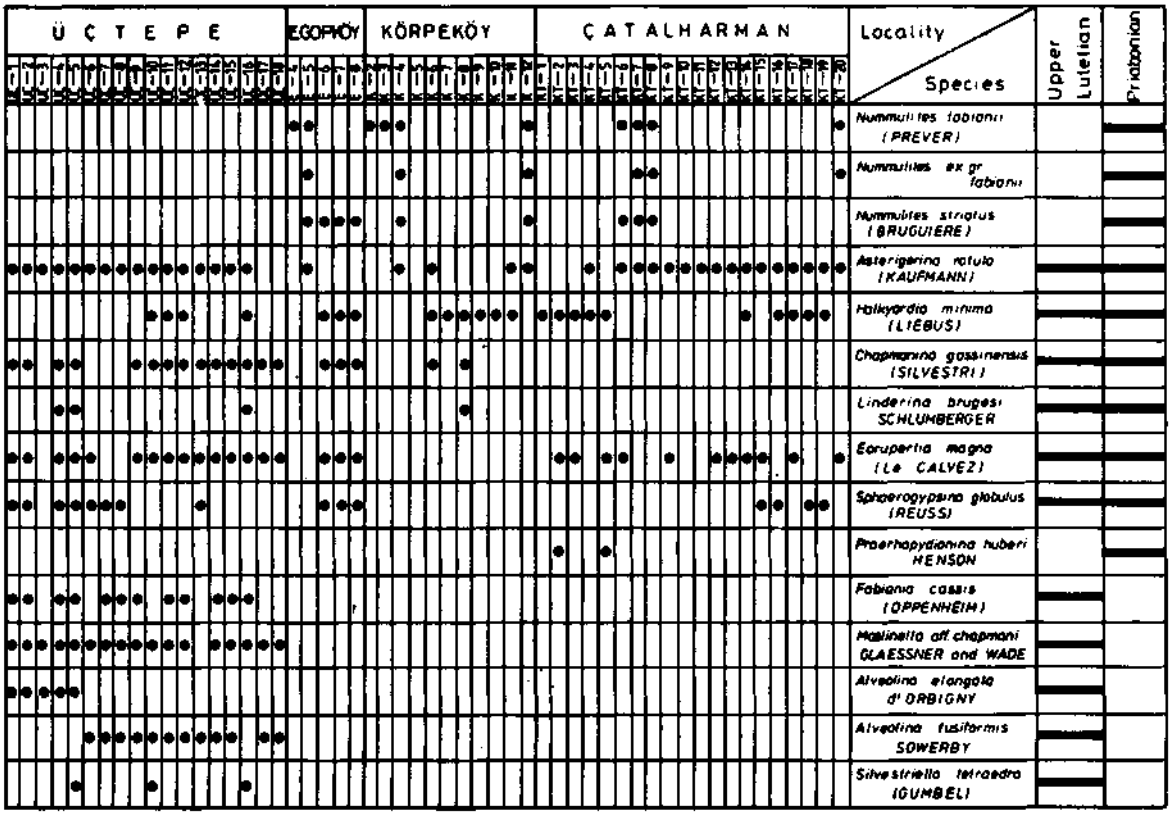

Fig.2- Biostratigraphic distribution of the foraminifers in limestone in Elazığ.

In addition, the same fossil is observed around the Baskil region (Turan, 1984; Asutay, 1985) together with the fossil assemblages: *Nummulites fabianii* (Prever), *Nummulites striatus* (Bruguiere), *Eorupertia magna* (Le Calve?.), *Chapmanina gassinensis* (Silvestri), *Fabiania cassis* (Oppenheim), *Halkyardia minima* (Liebus), *Sphaerogypsina globulus* (Reuss), *Amphistegina* sp., *Heterostegina* sp., and *Alveolina* sp

Stratigraphic level: Priabonian.

DISCUSSION AND CONCLUSIONS

The nummulites which belong to *Nummulites fabianii* (Prever) group are different from real *Nummulites fabianii* (Prever). Also, these species are diffrerent from *Nummulites fichteli* Michclotti which arc characteristic of Oligocene. Our species are found together with the characteristic foraminifers of Eocene; *Nummulites fabianii* (Prever), *Nummulites striatus* (Bruguiere), *Halkyardia minima* (Liebus), *Chapmanina gassinensis* (Silvestri), *Linderina brugesi* Schlumberger, *Asterigerina rotula* (Kaufmann), *Eorupertia magna* (Le Calvez) and *Sphaerogypsina globulus* (Reuss) and that is why there is no doubt about their age.

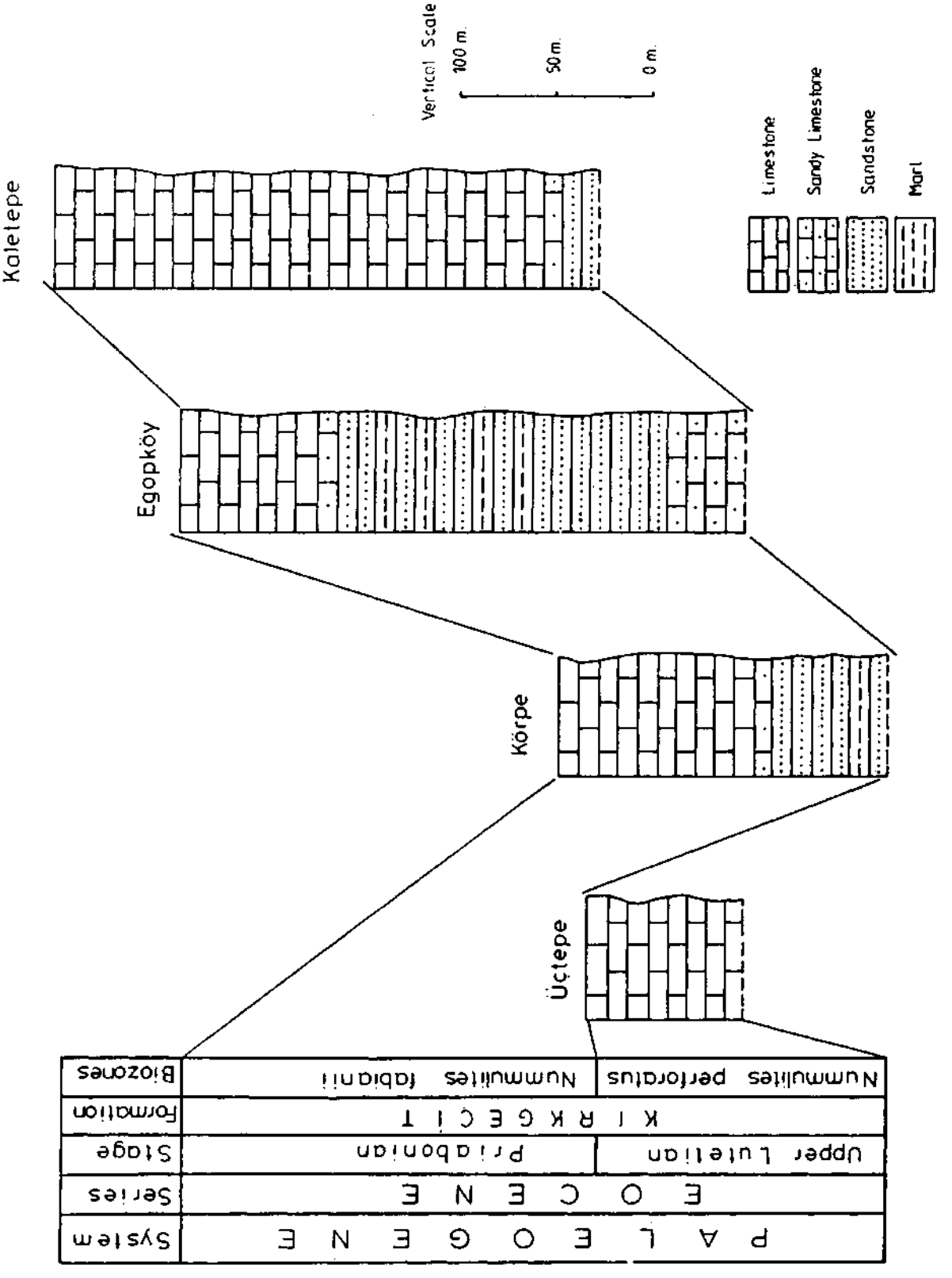

Fig.3- The correlation of the measured stratigraphic section in the study area.

However, paleontologists studied on the nummulites all over the world have indicated their problems about naming this kind of nummulites.

Boussac (1911) stated that there were transitional nummulites between *Nummulites fabianii* (Prever) and *Nummulites intermedius* (d'Archiac) in Biarritz, and showed evidence revealing that the latter originated from the former. In addition, the same author pointed out that typical *Nummulites fabianii* (Prever) posses a sparse net and more granules, and *Nummulites* ex gr. *fabianii* are not found in the lower part of the Priabonian (Bartonian) and they indicate a variation approaching typical *Nummulites intermedius* (d'Archiac).

Flandrin (1938) pointed out that the transitional forms were in the upper part of the Eocene beds, and the lower part of the Oligocene layers having studied the materials collected from Algeria. The nummulites in the Flandrin's thesis resemble those of the Hoia-Cluj samples.

Grigorian (1961) accepts *Nummulites reliatus* Roveda as a subspecies. In addition, the same researcher pointed out that *Nummulites fabianii reliatus* Roveda indicated a transitional morphology between *Nummulites fabianii* (Prever) and *Nummulites intermedius* (d'Archiac) and was found at the Upper Eocene-Lower Oligocene boundary.

Roveda (1970) indicated that the nummulites are faced with a dangerous inflation as being parallel to the other foraminifcral group as result of the author's comprehensive study. For this reason, Roveda (1970) produced forty-one species, subspecies and varieties *of Nummulites fabianii* (Prever) and accepted only five of them.

Bombita (1975) revealed that four laxons of the group followed each other in Transilvania, first of which has a little primitive character and was found in Lcgia-Cluj Limestones, second of which formed an epibole species in the marls with *Nummulites fabianii* (Prever), third of which diminished in the marls bearing Bryozoa, and fourth of which formed a transitional form to *Nummulites intermedius* (d'Archiac) in Hoia Limestones and described the forms as follows;

1- Having studied the initial form (Plate I, figs. 1-17) from subspecies of Transilvania (Bombita, 1975), it was determined that the diameters of microspheric forms vary between 7.5-11.5 mm. The superficial net of the test shows transitional aspects of great nets to irregularly trajectory and broken and elongated meshes disposed, sinuous and granules arranged parallel to that of central form *of Nummulites fabianii* (Prever). In the equatorial section, the spiral lamina is growing progressively until the end of the penultimate whorl, and towards the last whorls of the chambers are longer than higher. The surface of the macrospheric form is covered by a reticulum. The diameter of the macrospheric form (3.5-4.5) is bigger than the previous form. The diameter of the macrosphere is approximately 0.35 mm.

2- *Nummulites* ex *gr. fabianii* (Plate II, figs. 1-15; Plate VII, figs. 1-6) are found in the marls with *Nummulites fabianii* (Prever) in the epibole zone of the Baci (Cluj) region. The margin of the test at these forms is undulated, and the superficial net is sinuous, meandriform and of parallel bunched forms containing thin meshes. The diameter of the test is between 12-13.5 mm. The diameter of the macrospheric forms (3-4 mm.) are less than those of the species of Legia Limestones, but diameter of the macrosphere is slightly larger.

3- *Nummulites* ex gr. *fabianii* collected from the Hoia Limestones, cropped out the western part of the Cluj, formed the transitional form between *Nummulites fabianii* (Prever) and *Nummulites intermedius* (d'Archiac) (Plate IV, figs. 1-19). The diameters of the microspheric forms of the Hoia arp 5.9-9.3 mm. and generally vary between 7-7.5 mm. The margin of the test is often undulated and the central part is poorly prominent. In general, the secondary ramification of the superficial nets is not to be gathered in the nets but turminates in the meshes with or without granules. Unification as being net shaped can be seen at the polar, zone of the test in a narrow band. However, this unification docs not attain to the fineness revealed by the *Nummulites intermedius* (d'Archiac). The meshes of the net are more elongated in radial direction which form a similar type *of Nummulites fabianii* (Prever). Despite the fact that the diameter of the macrospheric form is found in the same variability limits in the marl with *Nummulites fabianii* (Prever), the diameter of the macrosphere indicated a slightly lessening magnitude (0.3-0.35 mm.). Most of the macrospheric forms, as seen in *Nummulites fabianii* (Prever), contain the rectangular mesh between septa and spiral lamina. In adult forms the lenghts of the final whorls arc more than their heights.

After having throughly studied all the general characteristics of *Nummulites* ex *gr.fabianii* collected from the Elazığ region (Eastern Anatolia), they are found to be within the same limits and to resemble the characteristics of *Nummulites* ex *gr.fabianii* determined from Baci, Legia and Hoia Limestones in Transilvania.

As pointed out before, a chaotic naming still continues. These nummulites are included in the *Nummulites fabianii* (Prever) group in this work because of the rarity of the nummulites.

Manuscript received April 19,1990

REFERENCES

Asutay, J., 1985, Baskil (Elazığ) çevresinin jeolojik ve petrografik incelenmesi: A.Ü. Fen Bil. Enst., Doctora thesis (unpublished), Ankara.

Bingöl, F., 1984, Geology of the Elazığ area in the Eastern Taurus region in: Tekeli, O. and Göncüoğlu, M.C. (eds), Geology of the Taurus Bell, MTA Publ., p. 209-216, Ankara.

Bombita, G., 1975, Remarques sur le groupe de Nummulites fabianii: Revista Espanole de Mikropalcontologia, v. VII, n.1, p. 33-90.

Boussac, J., 1911, Etudes stratigraphiqucs et palcontologiques sur le Nummulitique de Biarritz: Ann. Hebert, Paris, v. 5, pp. 1-95, Plate 4, figs. 4,7,9, Plate 6, fig. 4.

Flandrin, J., 1938, Contribution a l'etude palcontologique du Nummulitique algerien: Algeria, Service Carte Geol., Matcriaux Carte Geol. Algerie, Macon, France, ser. 1 (Pal.), no. 8, pp. 5-158, Plate 3, figs. 71-75.

Grigorian, S. M., 1961, Nouvelles sous-especes de Nummulites de l'Eocene supericur d'Armania (en russe): Dokl. Akad. Nauk. Arm. SSR 32/2.

Ketin, İ., 1946, Elazığ-Palu ve Pertek yöresinin jeolojisi: MTA Rep., 1708 (unpublished), Ankara.

Kipman, E., 1976, Kebanın jeolojisi ve volkanitlerinin petrolojisi: Doctora thesis, İst. Üniv. no. 134 (unpublished) İstanbul.

Özkul, M., 1982, Elazığ doğusu (Güneyçayırı) sedimantolojik incelemesi: F.Ü. Yüksek Lisans Tezi (unpublished), Elazığ.

Roveda, V., 1970, Revision of the Nummulites (Foraminiferida) of the Nummulites fabianii-fichteli group: Riv. Ital. Palcont. v.76, n.2, pp.235-324, tav.22-25, Milano.

Sirel, E.; Metin, S. and Sözeri, B., 1975, Palu (KD Elazığ) denizel Oligosenin stratigrafisi ve mikropalcontolojisi: Türkiye Jeol. Kur. Bull., 18.no.2, 175-180, Ankara.

Tolun, N., 1955, Elazığ-Keban-Çemişgezek ve Pertek bölgesinin jeolojisi: MTA Rep., 2227 (unpublished), Ankara.

Tuna, E., 1979, Elazığ-Palu ve Pertek dolayının jeolojisi: TPAO Rep., 1362 (unpublished), Ankara.

Turan, M., 1984, Baskil-Aydınlar (Muşar) yöresinin stratigrafisi ve tektoniği: F.Ü. Fen Bil. Enst. Doct. thesis (unpublished), Elazığ.

PLATES

PLATE -I

Nummulites ex gr. *fabianii*

Fig. 1- Equatorial section, microspheric form (E5-2f), X7.

Fig. 2-Equatorial section, microspheric form (E5/1), X7

Fig. 3- Equatorial section, microspheric form (E5-2i), X7.

Fig. 4- Equatorial section, microspheric form (E5-2h), X7.

Fig. 5- Axial section, microspheric form (E5-2b), X7.

Fig. 6- Equatorial section, microspheric form (E5-lk), X6.

Fig. 7- Equatorial section, microspheric form (E5-2k), X6.

Fig, 8- Axial section, microspheric form (K4-ld), X6.

Fig. 9-Equatorial section, microspheric form (E5-1n), X5.

Fig. 10- Equatorial section, microspheric form (E5-2g), X6.


1
2
3
4
5
8
9
10

PLATE - II

Nummulites ex gr. *fabianii*

Fig. 1-Equatorial section, macrospheric form (E5-2), X11.

Fig. 2-Equatorial section, macrospheric form (E5/3), X12.

Fig. 3-Axial section, macrospheric form (E5-lb), X9.

Fig. 4- Axial section, macrospheric form (E5-lc), X9.

Fig. 5- Equatorial section, macrospheric form (E5/4), XI2.

Fig. 6- Equatorial section, macrospheric form (KT-7/4), XI1.

Fig. 7- Equatorial section, macrospheric form (E5/5), X12.

Fig. 8- Surface view, macrospheric form (E5/6), X9.

Fig. 9- Surface view, macrospheric form (E5/8), X8.

Nummulites fabianii (Prever)

Fig. 10- Equatorial section, macrospheric form (E4/1), X5.

Fig. 11- Equatorial section, macrospheric form (E4/2), X4.

Fig. 12- Surface view, macrospheric form (K-3), X6.

Nunvnulites striatus (Bruguiere)

Fig. 13- Surface view, macrospheric form (K4-2/1), X7.

Fig. 14- Axial section, macrospheric form,(K4-2), X7.

Fig. 15-Axial section, macrospheric form (K4-2d), X10.

Fig. 16- Equatorial section, macrospheric form (K4-2/3), X8.

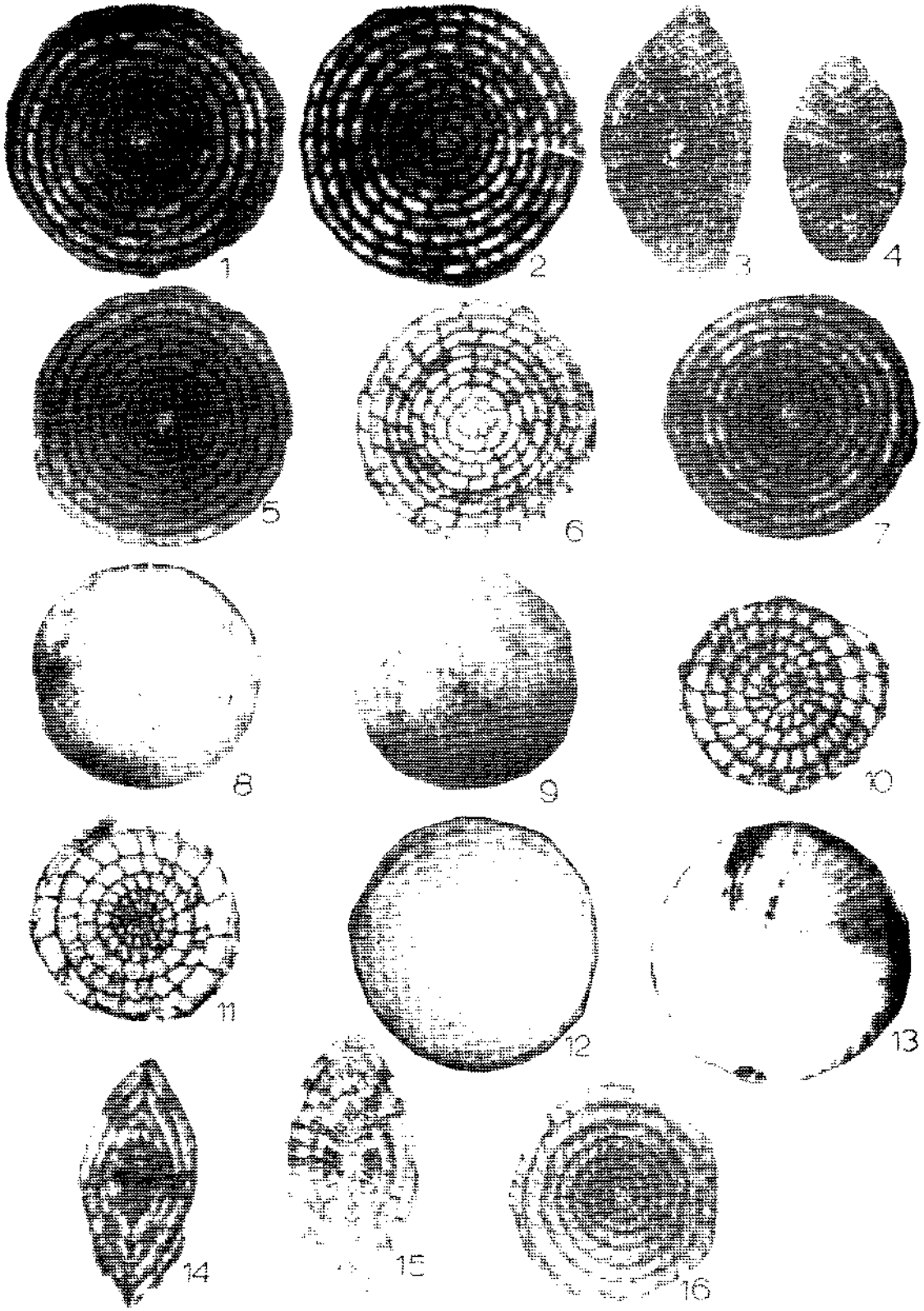
1
2
3
4
5
6
7
8
9
10
11
12
13
14
15
16

PLATE - III

Eorupertia magna (Le Calvez)

Fig. 1-Equatorial section (Üç-18/1), X28.

Fig. 2-Axial section (Üç-17), X25.

Fig. 3- Axial section (Al-7), X16.

Halkyardia minima (Liebus)

Fig. 4-Axial section (A1-1), X92.

Fig. 5- Axial section (KT-14/1), X51.

Praerhapydionina huberi Henson

Fig. 6- Vertical section (A1-21/6), X34.

Fig. 7-Vertical section (Al-21/12), X32.

Chapmanina gassinensis (Silvestri)

Fig. 8- Vertical section (N-8), X34.

Fig. 9- Basal section (N-9), X32.

Sphaerogypsina globulus (Reuss)

Fig. 10- Axial section (KT-15/1), X36.

Asterigerina rotula (Kaufmann)

Fig. 11- Axial section (KT-14/1), X45.

Fig. 12- Axial section (KT-14/2), X47.

Rotalia sp.

Fig. 13-Axial section (KT-15/2), X33.

Austrolrillina sp.

Fig. 14- Equatorial section (Al-21/12), X35.

Peneroplis sp.

Fig. 15- Axial section (Al-21/4), X20.

Linderina brugesi Schlumberger

Fig. 16- Vertical section (Al-4), X35.

Planorbulina sp.

Fig. 17- Axial section (KT-18), X75.

NiyaziAVŞARPLATE-III

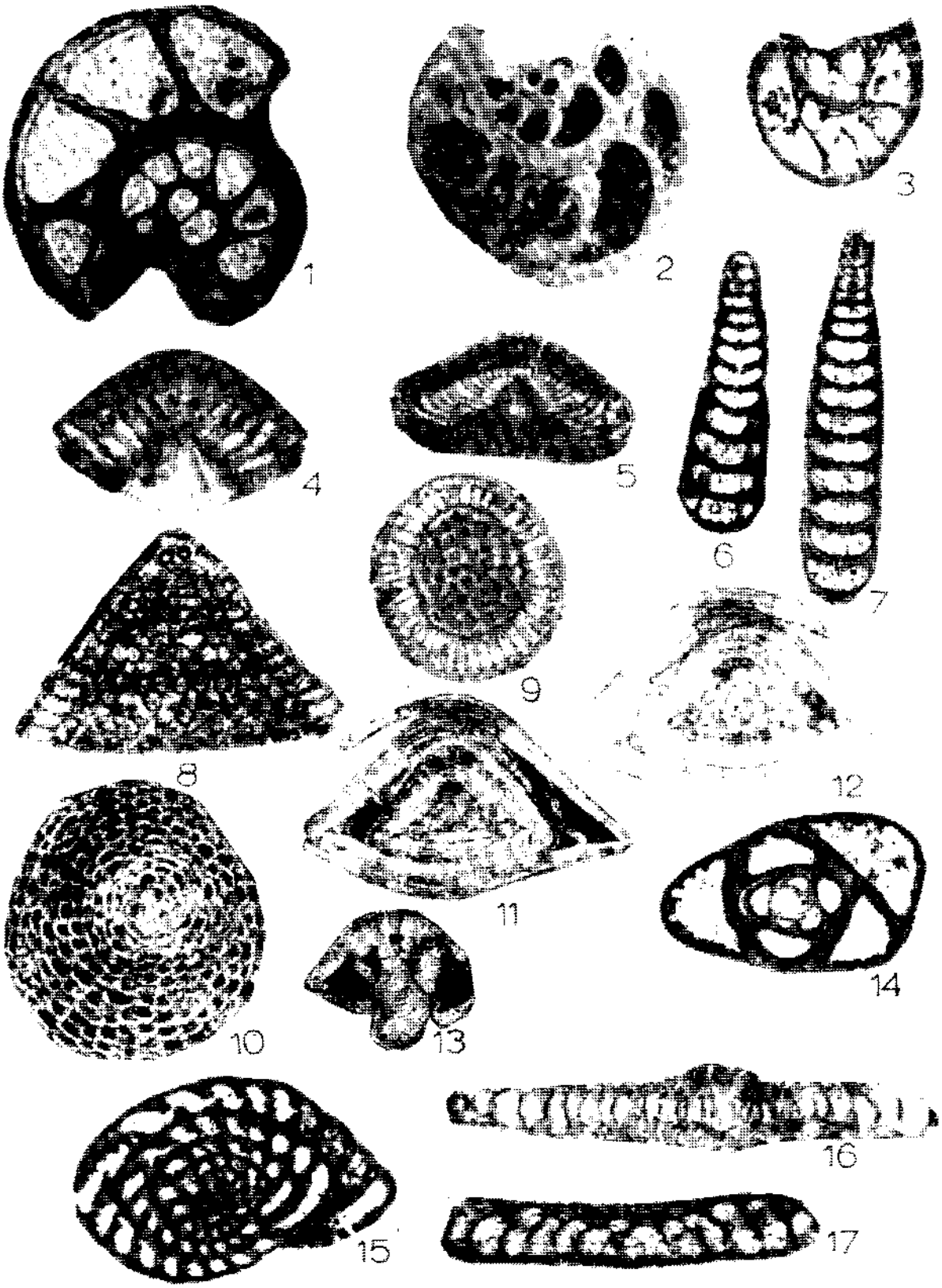

MACRO AND MICRO FOSSIL FLORA OF SOMA COAL AREA

Yusuf GEMİCİ****; Erol AKYOL*****; Funda AKGÜN***** and Özcan SEÇMEN****

ABSTRACT— The macro and micro fossil flora of Soma coal area (West Anatolia) embodying important lignite deposits of Turkey; has been investigated in this study in all 72 family, genus or species level have been determined from the area. The most distributed species are *Glyptostrobus europaeus* (Brong.) Unger, *Pinus* (cf. *P. taedaformis* Heer) and *Quercus.These* specimens point out that this flora belongs to Middle Miocenes age. It also depicts the presence of a subtropical hot and wet climatic conditions. The most probable vegetation could have been a marshy forest cover of *G. europaeus* alongside the lake with a mixed forest of *Pinus-Quercus* at its margin.